NASA Technical Memorandum 85835

GASP Cloud- and Particle-Encounter Statistics, and Their Application to LFC Aircraft Studies

Volume I: Analysis and Conclusions

William H. Jasperson, Gregory D. Nastrom,
Richard E. Davis, and James D. Holdeman

OCTOBER 1984

NASA

NASA Technical Memorandum 85835

GASP Cloud- and Particle-Encounter Statistics, and Their Application to LFC Aircraft Studies

Volume I: Analysis and Conclusions

William H. Jasperson and Gregory D. Nastrom
Control Data Corporation
Minneapolis, Minnesota

Richard E. Davis
Langley Research Center
Hampton, Virginia

James D. Holdeman
Lewis Research Center
Cleveland, Ohio

National Aeronautics
and Space Administration

**Scientific and Technical
Information Branch**

1984

CONTENTS

VOLUME I

VOLUME II

SUMMARY

Summary statistics, tabulations, and variability studies are presented for the entire cloud observation archive - nearly 88 000 samples - from the NASA Global Atmospheric Sampling Program (GASP), which was conducted from 1975 to 1979 aboard four commercial airliners in regular service. Summary statistics, tabulations, and variability studies are also presented for GASP particle-concentration data - nearly 56 000 samples - gathered concurrently with the cloud observations. Clouds were encountered in about 15 percent of the data samples, but the probability of cloud encounter is shown to vary significantly with altitude, latitude, and distance from the tropopause, and less significantly with season. Several meteorological circulation features, such as the Intertropical Convergence Zone, are apparent in the latitudinal distribution of cloud cover. The cloud-encounter statistics are shown to be consistent with the classical mid-latitude cyclone model, with more clouds encountered in the upper troposphere in highs than in lows. Observations of clouds spaced more closely than 90 minutes of flight time are shown to be statistically dependent.

The number density of particles with a diameter greater than 3 μm also varies with time and location. It depends primarily on the horizontal extent of cloudiness, that is, the portion of each sampling interval that is spent within clouds. Thus, the variability of time in clouds and the variability of particle number density are closely related.

The summary statistics for cloud and particle encounter are utilized to estimate the frequency of cloud encounter on long-range commercial transport routes and to assess the probability and extent of laminar flow (LF) loss due to cloud or particle encounter by aircraft utilizing laminar flow control (LFC). The observations of route-averaged time in clouds are found to fit an empirical model based on a gamma probability density function; this model can be used to estimate the probability of extended cloud encounter along a route. The analysis in this report shows that the probability of LF loss in clear air is negligible and that the probability of extended cloud encounter, and associated significant loss of LF, is too low, of itself, to make LFC impractical.

For user convenience, this report is presented in two volumes. Volume I contains the narrative, analysis, and conclusions. Volume II is composed of five appendixes, as follows: A - GASP Cloud and Particle Instrumentation; B - Individual Flight Summaries; C - Independence of Cloud Observation Periods; D - Cloud-Encounter Statistics as Functions of Latitude, Longitude, Northern Hemisphere Season, and Altitude; and E - Cloud-Encounter Statistics as Functions of Latitude, Longitude, Northern Hemisphere Season, and Distance From the National Meteorological Center (NMC) Tropopause.

INTRODUCTION

The purpose of this report is to present summary results of the analysis of all cloud- and particle-encounter measurements taken in the NASA Global Atmospheric Sampling Program (GASP) (refs. 1 to 3), which was conducted from 1975 to 1979 from as many as four Boeing 747 aircraft operating in regular commercial service worldwide.

This report extends and generalizes the preliminary results given earlier in references 4, 5, and 6, which were based on the fraction of GASP data from only December 1975 to December 1977. Those preliminary analyses were based on the first 52 000 cloud observation periods in the set, whereas the analyses in this report are based on the total set, approximately 88 000 cloud observation periods. The primary motivation for this study is evidence that the low-drag characteristics of laminar flow control (LFC) wings are lost (albeit temporarily) in visible clouds and are also occasionally lost in cirrus hazes. These increases in drag influence the economic feasibility of LFC-winged aircraft (refs. 7 to 10). The increase in drag is due to turbulent wakes behind particles which penetrate the boundary layer (ref. 10). Cloud ice particles also cause aerodynamic problems for reentry vehicle nose cones penetrating cirrus clouds (ref. 11). Therefore, using instrumentation described in references 12 to 14, the U.S. Air Force has also been pursuing a research effort on cirrus particle distributions.

The research reported here lies within the first of a two-part research effort by NASA to assess the impact of cloud particles on LFC performance. In the first part, a climatology of cloud and particle encounters is being developed to address the fundamental questions: What is the probability of cloud encounter on airline routes, and what is the variability of cloud encounter with altitude, season, and location? These climatological data, together with theoretical estimates of the effect of ice crystals on LFC (ref. 10), and USAF particle measurements in cirrus clouds (e.g., refs. 15 and 16) have already been used in making preliminary estimates of the portion of time that LFC would be lost in clouds and clear air (ref. 17). In the second part of the research effort, to be implemented during 1984, NASA will make precise in situ measurements of the cloud and particle environment on flights of an LFC-winged research aircraft in an attempt to quantify better the effects of clouds on LFC (refs. 18 and 19).

The location of clouds and their extent are also of interest for several meteorological reasons, such as the Earth's radiation balance (ref. 20), and long-term (climatic) variations of global temperature (refs. 21 and 22); thus, both the meteorological and the LFC applications of cloud-encounter results are discussed here. This report begins by describing the cloud-encounter and particle-concentration data sets used in this study. Then, cloud-encounter data are analyzed in terms of altitude, latitude, season, and distance from the tropopause; these data are also interpreted in terms of global meteorological circulation features and relative vorticity. The particle-concentration data are then analyzed. The report then shifts its emphasis to the applications of both cloud and particle data to the estimation of laminar flow loss for LFC aircraft and concludes with the presentation of an empirical model for the probability of cloud cover along airline routes. The five appendixes cited in this volume all appear in Volume II.

A much shortened version of this report, without appendixes and with primary emphasis on the meteorological conclusions, appears in reference 23.

SYMBOLS AND ABBREVIATIONS

ABV	above
ANOVA	analysis of variance
A1	pressure altitude band from 28.5 to 33.5 kft

A2 pressure altitude band from 33.5 to 38.5 kft

A3 pressure altitude band from 38.5 to 43.5 kft

BLO or BLW below

B747 Boeing 747 aircraft

CIV "clouds in vicinity" (i.e., clouds along the flight path)

CLAYR number of cloud patches encountered during a 256-second cloud observation

D diameter of particle, μm

EMD equivalent melted diameter of particle, μm (cf. ref. 15)

GASP Global Atmospheric Sampling Program (NASA)

ICAO International Civil Aviation Organization

ITCZ intertropical convergence zone

LF laminar flow

LFC laminar flow control

N number of observations, dimensionless

NH Northern Hemisphere

NMC National Meteorological Center (NOAA)

NOAA National Oceanic and Atmospheric Administration

P probability, percent

P(TIC>0) probability of cloud encounter, percent, numerically equivalent to PCE (q.v.)

PCE probability of cloud encounter, percent (see fig. 1)

PD5 total particle concentration or number density for particles larger than 3 μm in diameter, particles/m^3

ppbv parts per billion by volume (as in ozone concentration)

TIC time in clouds (total indicated time in clouds during an observation period divided by period observation time), percent (see fig. 1)

TIC_F average time in clouds per observation period for a given flight (percent TIC in appendix B listings (Vol. II))

TIC_R average time in cloud per observation period for all the flights on a given route, obtained from the average of TIC_F values; also termed "route-averaged time in clouds"

TICIV time in clouds with clouds along the flight path (as in TIC, but defined only for a set of non-zero TIC observations, i.e., observations with TIC > 0), percent (see fig. 1)

T1 tropopause separation band located 10 to 15 kft below the tropopause

T2 tropopause separation band located 5 to 10 kft below the tropopause

T3 tropopause separation band located 0 to 5 kft below the tropopause

T4 tropopause separation band located 0 to 5 kft above the tropopause

VLXXXX designator for GASP archive tape number XXXX

ζ relative vorticity, sec^{-1} (less than 0 for anticyclonic flow; greater than 0 for cyclonic flow)

η parameter in gamma probability density function model for TIC_F, equal to 0.7

σ standard deviation

A bar over a symbol or abbreviation denotes the mean value.

Additional Symbols in Tables and Appendixes (Vol. II)

SIGMA(x) standard deviation of quantity x, percent

N number of observations

$\bar{T}_{CLEAR}$ average temperature in clear air, °C

$\bar{T}_{CLOUD}$ average temperature in clouds, °C

$\overline{\Delta Z}_{CLEAR}$ distance from tropopause during flight in clear air, kft

$\overline{\Delta Z}_{CLOUD}$ distance from tropopause during flight in clouds, kft

DATA

The cloud-encounter and particle-concentration (particle-number-density) data used in this study were measured in the Global Atmospheric Sampling Program (GASP) from December 1975 to July 1979. These data are from GASP tapes VL0004 to VL0031, which have been archived at the NOAA National Climatic Center, Asheville, North Carolina. The contents and formats of these tapes are described in references 24 to 32. Briefly, the data acquisition phase of GASP began in March 1975; operational measurements began in December 1975 and continued to July 1979. Meteorological and trace constituent data were obtained with instruments placed aboard as many as four Boeing 747 airliners in routine commercial service. Data collected on these flights should thus be representative of conditions encountered by commercial airliners, even though the observations do not constitute a truly random sample of all possible atmospheric conditions from a statistical point of view. Observations were recorded at nominal 5- or 10-minute intervals at all altitudes above about 20 kft.

The presence of clouds at cruise altitude was determined with a light-scattering particle counter (refs. 24 to 34), hereinafter referred to as the "cloud detector." The GASP cloud and particle instrumentation is described further in appendix A (Vol. II). A cloud-detection threshold level for particles larger than 3 μm in diameter was set empirically, based on visual observation of a light haze outside the aircraft. The same threshold level was used for all GASP cloud detectors and resulted in an "in clouds" registration whenever the local particle concentration, or number density PD5 (of particles with diameter $D > 3$ μm), was greater than 66 000/m^3. The sampling time for the cloud detector was 256 sec (4 minutes 16 seconds), corresponding approximately to a horizontal distance of 36 n.mi. at a ground speed of 500 knots. At the end of each sampling cycle for the GASP system, the time (out of the last 256 sec) which registered as "in clouds" was recorded. Also, the number of cloud patches encountered during the sampling period was recorded; a new patch was registered if, having once entered a cloud (PD5 > 66 000/m^3) and subsequently left it (PD5 < 8250/m^3), the cloud detector again reached the cloud-detection threshold. (See discussion of CLAYR in refs. 24 to 32.)

During the first minute of each sampling period, the numbers of particles in selected size ranges were counted. Although GASP cloud data were first reported in December 1975 (ref. 24), particle count data were not reported until January 1977 because of a rather large uncertainty in the total particle count resulting from nonuniform illumination of the sample chamber and high noise-to-signal ratio on channels measuring particles smaller than 1.4 μm in diameter (refs. 28 to 32). While three channels were reported for the particle counter, only the largest particle channel (for $D > 3$ μm) has been used herein because only the largest particles are believed to be significant for laminar flow (LF) degradation.

The GASP data were recorded at nominal 5- or 10-minute intervals during flight above 20 kft. In addition to the basic GASP measurements, the tropopause pressure at each GASP data location has been time and space interpolated from the NOAA National Meteorological Center (NMC) grids, when available, and added to the archived tapes. Auxiliary meteorological data used herein, such as vorticity, have been computed from the NMC isobaric height fields for each GASP data location (ref. 35).

Before proceeding, it is necessary to establish three quantities of cloud-encounter nomenclature which will be used repeatedly in the analyses to follow: TIC, PCE, and TICIV. First, GASP observation periods are separated according to whether or not clouds are encountered during each 256-sec period. Figure 1 illustrates four successive observation periods, one with no cloud encounter and three with one or more cloud patches encountered. The time within each cloud patch is indicated (e.g., T_{21} denotes the time, in seconds, within the first cloud patch during the second observation period). The portion of time in clouds (TIC), expressed as a percentage, for the four observation periods in figure 1 is calculated as follows:

$$TIC_1 = \frac{T_{11} + T_{12}}{256} \times 100$$

$$TIC_2 = \frac{T_{21} + T_{22} + T_{23}}{256} \times 100$$

$$TIC_3 = \frac{T_{31} + T_{32} + T_{33}}{256} \times 100$$

$$TIC_4 = \frac{0}{256} = 0$$

The average portion of time in clouds for these four observation periods is

$$\overline{TIC} = \frac{TIC_1 + TIC_2 + TIC_3 + TIC_4}{4}$$

An observation period with TIC = 0 is appropriately termed "in clear air" because at no time during that observation period did the particle concentration exceed 66 000/m^3, the threshold concentration (TC). Those observation periods during which the particle concentrations exceeded the TC for some portion of the period (i.e., $0 < TIC \leq 100$ percent) had clouds along the flight path, or are said to have had "clouds in the vicinity" (CIV). A low TIC, for example, 10 to 40 percent, would indicate a scattered cloud layer; TIC = 50 to 90 percent would indicate a broken cloud layer; and TIC = 90 to 100 percent would indicate an overcast deck of clouds.

The probability of cloud encounter (PCE) during an observation period is obtained by dividing the number of observation periods with CIV (i.e., TIC > 0) by the total number of observation periods. For the example in figure 1,

$$PCE = \frac{3 \text{ observations with CIV}}{4 \text{ observations total}} = 0.75$$

Note that PCE is equivalent to the term P(TIC > 0) in references 4, 5, 6, and 17 and in appendixes D and E (Vol. II) of the present report.

Now consider only those observation periods with some cloud presence, that is, with TIC > 0. The average portion of time in clouds during an observation period with clouds in the vicinity (TICIV) is

$$TICIV = \frac{TIC_1 + TIC_2 + TIC_3}{3}$$

These three cloud-encounter quantities are related by

$$\overline{TIC} = PCE \times TICIV \qquad (1)$$

Equation (1) is demonstrated for the example in figure 1 as follows:

$$\frac{TIC_1 + TIC_2 + TIC_3 + TIC_4}{4} = 0.75 \frac{TIC_1 + TIC_2 + TIC_3 + TIC_4}{3}$$

For convenience, $\overline{TIC}$, PCE, and TICIV are all expressed as percentages.

From December 1975 to July 1979, 1748 GASP flights gathered cloud detection data (not necessarily cloud encounters). A summary of these flights, by month and contributing aircraft, is given in table I and a monthly and seasonal summary of all the flight routes is presented in table II. Note that particle count (PD5) was not reported until January 1977 (it is available for 1341 flights). Individual flight summaries and averaged data are listed in appendix B (Vol. II). The routes are listed alphabetically by airport pair and individual flights are ordered by date.

Cloud encounter and particle data are reported with respect to two different height references in this report. The first is the pressure altitude, with which all pilots are familiar. Each pressure altitude corresponds to a given value of atmospheric pressure according to the ICAO Standard Atmosphere (ref. 36). The second height reference is the distance from the National Meteorological Center (NMC) tropopause. The tropopause separates the weather-active troposphere from the thermally stable and generally cloud-free stratosphere. The actual tropopause height varies primarily with latitude and season with day-to-day changes superimposed as large-scale storms develop and decay. Figure 2 presents the average tropopause height over the world for each season (ref. 37). For simplicity, the term "altitude" will denote "pressure altitude" and the term "tropopause" will denote the "NMC tropopause."

The complete GASP data set consists of 87 922 cloud observation periods, 256 sec each, for a total of approximately 6250 hours in all. As shown in figure 3, these observations tend to be more numerous in the Northern Hemisphere (NH) mid-latitudes but are fairly uniformly distributed by Northern Hemisphere seasons. About 58 percent of the observations were made in winter and spring and about 42 percent were made in summer and autumn. The shaded areas in figure 3 (and subsequent similar figures) denote observation periods having clouds in the vicinity, that is, with TIC > 0. The numbers above the bars indicate the percentage of observation periods in each bar having clouds in the vicinity (i.e., the percentage is equal to the shaded area of the bar divided by the total area for each bar and multiplied by 100). Of the total 87 922 cloud observation periods, 13 206 (15.25 percent) were in the vicinity of clouds.

The distribution of cloud observation periods as a function of altitude is shown in figure 4(a). Over 96 percent of the observation periods fall between the normal airline cruise altitudes of 28.5 kft and 43.5 kft. Figure 4(b) shows that the distribution of cloud observation periods as a function of distance from the NMC tropopause is much more uniform. Because the NMC tropopause data were occasionally not available, only 70 340 observation periods are represented in figure 4(b). This panel clearly illustrates that very few clouds are encountered in the stratosphere (3 percent in the 5000 feet above the tropopause versus 19 percent in the 5000 feet below the tropopause). In fact, the frequency of clouds in the stratosphere may be even smaller than indicated because the GASP data are local measurements, whereas the tropopause pressures are interpolated from large-scale grids (2.5° latitude by 2.5° longitude by 12 hours), so that the small-scale undulations of the tropopause may be missed by the NMC grid. The graphical results of figures 3(b) and 4 are summarized numerically in table III.

Cloud-encounter data are used herein as reported, with all observation periods given equal weight. However, because cloudiness (or the lack thereof) is associated with large-scale weather systems, not all observation periods are independent. A study of the observation period independence is presented in appendix C (Vol. II). The results of this study indicate that to be considered statistically independent, observations of cloud or no cloud condition must be separated by 90 to 120 minutes of flight time. This study also analyzed the independence of TIC values <u>within</u> a cloud.

It was found that for TIC values of less than 50 percent, observations separated by 10 to 20 minutes could be considered independent. For TIC values larger than 50 percent, the sample-to-sample observations are highly correlated, and the time between independent observations cannot be reliably estimated. It can be assumed, however, to lie between 20 and 120 minutes.

Particle-concentration (PD5) data periods are shown in figure 5 to have nearly the same distributions with (a) latitude and (b) season as the cloud-detector data (fig. 3). In total, there were 70 304 particle-concentration observation periods, of which 55 718 were coincident with cloud observation periods, about 63 percent of the total number of cloud observation periods (87 922). About 13 percent of the particle data were gathered in clouds or in the vicinity of clouds; this compares with 15.25 percent for cloud observation periods. The distributions of particle-concentration observation periods presented in figure 6 as a function of (a) altitude and (b) distance from the NMC tropopause are also very similar to the distributions of cloud observation periods (fig. 5). There are 51 676 particle-concentration observation periods at times when the NMC tropopause data were available.

CLOUD-ENCOUNTER ANALYSIS

Complete tabulations of the cloud-encounter statistics as functions of latitude, longitude, and season (Northern Hemisphere) are given in appendix D (Vol. II) as functions of altitude and in appendix E (Vol. II) as functions of distance from the tropopause. A map to provide geographical orientation for the latitude-longitude cells is given at the front of appendix D, and the data entries are explained at the beginning of appendixes D and E. In the right column for each season and altitude band, the results from all data in each latitude band are given under the heading "zonal mean." For convenience, these zonal means of each variable are summarized in tables IV and V as functions of latitude and season. Table IV gives the results in terms of altitude and table V gives them in terms of distance from the tropopause. While the tabulations and summaries herein were formatted for optimum usefulness to the LFC aircraft studies, it is anticipated that the results will be of interest to a broader segment of the scientific community. Therefore, the results of the analysis of cloud-encounter variability and the relation of these data to other meteorological variables are discussed in the subsequent paragraphs.

The probability of cloud encounter (PCE) and the mean time in clouds ($\overline{TIC}$) both decrease rapidly above the tropopause, as shown in figure 7. Figure 8 shows the cumulative frequency distributions corresponding to the data shown in figure 7. These curves give the percentage of observations (on the ordinate) in which TIC equaled or exceeded any given percentage (on the abscissa). If these curves may be assumed to be representative of population-based probability values, then they may be considered cumulative probability distributions also and the ordinate label $P(\geq TIC)$ is appropriate.

Corresponding to figures 7 and 8, but as functions of altitude instead of distance from the tropopause, are figures 9(a) and 9(b), respectively. The decrease in cloudiness with altitude in figure 9(a) is primarily due to the increased likelihood of being in the stratosphere in the upper altitudes.

Although all available data were used in preparing figures 7 to 9, we do not intend to imply that these are universal curves. In fact, cloudiness varies significantly with both latitude and season. These variations may be seen in tables IV and V as well as in the figures presented with the following discussion.

Variations with latitude and season of the average percentage of time in clouds ($\overline{TIC}$) are presented in figure 10 for the three primary altitude ranges. Some of the variability in figures 10(a), 10(b), and 10(d) can be explained by seasonal variations of the mean height of the tropopause. Other features may be related to the global circulation or semipermanent circulation features (i.e., highs and lows), as discussed below.

Relation to Global Circulation Features

The general seasonal differences in maxima and minima in cloudiness are explained by the seasonal migration of the Intertropical Convergence Zone (ITCZ) and other general circulation features. The region of maximum cloudiness ranges between approximately 18°N in NH summer and 18°S in NH winter. The Hadley cell circulation to the north and south of the ITCZ shifts with the Zone resulting, for the Northern Hemisphere, in maximum descending motions (minimum cloudiness) near 35°N in summer and 15°N in winter. Thus, during winter (fig. 10(a)), the depressed values of cloud-encounter frequency in the 10°N to 20°N interval and enhanced values south of 10°N are consistent with the zonal mean Hadley circulation, which has its axis near 10°N with descending motions to the north and ascending motions to the south of the axis (ref. 38). Meteorologists will recognize that the following additional specific features are consistent with the mean global circulation:

1. The peak in mean cloudiness generally occurs near the subsolar latitude (Sun overhead at noon), lagging it by a few degrees. In the NH winter, the peak occurs near 15°S, in spring and autumn near the Equator, and in summer near 15°N. Some evidence of seasonal symmetry between hemispheres is shown in figure 11; this is not unexpected.

2. A secondary maximum, located between 40°N and 60°N, is noted in all the curves of figure 10. This is the result of the increased frequency of cyclone encounter along the Northern Hemisphere polar front. The effect is largest in winter, as would be expected because the maximum intensity of the mid-latitude baroclinic storm systems occurs then. Indeed, for the winter seasons of both hemispheres, the secondary and primary maxima are of nearly the same magnitude. Because of the lack of airline routes at high latitudes in the Southern Hemisphere, no comparable relative maximum appears in the figures; nevertheless, one related to the Southern Hemisphere polar front might be expected from symmetry considerations and is hinted at in figure 11.

3. When the minima of cloud encounter are studied, we see that a latitudinal displacement also occurs during the year, with the latitude of the minimum point preceding the poleward or equatorward movement of the subpolar point. In winter, this feature is farthest south, at about 15°N. In spring, the point moves to 30°N; in summer, it reaches 35°N; then in autumn, it retreats to 25°N again. The data for the Southern Hemisphere, although limited in latitudinal extent, suggest a relative minimum near 35°S in winter (Southern Hemisphere summer) and a minimum near 15°S to 25°S for the other seasons. The minima for each hemisphere, season and height combination all have values in a narrow range from 1 to 5 percent.

Figure 12 presents the average percentage of time in clouds ($\overline{TIC}$) as a function of latitude and distance from the tropopause for each season. The following conclusions can be made:

1. The primary maximum of $\overline{TIC}$ is located near the Equator, 10 to 15 kft below the tropopause. This peak corresponds to a $\overline{TIC}$ of about 20 percent except in winter when it reaches nearly 50 percent. There are very few data from altitudes above this distance interval because the tropical tropopause usually exceeds 50 kft in altitude.

2. In general, $\overline{TIC}$ decreases as the distance to the tropopause decreases. The primary exceptions to this pattern occur in spring and autumn when, in mid-latitudes, cloudiness tends to peak in the 5 to 10 kft interval below the tropopause.

The preceding results are consistent with the observations of Project Jet Stream and others (refs. 39 to 44), which showed a maximum occurrence of cirrus clouds from 3.3 to 6.6 kft below the tropopause at temperate latitudes. For tropical regions, it was reported in reference 45 that cirrus clouds are consistently 5 km (about 16 kft) or more below the tropopause, but that clouds occasionally are found above the tropopause in very high latitudes.

Variations with season of the vertical profile of cloud-encounter probability and the average time in clouds for data from 40°N to 50°N are shown in figure 13. The probability of cloud encounter (PCE) decreases with altitude in winter, spring, and autumn, but in summer there is a peak between 33.5 and 38.5 kft. This latter feature may result from cirrus clouds blown off the tops of summer thunderstorms near the tropopause. The values of TICIV range from 25 to 40 percent for spring, summer, and autumn. In the winter and spring, TICIV increases with altitude while $\overline{TIC}$ decreases, which suggests less haze or subvisible cirrus with increasing altitude. The winter TICIV varies from 48 percent at low altitudes to 66 percent at the highest altitude. These large values may reflect the dense cirrostratus shields of large baroclinic systems most persistent during winter, for example, the semistationary Icelandic and Aleutian low-pressure systems.

Cloudiness and Relative Vorticity

As noted previously in connection with the persistence of cloudiness, cloudiness is often related to large-scale storm systems (a general model is presented in ref. 46). An objective variable often used for separating the two fundamental dynamic regimes, cyclones and anticyclones, is the relative vorticity ζ (ref. 36). Figure 14 shows the cumulative frequency distribution for all data obtained at 0 to 10 kft below the tropopause separated only by the algebraic sign of the relative vorticity (cyclonic flow is positive; anticyclonic flow is negative). The difference between these curves is similar to the difference between the curves for the highest and lowest altitude bands in figure 9(b) and is larger than the difference between the curves for the layers below the tropopause (fig. 8). Therefore this difference is important. Figure 15 presents $\overline{TIC}$ as a function of distance from the tropopause and sign of the relative vorticity for each NH season for the latitude region from 30°N to 70°N. Indeed, the difference in cloudiness between cyclonic and anticyclonic conditions with respect to distance from the tropopause is very apparent on this figure and is consistent with the ozone distributions in cyclones and anticyclones reported in references 4 and 47 and the known negative correlation at these heights between ozone and water vapor. (See ref. 47.) For the LFC application, this result indicates that conditions significantly different from the average of all data can be expected if specific flight routes are likely to encounter more cyclonic than anticyclonic circulation systems, or vice versa.

From figure 15, the following conclusions can be drawn:

1. For winter, $\overline{TIC}$ is substantially larger for negative vorticity than for positive vorticity, particularly near the tropopause. The maximum occurs in the layer immediately below the tropopause. These results appear to contradict meteorological teachings, because most meteorologists are accustomed to associating positive relative vorticity with clouds, which is certainly the case at the Earth's surface. However, because of the vertical structure of the atmosphere and the tilting of the pressure systems with respect to altitude, the opposite tends to be true at aircraft flight altitudes.

2. During summer, $\overline{TIC}$ is nearly constant at 5 percent, independent of the vorticity and distance from the tropopause. This is consistent with the seasonal differences of fewer and weaker cyclones in summer with more clouds, relatively, stemming from convective storms, as discussed in the previous section.

3. The behavior during spring and autumn is appropriate for transition periods between winter and summer.

Figure 16 presents PCE as a function of sign of the relative vorticity, distance from the tropopause, latitude, and season (winter and summer). The following characteristics are observed in this figure:

1. The values of PCE for positive and negative relative vorticity differ most in the winter and at altitudes near the tropopause. As mentioned before, positive vorticity and clouds are correlated in the lower atmosphere and this is consistent with the crossover of the curves at 10 to 15 kft below the tropopause in winter.

2. For negative vorticity (heavy curve), winter values of PCE are much larger than summer values.

3. In winter, the maximum in PCE is at 0 to 5 kft below the tropopause when the relative vorticity is negative and at 10 to 15 kft below the tropopause when the relative vorticity is positive.

4. For both seasons and both signs of relative vorticity, PCE tends to be smaller for latitudes from 30°N to 40°N than for higher latitudes.

Figure 17 presents TICIV as a function of sign of relative vorticity, distance from the tropopause, latitude, and season (winter and summer). The following characteristics are observed in this figure:

1. In winter, TICIV is consistently larger at all altitudes when the relative vorticity is negative. This is consistent with earlier discussions.

2. In winter, the maximum in TICIV occurs 0 to 5 kft below the tropopause.

3. For both signs of relative vorticity, TICIV decreases sharply for altitudes more than 10 kft below the tropopause.

4. There is no distinguishable pattern between TICIV and distance from the tropopause in summer, although the magnitude of TICIV tends to be larger for positive vorticity than for negative vorticity.

Cloudiness, Temperature, and Ozone

Other trace constituents and meteorological variables measured by GASP aircraft during the time of the data analyzed herein (not all constituents were measured at all times) were water vapor, ozone, carbon monoxide, and wind. An in-depth synoptic and statistical analysis of the interrelationship between clouds and these variables is beyond the scope of this study, but considerable insight is available from the distribution of mean values of some of these parameters with respect to the tropopause.

Figure 18 presents the mean air temperature and ozone concentration, in and out of clouds, with respect to the distance from the tropopause. The mean air temperature in the vicinity of clouds is consistently cooler than in clear air, perhaps suggesting that clouds are more likely to form in cool air because less water vapor is required for saturation. However, as was shown in figure 15, clouds tend to occur in areas of anticyclonic vorticity (i.e., in ridges), where there is a pattern of upward vertical motions and where the tropopause is generally higher and colder than in troughs. Thus, cirrus clouds form more readily in ridges, not only because it is colder there but also because the pattern of vertical motions around the underlying cyclones tends to produce upward motions of sufficiently moist air from below.

It is also apparent from figure 18 that concentrations of ozone are consistently smaller in the vicinity of clouds than in clear air.[1] Perhaps the simplest explanation for the strong anticorrelation between cirrus clouds and ozone at commercial aircraft cruise altitudes is that cirrus clouds are associated with moist upward-moving air coming from the ozone-poor troposphere, and clear areas are associated with dry downward-moving air coming from the ozone-rich stratosphere. This explanation is consistent with the vertical motions at the tropopause level expected in baroclinic storms (ref. 46) and with the previous observation that there is less cloudiness in the upper atmosphere and more ozone in a cyclone than in an anticyclone. (See figs. 14 and 15 and refs. 4 and 47.)

Even though the preceding explanation is straightforward, at least three other factors may influence the observed level of correlation between cirrus clouds and ozone:

1. Sampling - The cloud and ozone data are from in situ GASP observations, but the tropopause data have been interpolated in time and space from NMC grid maps (2.5° latitude by 2.5° longitude) which are available only at 12-hour intervals. Thus, some of the high-frequency undulations of the tropopause (e.g., see ref. 48) are probably missed by these maps. This leads to errors in the calculated height of the tropopause.

2. Chemistry - Enhanced chemical and photochemical destruction of ozone may occur in the presence of high relative humidity. As reviewed in reference 49, ozone photochemistry is an area of very active research, and we leave assessment of this possibility to modelers working in the field.

---

[1] It was reported in reference 5 that the concentration of ozone in clear air is significantly different (higher) from that in cloudy air, at the 99.9 percent confidence level.

3. Mechanical destruction - Ozone is a relatively unstable gas and is known to dissociate on contact with a hard surface. The ice crystals and particles in a cloud provide a relatively large surface area for ozone destruction.

PARTICLE-CONCENTRATION ANALYSIS

As stated in the section entitled "Data," GASP cloud-encounter data are available beginning in December 1975, but particle-number-density data (PD5) do not begin until January 1977. Approximately 63 percent of the cloud observation periods have corresponding particle-concentration data. Figure 19 presents the cloudiness variables for only those observation periods having particle-concentration measurements. The similarity between this figure and figure 13, the corresponding figure for all cloud-encounter data, and the marked similarities of figures 5 and 6 to figures 3 and 4, all provide evidence that the particle-concentration data subset is statistically similar to the entire data set.

Concentrations in Clear and Cloudy Air

Figure 20 shows that the particle density PD5($D > 3$ μm) is about three orders of magnitude greater in cloudy air (TIC > 0) than in clear air (TIC = 0). Figure 21 shows the cumulative frequency distributions of all available PD5 data for several TIC values. Among observations in the vicinity of clouds ($0 < \text{TIC} \leq 100$), the probability of encountering any given particle density increases as TIC increases. However, this difference is small compared with the difference between clear and cloudy air shown by the TIC = 0 and the TIC > 0 curves.

Figure 22 presents the cumulative frequency distributions of particle number density for clear and cloudy air with respect to (a) altitude and (b) distance from the tropopause. The differences in these distributions for TIC > 0 and TIC > 75 with respect to altitude are very small, whereas more particles tend to be present in the 0 to 5 kft interval below the tropopause.

Figure 23 presents similar cumulative frequency distributions with respect to (a) latitude and (b) NH season. In the clear air, more particles are present between 0° and 60°N than outside these latitudes, and more particles are present in spring and summer than in winter and autumn. These same relationships also tend to hold for cloudy air, at least for particle concentrations smaller than about 10^4 m^{-3}.

As mentioned in the section entitled "Introduction," the goal of this research is the derivation of the climatology (i.e., the statistical behavior with location, season, altitude, etc.) of the particle number density to be encountered on airline routes worldwide, from which the economic feasibility of employing laminar-flow-control (LFC) wings may be assessed. In this regard, the PD5 data in the current investigation are most valuable when they pertain to flight conditions that are either totally in clear air or totally within clouds. It is crucial to know whether the particle number density in clear air is, on the average, sufficiently high to make LFC impractical as a low-drag method. If such is the case, then the LF loss within clouds is almost certain to be prohibitive. If, however, the loss in clear air is not critical, then cloud encounter is the limiting factor. Therefore, it is important to estimate the portion of the time that clouds will be encountered, as was examined in the section entitled "Cloud-Encounter Analysis." Most estimates to date assume that all clouds always cause LF loss and that LF loss in clear air does not

occur, but one purpose of the present research was to ascertain what subset, if any, of cloud encounters would not cause LF loss and what portion of the time LF would be lost in clear air.

In this study, the PD5 data were examined to derive statistics on particle concentrations to be encountered in clear air and cloudy air. The results are summarized in table VI, which presents a composite of the overall particle-encounter experience as a function of TIC. This table, from which figure 21 was plotted, includes all conditions from totally cloud-free to totally in clouds.

Application of GASP Particle-Concentration Data to LFC Aircraft Studies

The motivation for analyzing the GASP data for cloud-encounter statistics in the format previously discussed is the requirement for obtaining particle-concentration climatological data to be utilized in feasibility studies for new long-range aircraft designs. Such aircraft would use laminar-flow-control (LFC) wings, offering promise of up to a 30-percent drag reduction from that of current wing designs (ref. 7). The particular need of cloud-encounter estimates for this class of aircraft stems from the fact that LF is thought to be lost, albeit temporarily, whenever the aircraft is within clouds or ice-crystal concentrations containing a sufficiently large number density of hydrometeors larger than about 30 μm in equivalent melted diameter (EMD). (See ref. 15 for definition of EMD.) Experience with the USAF X-21, an early LFC-winged research aircraft, seemed to show (refs. 8 and 10) that LF was always lost in visible clouds and sometimes within cirrus hazes. Motivated by the X-21 experience, Hall (ref. 10) derived, from aerodynamic considerations, the range of ice-particle fluxes which should cause significant loss of LF. Figure 24 is adapted from the Hall analysis and is presented as an example of the estimated LF degradation. Particle concentration (m^{-3}) is plotted on the ordinate, against the equivalent melted diameter of the particles. From this figure, the following observations may be made:

1. No loss of LF is expected to result from particles with EMD smaller than 33 μm, regardless of their concentration, or from total particle concentrations smaller than $3.5 \times 10^2/m^3$, regardless of particle size.

2. Total loss of LF is expected if the concentration of particles with EMD equal to or larger than 33 μm is greater than or equal to 1.9×10^5 particles/m^3 (or, e.g., if the concentration of particles larger than 60 μm is greater than or equal to $1.3 \times 10^5/m^3$). Similar conclusions can be reached in this manner for other particle sizes.

3. Between no loss and total loss of LF, partial loss is expected (e.g., if the number density of particles with EMD equal to or larger than 33 μm is greater than $8.0 \times 10^2/m^3$ but less than $1.4 \times 10^5/m^3$. The threshold of LF loss was 10 percent in the Hall analysis. This threshold is represented by the lower boundary of the region labeled "Partial loss of LF" in figure 24.

The task at hand, then, is to utilize GASP data for deriving or estimating the probability that particle number densities sufficient to cause LF loss will be encountered in day-to-day operations. To estimate the probability and severity of LF loss in the presence of particles, not only the probability of cloud encounter must

be known, but also the particle number distribution within clouds and in clear air. All the elements of the problem are represented in the following equation:

$$P(\text{LFC loss}) = \left[P(\text{LFC loss})\big|_{\text{Cloudy}}\right]\left[P(\text{Flight in clouds})\right] + \left[P(\text{LFC loss})\big|_{\text{Clear}}\right]\left[P(\text{Flight in clear air})\right] \quad (2)$$

From the GASP cloud-encounter data presented earlier, the probability of flight both in and out of clouds can be estimated. The probabilities of LF degradation in and out of clouds are, however, not directly accessible from the GASP data analyzed herein, since these provide only the total number density of particles with EMDs larger than 3 μm. However, empirical particle-distribution data are available from missions carrying Knollenberg-probe-type instrumentation. The investigations of the U.S. Air Force Geophysics Laboratory (AFGL) are particularly valuable sources of these data (refs. 15, 16, and 50 to 56). These AFGL data were studied to determine the variability of the ratio of the number of particles larger than 3 μm to the number of particles larger than 33 μm. This ratio is best visualized as the ratio of the two hatched areas shown on figure 25, presented to show the concept. This ratio depends on the type of cloud encountered and ranges from about 10 for thick clouds to about 100 or more for very thin cirrus clouds (numerous very small crystals) and has a modal value of around 30. In practical usage, then, the number of particles larger than the LFC-critical size (EMD of 33 μm) could be estimated by dividing the number of particles in a GASP PD5 observation by the appropriate ratio. To provide a conservative estimate of LF loss, a worst case ratio in clouds is taken to be 10 and a worst case ratio in clear air is taken to be 100. Here "worst case" signifies the greatest upper bound for the concentration of LFC-critical particle sizes - hence, the greatest probability of LF loss.

With these assumptions, the Hall criteria in figure 24 and the PD5 analyses in the section entitled "Particle-Concentration Analysis" can be related to estimate the degree of LF loss to be expected, in both totally clear air and totally cloudy air. First, we recall from figure 24 that the LFC-critical density of particles larger than 33 μm in diameter is $8.0 \times 10^2/m^3$. Multiplying this density by the clear air ratio of 100, the critical density of particles larger than 3 μm in diameter would be $8 \times 10^4/m^3$. From figure 21 and table VI, we find that this particle density was never encountered in clear air. Therefore, the assumption that no LF loss occurs in truly clear air seems appropriate.

The assumption of no LF loss in clear air does not totally agree with data taken during the X-21 program, in which some LF loss evidently occurred in very light haze (refs. 8 and 10). However, no particle-concentration measurements were taken in conjunction with the X-21 missions, so the particle concentrations in the haze were unknown, and unfortunately cannot be used to refine the assumption of no loss in clear air. It is reported in references 57 and 58 that local concentrations of large particles, resulting from particle fallout into the clear air, may be encountered beneath cirrus cloud decks during flight in otherwise clear air. The observations in reference 57, and calculations in reference 58, show that these particles can survive falls of several kilometers. However, we believe that the concentrations of these particles will generally be too low to degrade LF, although the particles are large enough to cause a problem, if encountered in sufficient concentration.

In clouds, the critical number densities of particles with EMD > 3 μm are obtained by multiplying the worst case ratio (10) by the critical densities of particles with EMD > 33 μm: for 10-percent LF loss, $(8 \times 10^2/m^2)(10)$; for total loss, $(1.9 \times 10^5/m^2)(10)$. The curves for TIC ⩾ 75 in figure 21 suggest that the critical number density for a 10-percent LF loss, $8 \times 10^3/m^3$, would be exceeded 100 percent of the time. Total loss of LF(PD5 = $1.9 \times 10^6/m^3$) would be expected approximately 5 percent of the time. Thus, a significant degree of LF loss within clouds is obviously predicted, and the previously stated assumption that encounters with visible clouds always result in a loss of LF seems valid until further observations are obtained of LF degradation in clouds, with modern cloud-particle-sampling instrumentation. Such observations are planned for the near future in a NASA experiment (ref. 19), in which the Hall criteria can be validated for the first time. In that experiment, a Knollenberg probe particle sampler (ref. 59) will be flown aboard a NASA JetStar aircraft modified with LFC wing sections, to measure the particle environment simultaneously with the assessment of LFC system performance. The results of the experiment should allow validation of the assumption of no LF loss in clear air and a new determination of the level of LF degradation in a variety of cloud conditions. Pending these revised estimates of LF loss, no loss of LF in clear air and total loss of LF in all clouds are assumed; thus, the analysis in the next section will be centered around the GASP cloud-encounter data.

APPLICATION OF GASP CLOUD-ENCOUNTER DATA TO AIRLINE ROUTE STUDIES

In this section, the GASP cloud-encounter data are applied to the estimation of cloud-encounter statistics for airline application. First, the overall cloud-encounter variability is summarized in tables and discussed from the viewpoint of statistical significance. Then, an empirical statistical model for the route-averaged time in clouds is developed. This model is applied to seven high-density airline routes, and the implications for the economic feasibility of LFC transports are discussed.

Overall Results

Tables VII, VIII, and IX present statistics derived from cloud observation periods. Recall that each cloud observation period lasts only 256 sec, or approximately 36 n.mi. at a ground speed of 500 knots. It is important to realize that such statistics are derived from these 256-sec intervals and are only estimates of the cloud-detection probability over other time intervals or distances. It is shown in appendix C (Vol. II) that successive observations are not really statistically independent until about 20 intervening observations have elapsed. With these considerations firmly in mind, tables VII, VIII, and IX are still useful in studying the relative probability of cloud encounter as a function of altitude, NH season, and geographic location; this probability is of use in determining the feasibility of LFC flight.

Table VII presents a composite of TIC statistics as a function of altitude for the global data set (i.e., all seasons and latitudes) and represents an elaboration of the data plotted in figure 9(b). The benefits of higher cruise altitude for cloud avoidance are readily apparent from the table. For example, an aircraft cruising at 28.5 to 33.5 kft would be expected to fly through a 256-second time interval totally clear of clouds 78.8 percent of the time and to encounter clouds during that interval (TIC > 0) 21.2 percent of the time. There is a 16-percent probability of being in

clouds for more than 10 percent of the interval (25.6 sec) and an 8-percent probability of being in clouds half or more of the interval (128 sec). There is only a 1.6-percent probability that more than 90 percent of the interval would be cloudy. By cruising at a higher altitude, 33.5 to 38.5 kft, however, the probability of encountering clouds in any 256-sec interval is reduced from 21.2 to 15.8 percent. In the cruise altitude range from 38.5 to 43.5 kft, representing the upper range of current transport aircraft, the probability of cloud encounter in each 256-sec interval is reduced still further to 8.5 percent. Above 43.5 kft, there is virtually no probability of encountering clouds.

Results Analyzed With Respect to Altitude

The values just presented in table VII are useful for estimating the relative cloud-encounter frequency on a worldwide basis, but for the operations of most airlines, statistics for more limited geographic regions are of more practical interest. For this reason, the data of table VIII were extracted from appendix D (Vol. II). For table VIII, only the average value of TIC ($\overline{TIC}$) the probability of cloud encounter (PCE, numerically equal to P(TIC > 0) in appendix D), and the number of independent observation periods making up the sample in each cell of the latitude-season-altitude grid are presented. These parameters were chosen from all those in appendix D because they are of most direct usefulness in assessing the relative magnitudes of cloud-encounter frequencies.

The data in table VIII are presented for 10° latitude zones between 40°S and 80°N, and for the three primary altitude bands analyzed in this report, denoted for convenience as follows:

Band A1: 28.5 to 33.5 kft

Band A2: 33.5 to 38.5 kft

Band A3: 38.5 to 43.5 kft

The data are further subdivided by NH season. It is immediately apparent that most data were obtained between 30°N and 60°N latitude. For completeness, data are presented for every latitude zone having observations; blanks indicate that no data were taken in a zone. The reader is strongly cautioned that the statistics within zones having fewer than 30 independent samples may not be representative of population values.

Latitude zone from 30°N to 60°N.- Most confidence may be placed in the variability of data in table VIII occurring within the 30°N to 60°N latitude band. This variability was further tested for statistical significance, using the analysis of variance (ANOVA) technique (ref. 60) as implemented through a well-proven software package (ref. 61). The following general conclusions were reached for the 30°N to 60°N latitude region:

1. The average value of TIC ranges from 0 percent, for altitude band A3, to 13.7 percent, for band A1. The respective probability of cloud encounter, PCE, ranges from 0 to 32.4 percent.

2. In comparing the $\overline{TIC}$ statistics from different altitude bands by the ANOVA technique, we note that the $\overline{TIC}$ value in band A3 (highest altitude band) is significantly lower (thus affording a smaller chance of losing LF) than the values in

bands A1 and A2, and that the $\overline{TIC}$ value in band A2 is probably significantly lower than that in band A1. Thus, in this latitude region, an increase in altitude provides a significantly lower probability of cloud encounter. (In this report, an event is termed "significant" if it could have occurred by random chance 1 percent or less of the time. It is termed "probably significant" if it could have occurred no more than 5 percent of the time by chance. Events occurring more than 5 percent of the time by random chance were considered not statistically significant.)

3. With all seasons and altitudes considered together, the average time in clouds ($\overline{TIC}$) varies significantly with altitude, season, and latitude, and the probability of cloud encounter (PCE) varies significantly with altitude and latitude, but not with season.

4. When only spring and summer are compared, $\overline{TIC}$ variability with altitude and latitude is probably significant, but variability with season is not significant. For PCE, only altitude is probably significant, but latitude and season are not significant.

5. When autumn and winter are compared, $\overline{TIC}$ variability with season and altitude is significant and variability with latitude is probably significant. For PCE, season is still not significant, but altitude is significant, and latitude is probably significant.

6. From items 4 and 5 above, we conclude that the greatest variability occurs in winter. This is consistent with meteorological experience, which tells us that there is both more latitudinal and altitudinal variability in the winter than in the other seasons.

7. Comparing altitude bands A1 and A2, over all seasons, we note significant variability with season and latitude, and probably significant variability with altitude for $\overline{TIC}$. For PCE, only the variability with altitude is significant, at the 95 percent level.

8. Comparing altitude bands A2 and A3 over all seasons, we note significant variability with latitude and altitude, but no significant seasonal difference. For PCE, season is not significant, but altitude and latitude are significant.

9. To summarize items 1 to 8 above, altitude is always important, latitude is of less importance, and season of least importance to the variability of $\overline{TIC}$ and PCE.

Other latitude zones.- With the cautions imposed by small sample size firmly in mind, we conclude that the following trends seem to be present in table VIII for the other latitude bands:

1. For regions poleward of 20° latitude in both the Northern and Southern Hemispheres, the superiority of altitude band A3 for cloud avoidance becomes more evident the more poleward one goes.

2. For the tropical region, 20°N to 20°S, altitude band A3 is no longer obviously better for cloud avoidance than bands A1 and A2; in fact, band A2 is probably the best, overall. Values for $\overline{TIC}$ of 10 percent and PCE of 30 percent are good representative values for this region and band. The tropopause is at its highest in the tropics, at 50 to 55 kft, so that even band A3 is still well below the tropopause and within the convective region of the atmosphere; it is thus subject to cloud

occurrence and vertical development. The fact that the highest values of $\overline{TIC}$ and PCE in the tropical region both occur in band A3 is consistent with the results of other research (ref. 45) showing cirrus consistently occurring 5 km or more beneath the tropical tropopause - exactly within band A3. Thus, for the tropical region, no strongly favored altitude band for minimum cloud encounter exists, and we recommend that a $\overline{TIC}$ of at least 10 percent and a PCE of 30 percent be assumed for planning purposes.

Results Analyzed With Respect to Distance From the Tropopause

A companion analysis to that for table VIII was performed, in which the data were analyzed with respect to distance from the tropopause rather than altitude. For convenience, the four tropopause separation bands are denoted as follows:

Band T1: 10 to 15 kft below the tropopause

Band T2: 5 to 10 kft below the tropopause

Band T3: 0 to 5 kft below the tropopause

Band T4: 0 to 5 kft above the tropopause

As before, the data were analyzed by 10° latitude zones and by NH season, and the parameters presented are again $\overline{TIC}$, PCE, and the number of independent observations. The results are presented in table IX. These data were extracted from appendix E (Vol. II). However, much of the variance that occurs with respect to season and latitude is contained in the single variable "distance from the tropopause." Therefore, the ANOVA technique used in the previous section could not be used to provide meaningful results for the data stratified by separation from the tropopause. An ANOVA of these data would give statistically confounded results. Nevertheless, from an inspection of table IX, the following conclusions appear reasonable without further statistical confirmation:

Latitude zone from 30°N to 60°N.- The following tentative conclusions can be made for latitudes from 30°N to 60°N:

1. Band T4 (the uppermost) seems to have markedly lower values of $\overline{TIC}$ and PCE than the other bands. The textbook maxim that clouds do not often exist at altitudes above the tropopause is again proven here.

2. The values in the two lowest bands, T1 and T2, do not appear markedly different. But cloud encounter appears less probable for band T3 than for bands T1 and T2.

Other latitude zones.- For the three latitude zones from 20°N to 30°N, from 20°S to 40°S, and from 60°N to 80°N, there are generally too few observations to make reliable conclusions, but conclusions 1 and 2 above seem to be borne out.

For the tropical region 20°N to 20°S, all data, as noted previously for the altitude data, were obtained well below the tropical tropopause; in most cases, band T1 was the only one having data. Therefore, no comparisons were possible; any comparison in this latitude zone must be made on altitude data (table VIII).

Results Derived Directly From Route Statistics

Although the data in tables VIII and IX are helpful in estimating the cloud-encounter variability with altitude, season, and latitude zone, further longitudinal detail, imposed by geographic and seasonal climatological differences, is needed to derive the variability pertinent to various city or regional pairs. Examples of implicit climatological effects would include jet streams with their associated cloud patterns, the presence of semipermanent synoptic features such as the Aleutian and Icelandic lows, and monsoon cloud patterns in connection with the Indian subcontinent. No attempt was made to model the effect of these features directly, but they and others undoubtedly influence the statistics for the various city pairs in ways that are not apparent in the zonal mean values. Also it is important to realize that the statistics used in these tables pertain to the ensemble behavior of 256-sec observation periods within each cell in a latitude-longitude-season-altitude grid. In earlier reports, the gridded data were used directly in a first attempt to provide an estimate of cloud-encounter statistics along several routes and altitudes (refs. 5, 6, and 17). However, because weather systems have appreciable horizontal extent, a high or low pressure system can cover several cells, so, as discussed in appendix C, the data from adjacent cells are not independent. Thus, there are problems in using cell statistics to estimate the probability of encountering a given average amount of cloudiness along an airline route that traverses one or more cells - the estimate that is needed in assessing the feasibility of employing LFC on airline routes. For all these reasons, another approach was sought.

Empirical Model

A more direct approach is to compute the cloud-encounter statistics for routes of interest by studying the frequency distribution of route-averaged time-in-cloud values for all flights on a given route. A model based on this approach was developed as follows:

1. The ensemble of flights between each city pair (e.g., JFK-LHR) was extracted from appendix B and each flight placed into one of three primary altitude bands (28.5 to 33.5 kft, 33.5 to 38.5 kft, and 38.5 to 43.5 kft) according to the average altitude during the entire flight.

2. For each flight, the value of %TIC was obtained from appendix B. This value will be denoted TIC_F and is the average percentage of time in clouds along the route for <u>that</u> flight.

3. Frequency distributions of TIC_F were prepared for each route and altitude band. An average value of TIC_F for the route, TIC_R, was then computed by averaging all the values of TIC_F from all flights along the route.

4. For each route where a relatively large number of flights (i.e., more than 30) were in the sample, the frequency distribution of TIC_F was plotted and its character studied. This study disclosed that for all routes the most frequent TIC_F value was 0 (i.e., flight in clear air at these altitudes is the most frequent experience), that a TIC_F value of 100 percent was never obtained, and that the frequency of TIC_F values usually decreased monotonically as TIC_F increased. This behavior suggested

that the observations for each route could perhaps be modeled by either a negative exponential probability density function,

$$f(t) = \exp(-t) \tag{3}$$

where $t = TIC_F/\overline{TIC}_F = TIC_F/TIC_R$, $TIC_R > 0$ percent, and $TIC_F \leq 100$ percent; or by a gamma probability density function,

$$f(t') = \exp(-t')(t')^{\eta-1}/\Gamma(\eta) \tag{4}$$

where $t' = 0.7TIC_F/TIC_R$ and $\eta = 0.7$. Further study showed that, while the simple negative exponential probability density function (eq. (3)) modeled several of the distributions well (ref. 23), the gamma probability density function (eq. (4)) gave a better fit, overall, to all of the distributions studied. As an example, figure 26 shows histogram frequency plots of TIC_F for the route between the East Coast of the United States and Northwest Europe. A plot for the 99 flights with an average cruise altitude of 33.5 to 38.5 kft is shown in figure 26(a), and figure 26(b) shows a plot for the 38 flights with an average cruise altitude of 28.5 to 33.5 kft. On each figure, both the observed frequency and the frequency from the gamma probability density function are shown. The apparent agreement of observed and modeled plots on each figure was verified by chi-squared goodness-of-fit testing at the 95-percent confidence level. Similar good agreement was obtained in other cases as well. Therefore, equation (4) was used to model the distribution of time in clouds for all cases, using the sample value $t' = 0.7TIC_F/TIC_R$ appropriate to each route and altitude combination. The probability of encountering a value of TIC_F that equals or exceeds a value X is found by integrating equation (4).

$$P(TIC_F \geq X) = P(t' \geq 0.7X/TIC_R) = \int_{0.7X/TIC_R}^{\infty} f(t')\,dt' \tag{5}$$

The integral does not exist in closed form and so must be computed by numerical methods.

This model was applied to seven high-density routes. For each route and altitude band, the following parameters are given in table X: the number of flights actually in the sample; TIC_R, the sample route-averaged percentage time in clouds at that altitude; $P(TIC_F < 1\%)$ and $P(TIC_F < 5\%)$, the probabilities that the average time in clouds will be below 1 and 5 percent; $P(TIC_F \geq 5\%)$, $P(TIC_F \geq 10\%)$, $P(TIC_F \geq 25\%)$, and $P(TIC_F \geq 50\%)$, and the probabilities that the average time in clouds will equal or exceed 5, 10, 25, and 50 percent. All probabilities are expressed as percentages. Conclusions reached from studying table X are as follows:

1. For all routes except Australia to SE Asia, TIC_R, $P(TIC_F \geq 5\%)$, $P(TIC_F \geq 10\%)$, $P(TIC_F \geq 25\%)$, and $P(TIC_F \geq 50\%)$ all generally decrease with

altitude. For Australia and SE Asia and other subtropical routes, the tropopause lies well above the aircraft cruise altitude, and TIC increases with height, as remarked earlier.

2. The abnormally low value of TIC_R for 33.5 to 38.5 kft on the West Coast-to-NW Europe route reflects the low tropopause height at the high latitudes traversed on this route.

3. There is a statistically significant difference in TIC_R values between flights from the West Coast to Japan and those in the opposite direction. These flights are routed to take into account the strong west-to-east North Pacific Jet Stream; the higher TIC_R on the west-to-east route, where the Jet Stream is utilized for a tail wind, probably reflects the increased cloudiness from the cirrus shield which typically accompanies the Jet Stream.

4. For the routes and altitudes in the table, the probability of encountering clouds on more than 10 percent of a route is less than 35 percent. The probability of encountering clouds on more than 25 percent of a route is less than 10 percent, and the probability of encountering clouds on more than 50 percent of a route is less than 2 percent.

5. The above conclusions are consistent with an earlier estimate (ref. 8) that cirrus clouds exist no more than 6 percent of the time at LFC transport cruise altitudes.

EFFECT OF CLOUDS ON LFC

The impact of the above results on the feasibility of LFC for long-range transports may be estimated as follows. If it is assumed that LFC is totally lost within clouds and that it is totally effective outside of clouds, then the fractional effectiveness of LFC on a route is equal to the fraction of the route that is flown in clear air. It is estimated (ref. 7) that use of LFC will result in a 30-percent drag reduction outside of clouds. Therefore, the net drag reduction over a route will range from the full 30 percent, when no clouds are encountered on the route, to 0 percent, when the route lies totally within clouds. By this reasoning, for example, on a route that is 25-percent cloud covered, the net effectiveness of LFC is decreased to 75 percent of 30 percent, or 22.5 percent. On a route that is 50-percent cloud covered, LFC effectiveness is reduced by half, to 15 percent. Combining these results with the probability of cloud encounter for the routes and altitudes in table X (see item 4 above), we estimate that the probability of losing 10 percent or more of LFC effectiveness is less than 35 percent. Similarly, the probability of losing 25 percent or more of LFC effectiveness is less than 10 percent, and the probability of losing at least 50 percent of LFC is less than 2 percent. Therefore, we conclude for these routes and altitudes that the probability of encountering extensive cloud cover on long routes is not large enough, of itself, to make LFC impractical.

CONCLUSIONS

The motivation for the study reported herein is the need for estimates of the probability of cloud encounter and of the ice-particle size distribution and number density, both in and out of clouds, existing at airliner cruise altitudes in the

range from 25.0 kft to 45.0 kft (7.62 to 13.72 km). These estimates are needed for application to design of aircraft employing laminar flow control (LFC) to reduce drag. Accordingly, summary statistics, tabulations, and variability studies have been derived and presented for cloud-encounter data and particle-concentration data taken as part of the National Aeronautics and Space Administration (NASA) Global Atmospheric Sampling Program (GASP) aboard commercial airliners. The GASP data analyzed herein were from December 1975 to July 1979, and represent all of the cloud- and concurrent particle-encounter data obtained during the program.

From this GASP archive, nearly 88 000 cloud observation periods, each of 256-sec duration (horizontal distance of approximately 36 n.mi. (66 km) at a ground speed of 500 knots) were available. On the average, cloud encounters were shown on about 15 percent of these data samples. However, this value was found to vary significantly with altitude, latitude, and distance from the tropopause, and less significantly with season.

Several meteorological circulation features, such as the Intertropical Convergence Zone, are apparent in the latitudinal distribution of cloudiness as derived from the GASP data.

The probability of encountering clouds varies with synoptic weather systems. In agreement with classical storm models, the present data show relatively more cloudiness in the upper troposphere in anticyclones (negative vorticity) than in cyclones (positive vorticity). Marked differences in cloudiness between anticyclonic and cyclonic conditions with respect to the distance from the tropopause were found.

Observations of clouds spaced more closely than 90 minutes are shown to be statistically dependent.

The number densities of particles with diameters larger than 3 μm were also sampled over a shorter time period beginning in January 1977; 70 304 total observations made up this set; 55 718 particle-concentration observation periods, coincident with cloud observation periods, were analyzed. The particle-concentration data have nearly the same latitudinal distribution as the cloud-detector data, but relatively more observations in summer, fewer in spring, and more at higher altitudes. About 13 percent of the particle data were gathered in clouds or in the vicinity of clouds. Because of the application to laminar flow control (LFC) aircraft, attention was focused on the concentration of the larger particles (those larger than 3 μm). It was found that the number density of such particles also varies with season and location and is closely related to the horizontal extent of cloudiness.

The summary statistics for cloud encounter show that the probability of LFC loss in clear air is negligible, but that a significant degree of LF loss is always to be expected in clouds.

The observations of route-averaged time in cloud are found to fit a gamma probability density function model, which can be used to estimate the probability of extended cloud encounter along a route.

From study of seven high-density airline routes with the above model, it is shown that the probability of extended cloud encounter and significant loss of LFC effectiveness should be too low, of itself, to make LFC impractical for commercial use.

The data show that in temperate latitudes, the uppermost altitude band studied (38.5 to 43.5 kft) has the most promise for cloud avoidance. For equatorial regions, no band studied has a clear superiority; it is recommended that route-averaged time-in-clouds value of 10 percent be employed in simulations for these regions.

Langley Research Center
National Aeronautics and Space Administration
Hampton, VA 23665
July 31, 1984

REFERENCES

1. Perkins, Porter; and Gustafsson, Ulf R. C.: An Automated Atmospheric Sampling System Operating on 747 Airliners. NASA TM X-71790, 1975.

2. Gauntner, Daniel J.; Holdeman, J. D.; Briehl, Daniel; and Humenik, Francis M.: Description and Review of Global Measurements of Atmospheric Species From GASP. NASA TM-73781, 1977.

3. Perkins, Porter J.; and Papathakos, Leonidas C.: Global Sensing of Gaseous and Aerosol Trace Species Using Automated Instrumentation on 747 Airliners. NASA TM-73810, 1977.

4. Nastrom, Gregory D.; Holdeman, J. D.; and Davis, R. E.: Cloud Encounter and Particle Density Variabilities From GASP Data. AIAA-81-0308, Jan. 1981.

5. Nastrom, Gregory D.; Holdeman, James D.; and Davis, Richard E.: Cloud Encounter and Particle-Concentration Variabilities From GASP Data. NASA TP-1886, 1981.

6. Nastrom, G. D.; Holdeman, J. D.; and Davis, R. E.: Cloud Encounter and Particle Number Density Variabilities From GASP Data. J. Aircr., vol. 19, no. 4, Apr. 1982, pp. 272-277.

7. Braslow, Albert L.; and Muraca, Ralph J.: A Perspective of Laminar-Flow Control. AIAA Paper 78-1528, Aug. 1978.

8. Whites, R. C.; Sudderth, R. W.; and Wheldon, W. G.: Laminar Flow Control on the X-21. Astronaut. & Aeronaut., vol. 4, no. 7, July 1966, pp. 38-43.

9. Wagner, Richard D.; and Fischer, Michael C.: Developments in the NASA Transport Aircraft Laminar Flow Program. AIAA-83-0090, Jan. 1983.

10. Hall, G. R.: On the Mechanics of Transition Produced by Particles Passing Through an Initially Laminar Boundary Layer and the Estimated Effect on the LFC Performance of the X-21 Aircraft. Northrop Corp., Oct. 1964.

11. Conover, John H.; and Bunting, James T.: Estimates From Satellites of Weather Erosion Parameters for Reentry Systems. AFGL-TR-77-0260, U.S. Air Force, Nov. 29, 1977. (Available from DTIC as AD A053 654.)

12. Barnes, Arnold A., Jr.: New Cloud Physics Instrumentation Requirements. AFGL-TR-78-0093, U.S. Air Force, Apr. 17, 1978. (Available from DTIC as AD A053 235.)

13. Dyer, Rosemary M.; and Barnes, Arnold A., Jr.: The Microphysics of Ice Clouds - A Survey. AFGL-TR-79-0103, U.S. Air Force, May 8, 1979. (Available from DTIC as AD A077 020.)

14. Hallett, John: Characteristics of Atmospheric Ice Particles: A Survey of Techniques. AFGL-TR-80-0308, U.S. Air Force, Sept. 1980. (Available from DTIC as AD A093 927.)

15. Varley, D. J.: Cirrus Particle Distribution Study, Part 1. AFGL-TR-78-0192, U.S. Air Force, Aug. 7, 1978. (Available from DTIC as AD A061 485.)

16. Cohen, Ian D.: Cirrus Particle Distribution Study, Part 8. AFGL-TR-81-0316, U.S. Air Force, Oct. 28, 1981. (Available from DTIC as AD A118 715.)

17. Davis, Richard E.: Probability of Laminar Flow Loss Because of Ice Crystal Encounters. Laminar Flow Control - 1981 Research and Technology Studies, Dal V. Maddalon, ed., NASA CP-2218, 1982, pp. 75-93.

18. Fischer, M. C.; Wright, A. S., Jr.; and Wagner, R. D.: A Flight Test of Laminar Flow Control Leading-Edge Systems. AIAA-83-2508, Oct. 1983.

19. Davis, Richard E.; and Fischer, Michael C.: Cloud Particle Effects on Laminar Flow, and Instrumentation for Their Measurement Aboard a NASA LFC Aircraft. AIAA-83-2734, Nov. 1983.

20. Platt, C. M. R.: Remote Sounding of High Clouds: I. Calculation of Visible and Infrared Optical Properties From Lidar and Radiometer Measurements. J. Appl. Meteorol., vol. 18, no. 9, Sept. 1979, pp. 1130-1143.

21. Schneider, Stephen H.: Cloudiness as a Global Climatic Feedback Mechanism: The Effects on the Radiation Balance and Surface Temperature of Variations in Cloudiness. J. Atmos. Sci., vol. 29, no. 8, Nov. 1972, pp. 1413-1422.

22. Cess, Robert D.: Climate Change: An Appraisal of Atmospheric Feedback Mechanisms Employing Zonal Climatology. J. Atmos. Sci., vol. 33, no. 10, Oct. 1976, pp. 1831-1843.

23. Jasperson, W. H.; Nastrom, G. D.; Davis, R. E.; and Holdeman, J. D.: Cloud Encounter Statistics in the 28.5-43.5 KFT Altitude Region From Four Years of GASP Observations. Ninth Conference on Aerospace and Aeronautical Meteorology, American Meteorological Soc., 1983, pp. 159-164.

24. Holdeman, J. D.; Humenik, F. M.; and Lezberg, E. A.: NASA Global Atmospheric Sampling Program (GASP) Data Report for Tape VL0004. NASA TM X-73574, 1976.

25. Holdeman, J. D.; and Humenik, F. M.: NASA Global Atmospheric Sampling Program (GASP) Data Report for Tape VL0005. NASA TM X-73608, 1977.

26. Gauntner, Daniel J.; Holdeman, J. D.; and Humenik, Francis M.: NASA Global Atmospheric Sampling Program (GASP) Data Report for Tape VL0006. NASA TM-73727, 1977.

27. Holdeman, J. D.; Gauntner, Daniel J.; Humenik, Francis M.; and Briehl, Daniel: NASA Global Atmospheric Sampling Program (GASP) Data Report for Tapes VL0007 & VL0008. NASA TM-73784, 1977.

28. Holdeman, J. D.; Dudzinski, Thomas J.; Nyland, Ted W.; and Tiefermann, Marvin W.: NASA Global Atmospheric Sampling Program (GASP) Data Report for Tape VL0009. NASA TM-79058, 1978.

29. Holdeman, J. D.; Dudzinski, Thomas J.; Tiefermann, Marvin W.; and Nyland, Ted W.: NASA Global Atmospheric Sampling Program (GASP) Data Report for Tapes VL0010 & VL0012. NASA TM-79061, 1979.

30. Holdeman, J. D.; Dudzinski, Thomas J.; and Tiefermann, Marvin W.: NASA Global Atmospheric Sampling Program (GASP) Data Report for Tapes VL0011 and VL0013. NASA TM-81462, 1980.

31. Briehl, Daniel; Dudzinski, Thomas J.; and Liu, David C.: NASA Global Atmospheric Sampling Program (GASP) Data Report for Tape VL0014. NASA TM-81579, 1980.

32. Papathakos, Leonidas C.; and Briehl, Daniel: NASA Global Atmospheric Sampling Program (GASP) Data Report for Tape VL0015, VL0016, VL0017, VL0018, VL0019, and VL0020. NASA TM-81661, 1981.

33. Liu, Benjamin Y. H.; Berglund, Richard N.; and Agarwal, Jugal K.: Experimental Studies of Optical Particle Counters. Atmos. Environ., vol. 8, no. 7, July 1974, pp. 717-732.

34. Reck, Gregory M.; Briehl, Daniel; and Nyland, Ted W.: In Situ Measurements of Arctic Atmospheric Trace Constituents From an Aircaft. NASA TN D-8491, 1977.

35. Nastrom, G. D.: Variability and Transport of Ozone at the Tropopause From the First Year of GASP Data. NASA CR-135176, 1977.

36. Huschke, Ralph E., ed.: Glossary of Meteorology. American Meteorol. Soc., 1959.

37. Crutcher, H. L.; and Davis, O. M.: U.S. Navy Marine Climatic Atlas of the World. Volume VIII - The World. NAVAIR 50-1C-54, U.S. Navy, Mar. 1, 1969.

38. Newell, Reginald E.; Kidson, John W.; Vincent, Dayton G.; and Boer, George J.: The General Circulation of the Tropical Atmosphere. Volume 1. MIT Press, c.1972.

39. Endlich, R. M.; Harney, Patrick; McLean, G. S.; Rados, Robert M.; Tibbets, O. J.; and Widger, W. K., Jr.: Project Jet Stream - The Observation and Analysis of the Detailed Structure of the Atmosphere Near the Tropopause. Bull. American Meteorol. Soc., vol. 35, no. 4, Apr. 1954, pp. 143-153.

40. McLean, George S.: Cloud Distributions in the Vicinity of Jet Streams. Bull. American Meteorol. Soc., vol. 38, no. 10, Dec. 1957, pp. 579-583.

41. Endlich, R. M.; and McLean, G. S.: Analyzing and Forecasting Meteorological Conditions in the Upper Troposphere and Lower Stratosphere. AFCRC-TN-60-262, U.S. Air Force, Apr. 1960.

42. Murgatroyd, R. J.; and Goldsmith, P.: High Cloud Over Southern England. Prof. Notes No. 119 (M.O. 524S), Meteorol. Off., British Air Ministry, 1956.

43. James, D. G.: Investigations Relating to Cirrus Cloud. Meteorol. Mag., vol. 86, no. 1015, Jan. 1957, pp. 1-12.

44. Clodman, J.: Some Statistical Aspects of Cirrus Cloud. Mon. Weather Rev., vol. 85, no. 2, Feb. 1957, pp. 37-41.

45. Graves, Maurice E.: Aircraft Reports of Cirriform Clouds on Certain High Latitude Routes and California to Honolulu. Mon. Weather Rev., vol. 96, no. 11, Nov. 1968, pp. 809-812.

46. Palmén, E.; and Newton, C. W.: Atmospheric Circulation Systems - Their Structure and Physical Interpretation. Academic Press, Inc., 1969.

47. Holdeman, J. D.; Nastrom, G. D.; and Falconer, P. D.: An Analysis of the First Two Years of GASP Data. NASA TM-73817, 1977.

48. Danielsen, E. F.: Stratospheric Source for Unexpectedly Large Values of Ozone Measured Over the Pacific Ocean During GAMETAG, August 1977. J. Geophys. Res., vol. 85, no. C1, Jan. 20, 1980, pp. 401-412.

49. Hudson, Robert D.; and Reed, Edith I., eds.: The Stratosphere: Present and Future. NASA RP-1049, 1979.

50. Plank, Vernon G.: Hydrometeor Parameters Determined From the Radar Data of the SAMS Rain Erosion Program - AFCRL/SAMS Report No. 2. AFCRL-TR-74-0249, U.S. Air Force, May 15, 1974. (Available from DTIC as AD A005 391.)

51. Varley, D. J.: Cirrus Particle Distribution Study, Part 2. AFGL-TR-78-0248, U.S. Air Force, Oct. 10, 1978. (Available from DTIC as AD A063 807.)

52. Varley, Donald J.: Cirrus Particle Distribution Study, Part 3. AFGL-TR-78-0305, U.S. Air Force, Dec. 11, 1978. (Available from DTIC as AD A066 975.)

53. Varley, D. J.; and Barnes, A. A., Jr.: Cirrus Particle Distribution Study, Part 4. AFGL-TR-79-0134, U.S. Air Force, June 18, 1979. (Available from DTIC as AD A074 763.)

54. Cohen, Ian D.: Cirrus Particle Distribution Study, Part 5. AFGL-TR-79-0155, U.S. Air Force, July 13, 1979. (Available from DTIC as AD A077 361.)

55. Cohen, Ian D.; and Barnes, Arnold A., Jr.: Cirrus Particle Distribution Study, Part 6. AFGL-TR-80-0261, U.S. Air Force, Sept. 4, 1980.

56. Varley, Donald J.; Cohen, Ian D.; and Barnes, Arnold A., Jr.: Cirrus Particle Distribution Study, Part 7. AFGL-TR-80-0324, U.S. Air Force, Oct. 16, 1980.

57. Barnes, A. A., Jr.: Ice Particles in Clear Air. Communications From the Eighth International Conference on Physics of Clouds (Clermont-Ferrand - France), July 15-19, 1980.

58. Braham, Roscoe R., Jr.; and Spyers-Duran, Paul: Survival of Cirrus Crystals in Clear Air. J. Appl. Meteorol., vol. 6, no. 6, Dec. 1967, pp. 1053-1061.

59. Knollenberg, R. G.: Techniques for Probing Cloud Microstructure. Clouds - Their Formation, Optical Properties, and Effects, Peter V. Hobbs and Adarsh Deepak, eds., Academic Press, Inc., 1981, pp. 15-91.

60. Hicks, Charles R.: Fundamental Concepts in the Design of Experiments, Second ed. Holt, Rinehart and Winston, Inc., c.1973.

61. Nie, Norman H.; Hull, C. Hadlai; Jenkins, Jean G.; Steinbrenner, Karin; and Bent, Dale H.: SPSS - Statistical Package for the Social Sciences, Second ed. McGraw-Hill, Inc., c.1970.

TABLE I.- GASP FLIGHTS SUMMARIZED BY MONTH, CONTRIBUTING AIRCRAFT, AND TYPE OF DATA TAKEN

Year	Month	Aircraft	Tape	File	Data (a)	Reference
1975	December	N4711U	VL0004	1	C	24
1976	January	N4711U	VL0004	1	C	24
		N655PA	VL0004	2		24
	February	N4711U	VL0004	1		24
		N655PA	VL0004	2		24
	March	N4711U	VL0004	1		24
			VL0005	1		25
		N655PA	VL0004	2		24
			VL0005	2		25
	April	N4711U	VL0005	1		25
		N655PA	VL0005	2		25
	May	N4711U	VL0005	1		25
		N655PA	VL0005	2		25
	June	None				
	July	None				
	August	VH-EBE	VL0006	3	C	26
	September	N655PA	VL0006	1	C	26
	October	None				
	November	VH-EBE	VL0008	2	C	27
	December	VH-EBE	VL0008	2		27
		N533PA	VL0007	3		27
1977	January	N533PA	VL0007	3	C	27
			VL0010	1	C,P	29
		VH-EBE	VL0008	2	C	27
			VL0011	1	C,P	30
	February	VH-EBE	VL0011	1		30
		N533PA	VL0010	1		29
	March	N533PA	VL0010	1		29
	April	N533PA	VL0010	2		29
	May	N533PA	VL0010	2		29
	June	N533PA	VL0010	4		29
	July	N533PA	VL0010	4		29
	August	N533PA	VL0010	4		29
	September	N533PA	VL0010	5		29
	October	N533PA	VL0010	5	C	29
			VL0009	1 to 4	C,P	28
			VL0014	1		31
		N655PA	VL0014	3		31
	November	N533PA	VL0014	1		31
		N655PA	VL0014	3		31
	December	N655PA	VL0012	3		29

[a]C represents cloud detector observations; P represents particle concentration observations.

TABLE I.- Concluded

Year	Month	Aircraft	Tape	File	Data (a)	Reference
1978	January	N533PA	VL0015	1	C,P	32
	February	N533PA	VL0015	1	C,P	32
	March	None				
	April	N533PA	VL0015	2	C,P	32
	May	N533PA	VL0015	2,3	↓	32
		N655PA	VL0020	1	↓	32
	June	N4711U	VL0017	3	↓	32
			VL0018	1	↓	32
		N655PA	VL0020	1,2	↓	32
	July	N4711U	VL0018	1	↓	32
		N655PA	VL0020	2	P	32
	August	None				
	September	N4711U	VL0018	2	P	32
		N655PA	VL0020	3	C,P	32
	October	N4711U	VL0018	2	P	32
			VL0027	1	P	
		N655PA	VL0020	3	C,P	32
			VL0023	1	C,P	
	November	N4711U	VL0027	1	P	
		N655PA	VL0023	1	C,P	
	December	N4711U	VL0027	1	P	
			VL0028	1	P	
		N655PA	VL0023	1	C,P	
			VL0024	1	C,P	
1979	January	N655PA	VL0024	1	C,P	
	February	N4711U	VL0029	1	↓	
		N655PA	VL0024	1	↓	
			VL0025	1	↓	
	March	N4711U	VL0029	1	↓	
			VL0030	1	↓	
		N655PA	VL0025	1	↓	
			VL0026	1	↓	
	April	N4711U	VL0030	1	↓	
	May	N4711U	VL0031	1	↓	
		N655PA	VL0026	2	↓	
	June	N4711U	VL0031	1	↓	
		N655PA	VL0026	2	↓	

[a]C represents cloud detector observations; P represents particle concentration observations.

TABLE II.- *MONTHLY AND SEASONAL SUMMARY OF THE NUMBER OF GASP FLIGHTS WITH CLOUD-ENCOUNTER DATA, BY CITY PAIRS FOR ROUTES WITHIN GEOGRAPHIC REGIONS*

(a) Intercontinental routes

Route	Region / City-pair	City-pair coordinates				Distance, n.mi.	Month												Seasonal totals				
							J	F	M	A	M	J	J	A	S	O	N	D	W	Sp	Su	Au	Total
1	U.S. WEST COAST -- HAWAII																						
	SFO HNL	37.6N	122.4W	21.3N	157.9W	2079	6	24	8	9	7	11	10	0	0	0	3	17	38	27	10	20	95
	LAX HNL	34.0N	118.4W	21.3N	157.9W	2217	2	22	18	7	7	14	12	0	0	1	6	5	42	28	12	12	94
	LAX ITO	34.0N	118.4W	19.7N	155.0W	2124	0	4	4	1	3	1	1	0	0	0	0	0	8	5	1	0	14
	SEA HNL	47.6N	122.3W	21.3N	157.9W	2329	0	1	4	6	0	0	0	0	0	0	0	2	5	6	0	2	13
	PDX HNL	45.7N	122.5W	21.3N	157.9W	2267	0	0	0	0	0	0	0	0	0	4	0	0	0	0	0	4	4
	LAS HNL	36.0N	115.2W	21.3N	157.9W	2392	0	0	0	0	1	0	0	0	0	0	0	0	0	1	0	0	1
																			93	67	23	38	221
2	CENTRAL USA -- HAWAII																						
	ORD HNL	42.0N	87.9W	21.3N	157.9W	3679	0	5	9	13	8	7	7	0	0	0	0	2	14	28	7	2	51
	DFW HNL	32.9N	97.1W	21.3N	157.9W	3277	0	0	2	0	6	0	0	0	0	0	0	6	2	6	0	6	14
	ORD ITO	42.0N	87.9W	19.7N	155.1W	3613	0	1	0	0	1	2	2	0	0	0	0	0	1	3	2	0	6
	DTW HNL	42.2N	83.4W	21.3N	157.9W	3878	0	0	0	1	0	0	0	0	0	0	0	0	0	1	0	0	1
																			17	38	9	8	72
3	WESTERN NORTH AMERICA -- JAPAN																						
	LAX HND	34.0N	118.4W	35.5N	139.8E	4754	7	3	1	17	2	1	6	8	12	5	2	0	11	20	26	7	64
	SFO HND	37.6N	122.4W	35.5N	139.8E	4472	1	0	2	1	4	0	0	0	1	3	0	0	3	5	1	3	12
	LAX NRT	34.0N	118.4W	35.7N	140.4E	4727	0	1	0	0	2	0	0	0	0	0	1	2	1	2	0	3	6
	SFO NRT	37.6N	122.4W	35.7N	140.4E	4441	1	1	1	0	0	0	0	0	0	2	1	0	3	0	0	3	6
	YVR HND	49.2N	123.2W	35.5N	139.8E	4079	0	0	0	0	0	0	0	0	0	1	0	0	0	0	0	1	1
																			18	27	27	17	89
4	U.S. EAST COAST -- JAPAN																						
	JFK HND	40.6N	73.8W	35.5N	139.8E	5872	8	1	1	18	7	3	9	9	11	4	1	0	10	28	29	5	72
	JFK CTS	40.6N	73.8W	42.8N	141.7E	5439	0	1	0	0	0	0	0	0	0	0	0	0	1	0	0	0	1
																			11	28	29	5	73
5	U.S. WEST COAST -- NW EUROPE																						
	SEA LHR	47.6N	122.3W	51.5N	.5W	4146	0	2	2	3	0	15	0	0	0	4	0	4	4	18	0	8	30
	SFO LHR	37.6N	122.4W	51.5N	.5W	4648	0	0	0	0	0	15	0	0	0	4	0	0	0	15	0	4	19
	LAX LHR	34.0N	118.4W	51.5N	.5W	4721	0	1	0	0	1	0	0	0	0	0	5	2	1	1	0	7	9
	LAX PIK	34.0N	118.4W	55.4N	4.6W	4459	0	0	0	0	0	0	0	0	0	0	1	0	0	0	0	1	1
																			5	34	0	20	59

TABLE II.- Continued

Route	Region / City-pair	City-pair coordinates				Distance, n.mi.	Month												Seasonal totals				
							J	F	M	A	M	J	J	A	S	O	N	D	W	Sp	Su	Au	Total
6	CENTRAL USA -- NW EUROPE																						
	DTW LHR	42.2N	83.4N	51.5N	.5W	3262	0	0	0	0	2	0	0	0	0	0	0	0	0	2	0	0	2
7	U.S. EAST COAST -- NW EUROPE																						
	JFK LHR	40.6N	73.8W	51.5N	.5W	2990	8	3	6	3	10	2	0	0	9	11	3	3	17	15	9	17	58
	JFK FRA	40.6N	73.8W	50.1N	8.5E	3338	6	3	10	8	2	0	0	0	10	8	5	2	19	10	10	15	54
	IAD LHR	38.9N	77.5W	51.5N	.5W	3186	0	0	0	0	0	2	0	0	7	4	4	2	0	2	7	10	19
	JFK CPH	40.6N	73.8W	55.5N	12.8E	3345	0	0	0	0	0	0	6	2	6	0	0	0	0	0	14	0	14
	BOS LHR	42.4N	71.0W	51.5N	.5W	2824	0	0	0	0	4	0	0	0	9	0	0	0	0	4	9	0	13
	JFJ SNN	40.6N	73.8W	52.7N	8.9W	2672	1	0	0	0	0	0	0	0	0	0	1	0	1	0	0	1	2
																			37	31	49	43	160
8	EASTERN NORTH AMERICA -- SE EUROPE																						
	JFK FCO	40.6N	73.8W	41.8N	12.2E	3705	4	2	1	2	2	0	0	0	3	0	6	7	7	4	3	13	27
	YQX FCO	49.0N	54.5W	41.8N	12.2E	2751	1	0	0	0	0	0	0	0	0	0	0	0	1	0	0	0	1
	JFK ATH	40.6N	73.8W	37.8N	23.8E	4282	0	0	0	0	0	0	0	0	0	0	1	0	0	0	0	1	1
	BGR ATH	44.8N	68.8W	37.8N	23.8E	3961	0	0	0	0	0	0	0	0	0	0	1	0	0	0	0	1	1
																			8	4	3	15	30
9	U.S. WEST COAST -- AUSTRALIA																						
	SFO AKL	37.6N	122.4W	37.0S	174.7E	5672	1	1	1	0	5	1	2	0	2	2	0	8	3	6	4	10	23
	SFO SYD	37.6N	122.4W	33.9S	151.2E	6444	1	0	0	0	1	0	1	0	0	1	0	2	1	1	1	3	6
	LAX AKL	34.0N	118.4W	37.0S	174.7E	5664	0	0	0	0	4	0	0	0	0	0	0	0	0	4	0	0	4
																			4	11	5	13	33
10	U.S. WEST COAST -- SOUTHEAST ASIA																						
	SFO HKG	37.6N	122.4W	22.3N	114.1E	5998	6	1	0	0	6	0	0	0	0	0	0	0	7	6	0	0	13
11	CONTERMINOUS USA -- CENTRAL AND SOUTH AMERICA																						
	LAX GUA	34.0N	118.4W	14.7N	90.5W	1903	0	0	0	3	3	0	0	0	2	0	0	0	0	6	2	0	8
	JFK GIG	40.7N	73.8W	22.8S	43.2W	4175	0	0	0	7	0	0	0	0	0	0	0	0	0	7	0	0	7
	IAH MEX	30.0N	95.4W	19.4N	99.1W	667	0	2	2	0	2	0	0	0	0	0	0	0	4	2	0	0	6
	JFK CUN	40.6N	73.8W	21.0N	86.9W	1352	0	0	2	0	0	0	0	0	0	0	0	0	2	0	0	0	2
	MIA CCS	25.8N	80.3W	10.6N	67.0W	1184	0	0	0	1	0	0	0	0	0	0	0	0	0	1	0	0	1
																			6	16	2	0	24

TABLE II.- Continued

Route	Region / City-pair	City-pair coordinates				Distance, n.mi.	Month												Seasonal totals				
							J	F	M	A	M	J	J	A	S	O	N	D	W	Sp	Su	Au	Total
12	EASTERN USA -- MIDDLE EAST																						
	JFK BAH	40.6N	73.8W	26.1N	50.5E	5737	2	0	1	0	2	0	2	2	0	0	0	0	3	2	4	0	9
13	HAWAII -- OCEANIA																						
	HNL NAN	21.3N	157.9W	17.8S	177.5E	2756	2	4	0	0	0	2	0	0	0	0	4	12	6	2	0	16	24
	HNL PPG	21.3N	157.9W	14.2S	170.6W	2258	0	2	2	0	8	0	0	0	0	1	1	8	4	8	0	10	22
	HNL AKL	21.3N	157.9W	37.0S	174.7E	3826	0	0	0	0	0	0	0	0	0	0	1	0	0	0	0	1	1
																			10	10	0	27	47
14	HAWAII -- JAPAN																						
	HNL NRT	21.3N	157.9W	35.7N	140.4E	3312	2	3	2	0	1	1	0	0	0	4	1	0	7	2	0	5	14
	HNL OSA	21.3N	157.9W	34.8N	135.5E	3556	2	4	0	0	0	0	0	0	0	2	2	0	6	0	0	4	10
																			13	2	0	9	24
15	HAWAII -- GUAM																						
	HNL GUM	21.3N	157.9W	13.4N	144.8E	3321	0	1	2	1	6	0	0	0	0	0	0	4	3	7	0	4	14
16	AUSTRALIA -- SOUTHEAST ASIA																						
	SYD SIN	33.9S	151.2E	1.4N	103.9E	3402	3	3	0	0	0	0	0	0	0	0	3	3	6	0	0	6	12
	SYD MNL	33.9S	151.2E	14.6N	120.9E	3386	4	0	0	0	0	0	0	2	0	0	0	0	4	0	2	0	6
	MEL BKK	37.7S	144.8E	13.9N	100.7E	3968	0	0	0	0	0	0	0	6	0	0	0	0	0	0	6	0	6
	MEL SIN	37.7S	144.8E	1.4N	103.9E	3261	0	2	0	0	0	0	0	0	0	0	0	2	2	0	0	2	4
	SYD KUL	33.9S	151.2E	3.1N	101.5E	3577	0	0	0	0	0	0	0	0	0	0	0	2	0	0	0	2	2
	MEL KUL	37.7S	144.9E	3.1N	101.5E	3431	0	0	0	0	0	0	0	0	0	0	0	2	0	0	0	2	2
	DRW BKK	12.4S	130.9E	13.9N	100.7E	2391	0	0	0	0	0	0	0	2	0	0	0	0	0	0	2	0	2
	SYD BKK	33.9S	151.2E	13.9N	100.7E	4066	0	0	0	0	0	0	0	2	0	0	0	0	0	0	2	0	2
																			12	0	12	12	36
17	AUSTRALIA -- INDIA																						
	PER BOM	31.9S	116.0E	19.0N	72.9E	3932	4	0	0	0	0	0	0	4	0	0	1	3	4	0	4	4	12
18	AUSTRALIA -- SOUTHERN AFRICA AND INDIAN OCEAN																						
	PER MRU	31.9S	116.0E	20.5S	57.7E	3175	2	3	0	0	0	0	0	0	0	0	0	0	5	0	0	0	5
	AKL CPT	37.0S	174.7E	34.0S	18.6E	6336	0	0	0	0	0	0	0	0	0	1	0	0	0	0	0	1	1
																			5	0	0	1	6

TABLE II.- Continued

Route	Region / City-pair	City-pair coordinates				Distance, n.mi.	Month												Seasonal totals				
							J	F	M	A	M	J	J	A	S	O	N	D	W	Sp	Su	Au	Total
19	NW EUROPE -- SE EUROPE																						
	FRA IST	50.1N	8.5E	41.0N	28.8E	1008	2	0	2	1	0	0	0	0	0	0	0	0	4	1	0	0	5
	LHR ATH	51.5N	.5W	37.9N	23.7E	1305	0	0	0	0	0	0	0	4	0	0	0	0	0	0	4	0	4
	ORY BEG	48.8N	2.4E	44.8N	20.3E	771	0	0	0	0	0	0	0	2	0	0	0	0	0	0	2	0	2
	LHR BEG	51.5N	.5W	44.8N	20.3E	920	0	0	0	0	0	0	0	0	0	0	0	1	0	0	0	1	1
	SNN FCO	52.7N	8.9W	41.8N	12.3E	1076	1	0	0	0	0	0	0	0	0	0	0	0	1	0	0	0	1
	AMS ATH	52.3N	4.8E	37.8N	23.8E	1178	1	0	0	0	0	0	0	0	0	0	0	0	1	0	0	0	1
	LHR FCO	51.5N	.5W	41.8N	12.3E	783	0	0	0	0	0	0	0	0	1	0	0	0	0	0	1	0	1
																			6	1	7	1	15
20	NW EUROPE -- MIDDLE EAST																						
	FRA THR	50.1N	8.5E	35.7N	51.3N	2035	0	0	0	0	1	0	0	0	1	4	3	2	0	1	1	9	11
	FRA BAH	50.1N	8.5E	26.1N	50.5E	2402	3	2	0	0	0	0	0	0	0	0	3	1	5	0	0	4	9
	AMS BAH	52.3N	4.8E	26.1N	50.5E	2579	0	0	0	0	0	0	0	0	0	0	0	1	0	0	0	1	1
																			5	1	1	14	21
21	NW EUROPE -- MIDDLE EAST																						
	LHR BOM	51.5N	.5W	19.0N	72.9E	3899	4	0	0	0	0	0	0	4	0	0	1	3	4	0	4	4	12
	FRA DEL	50.1N	8.5E	28.6N	77.1E	3304	0	3	2	0	0	0	0	0	0	0	0	0	5	0	0	0	5
	FRA KHI	50.1N	8.5E	24.9N	67.2E	3078	0	0	0	0	1	1	0	0	0	0	0	0	0	2	0	0	2
	FRA BOM	50.1N	8.5E	19.0N	72.9E	3553	0	0	0	0	1	0	0	0	0	0	0	0	0	1	0	0	1
																			9	3	4	4	20
22	NW EUROPE -- SOUTH AFRICA																						
	LHR CPT	51.5N	.4W	33.9S	18.7E	5222	0	0	0	0	0	0	0	0	0	1	0	0	0	0	0	1	1
23	SE EUROPE -- MIDDLE EAST																						
	IST THR	41.0N	28.8E	35.7N	51.3E	1102	2	1	4	0	0	0	0	0	0	0	6	5	7	0	0	11	18
	ATH THR	37.8N	23.7E	35.7N	51.3E	1328	0	2	0	0	0	0	0	4	0	0	0	1	2	0	4	1	7
	ATH DAM	37.8N	23.7E	33.4N	36.5E	677	0	0	0	0	0	0	0	1	0	0	0	1	0	0	1	1	2
	BEG BAH	44.8N	20.3E	26.1N	50.5E	1836	0	0	0	0	0	0	0	0	0	0	0	1	0	0	0	1	1
	ATH BAH	37.8N	23.7E	26.1N	50.5E	1527	1	0	0	0	0	0	0	0	0	0	0	0	1	0	0	0	1
																			10	0	5	14	29

TABLE II.- Continued

Route	Region / City-pair	City-pair coordinates				Distance, n.mi.	Month												Seasonal totals				
							J	F	M	A	M	J	J	A	S	O	N	D	W	Sp	Su	Au	Total
24	SE EUROPE -- INDIA																						
	IST BOM	41.0N	28.8E	19.0N	72.9E	2607	1	1	0	0	0	0	0	0	0	0	0	0	2	0	0	0	2
	IST DEL	41.0N	28.8E	28.6N	77.1E	2459	1	0	0	0	0	0	0	0	0	0	0	0	1	0	0	0	1
	ATH DEL	37.8N	23.7E	28.6N	77.1E	2700	0	0	0	0	0	0	0	1	0	0	0	0	0	0	1	0	1
																			3	0	1	0	4
25	SE EUROPE -- SOUTHEAST ASIA																						
	ATH BKK	37.8N	23.7E	13.9N	100.7E	4281	0	0	0	0	0	0	0	4	0	0	0	0	0	0	4	0	4
26	SOUTHEAST ASIA -- MIDDLE EAST																						
	BKK THR	13.9N	100.7E	35.7N	51.3E	2953	0	2	0	0	0	0	0	4	0	0	1	1	2	0	4	2	8
	BKK BAH	13.9N	100.7E	26.1N	50.5E	2905	1	3	0	0	0	0	0	0	0	0	3	1	4	0	0	4	8
	KUL BAH	3.1N	101.6E	26.3N	50.5E	3239	1	0	0	0	0	0	0	0	0	0	0	2	1	0	0	2	3
	BKK DAM	13.9N	100.7E	33.4N	36.5E	3659	0	0	0	0	0	0	0	1	0	0	0	1	0	0	1	1	2
	SIN BAH	1.4N	103.9E	26.1N	50.5E	3414	1	0	0	0	0	0	0	0	0	0	0	0	1	0	0	0	1
																			8	0	5	9	22
27	SOUTHEAST ASIA -- JAPAN																						
	HKG NRT	22.3N	114.1E	35.8N	140.4E	1592	1	3	1	0	3	1	0	0	0	2	1	2	5	4	0	5	14
	HKG HND	22.3N	114.1E	35.5N	139.8E	1558	1	0	2	1	0	0	0	0	1	2	0	0	3	1	1	2	7
																			8	5	1	7	21
28	SOUTHEAST ASIA -- INDIAN SUBCONTINENT																						
	HKG DEL	22.3N	114.1E	28.6N	77.1E	2032	1	3	2	0	2	1	0	0	0	2	0	1	6	3	0	3	12
	BKK DEL	13.9N	100.7E	28.6N	77.1E	1582	1	0	2	1	0	0	0	1	1	1	0	1	3	1	2	2	8
	BKK BOM	13.9N	100.7E	19.0N	72.9E	1627	0	0	0	0	1	0	0	0	0	0	0	0	0	1	0	0	1
	BKK KHI	13.9N	100.7E	24.9N	67.2E	2001	0	0	0	0	0	0	0	0	0	1	0	0	0	0	0	1	1
																			9	5	2	6	22
29	INDIAN SUBCONTINENT -- MIDDLE EAST																						
	DEL THR	28.6N	77.1E	35.7N	51.3E	1373	1	0	2	0	1	0	0	0	1	3	0	2	3	1	1	5	10
	BOM THR	19.0N	72.9E	35.7N	51.3E	1519	1	1	0	0	0	0	0	0	0	0	2	4	2	0	0	6	8
	KHI THR	24.9N	67.2E	35.7N	51.3E	1046	0	0	2	0	0	0	0	0	0	1	2	2	2	0	0	5	7
	KHI IST	24.9N	67.2E	41.0N	28.8E	2138	0	0	0	1	0	0	0	0	0	0	0	0	0	1	0	0	1
																			7	2	1	16	26

TABLE II.- Continued

Route	Region / City-pair	City-pair coordinates				Distance, n.mi.	Month												Seasonal totals				
							J	F	M	A	M	J	J	A	S	O	N	D	W	Sp	Su	Au	Total
30	MISCELLANEOUS, WITHIN ATLANTIC REGION																						
	LHR LPA	51.5N	.5W	27.9N	15.4W	1567	0	0	0	0	0	0	0	0	0	0	0	1	0	0	0	1	1
	BGR LPA	44.9N	68.8W	27.9N	15.4W	2717	0	0	0	0	0	0	0	0	0	0	0	1	0	0	0	1	1
																			0	0	0	2	2
31	MISCELLANEOUS, WITHIN PACIFIC REGION																						
	LAX PPT	33.9N	118.4W	17.5S	149.5W	1939	0	0	0	0	2	0	0	0	0	1	1	2	0	2	0	4	6
	GUM NRT	13.4N	144.4E	35.7N	140.4E	1355	0	0	0	0	4	0	0	0	0	0	0	2	0	4	0	2	6
	TPE OKA	25.1N	121.6E	26.2N	127.7E	336	0	0	0	1	0	0	0	0	0	0	0	0	0	1	0	0	1
																			0	7	0	6	13

(b) Transcontinental or shorter routes

32	COAST TO COAST IN CONTINENTAL USA																						
	LAX JFK	34.0N	118.4W	40.6N	73.8W	2142	1	13	13	0	4	4	5	0	0	0	1	0	27	8	5	1	41
	JFK SFO	40.6N	73.8W	37.6N	122.4W	2241	0	5	3	0	4	6	3	0	1	2	0	5	8	10	4	7	29
	SFO BOS	37.6N	122.4W	42.4N	71.0W	2344	0	0	0	0	0	0	0	0	0	0	0	2	0	0	0	2	2
	BGR LAX	44.9N	68.8W	34.0N	118.4W	2350	0	0	0	0	0	0	0	0	0	0	1	1	0	0	0	2	2
																			35	18	9	12	74
33	MID USA TO WEST COAST																						
	ORD LAX	42.0N	87.9W	34.0N	118.4W	1510	1	9	13	1	8	4	2	0	0	0	0	0	23	13	2	0	38
	ORD LAS	42.0N	87.9W	36.1N	115.1W	1310	2	0	4	3	6	0	0	0	0	0	0	0	6	9	0	0	15
	ORD SFO	42.0N	87.9W	37.6N	122.4W	1601	2	0	0	4	0	2	2	0	0	0	0	0	2	6	2	0	10
	ORD SEA	42.0N	87.9W	47.6N	122.3W	1490	0	1	0	2	0	0	0	0	0	0	0	0	1	2	0	0	3
	IAH SFO	30.0N	95.4W	37.6N	122.4W	1415	0	0	0	0	0	0	0	0	0	1	0	0	0	0	0	1	1
																			32	30	4	1	67
34	TEXAS -- EAST COAST																						
	DFW JFK	32.9N	97.0W	40.6N	73.8W	1203	0	0	2	0	6	0	0	0	0	0	0	6	2	6	0	6	14
	IAH JFK	30.0N	95.4N	40.6N	73.8W	1229	0	2	2	0	2	0	0	0	0	3	2	0	4	2	0	5	11
																			6	8	0	11	25

TABLE II.- Continued

Route	Region / City-pair	City-pair coordinates				Distance, n.mi.	Month												Seasonal totals				
							J	F	M	A	M	J	J	A	S	O	N	D	W	Sp	Su	Au	Total
35	GREAT LAKES -- EAST COAST																						
	ORD JFK	42.0N	87.9W	40.6N	73.8W	640	0	3	4	0	1	3	4	0	0	0	0	0	7	4	4	0	15
	DTW IAD	42.2N	83.4W	39.0N	77.4W	334	0	0	0	0	0	2	0	0	1	4	2	2	0	2	1	8	11
	DTW BOS	42.2N	83.4W	42.4N	71.0W	550	0	0	0	0	4	0	0	0	6	0	0	0	0	4	6	0	10
																			7	10	11	8	36
36	WEST COAST ROUTES (LONG)																						
	SFO SEA	37.6N	122.4W	47.5N	122.3W	600	0	2	2	2	0	1	0	0	0	0	0	4	4	3	0	4	11
	LAX SEA	34.0N	118.4W	47.6N	122.3W	835	0	0	0	0	0	1	0	0	0	0	0	0	0	1	0	0	1
	SFO VYR	37.6N	122.4W	49.2N	123.2W	697	0	0	0	0	0	0	0	0	0	1	0	0	0	0	0	1	1
																			4	4	0	5	13
37	LOS ANGELES -- SAN FRANCISCO																						
	SFO LAX	37.6N	122.4W	34.0N	118.4W	291	1	4	0	2	5	0	0	0	2	2	1	3	5	7	2	6	20
38	LOS ANGELES -- DENVER																						
	LAX DEN	34.0N	118.4W	39.8N	104.9W	734	0	3	6	3	2	4	3	0	0	1	0	0	9	9	3	1	22
39	DENVER -- CHICAGO																						
	DEN ORD	39.8N	104.9W	42.0N	87.9W	781	0	2	6	0	0	4	3	0	0	0	0	0	8	4	3	0	15
40	WITHIN GREAT LAKES REGION																						
	ORD DTW	42.0N	87.9W	42.2N	83.4W	201	0	2	6	0	0	4	3	0	0	0	0	0	8	4	3	0	15
	ORD CLE	42.0N	87.9W	41.4N	81.8W	276	0	0	4	6	4	0	0	0	0	0	0	0	4	10	0	0	14
	ORD YYZ	42.0N	87.9W	43.7N	79.6W	379	0	2	2	4	0	0	0	0	0	0	0	2	4	4	0	2	10
	ORD PIT	42.0N	87.9W	40.5N	80.2W	359	0	2	0	0	6	0	0	0	0	0	0	0	2	6	0	0	8
																			18	24	3	2	47
41	MISCELLANEOUS, WITHIN NORTH AMERICA																						
	SEA FAI	47.6N	122.3W	64.8N	147.8W	1319	0	0	0	0	0	0	0	0	0	0	0	2	0	0	0	2	2
	LAS LAX	36.1N	115.1W	34.0N	118.4W	205	0	1	0	0	1	0	0	0	0	0	0	0	1	1	0	0	2
	YQX JFK	49.0N	54.6W	40.6N	73.8N	956	1	0	0	0	0	0	0	0	0	0	0	0	1	0	0	0	1
	JFK LAS	40.6N	73.8W	36.1N	115.1W	1944	0	1	0	0	0	0	0	0	0	0	0	0	1	0	0	0	1
	JFK JFK	40.6N	73.8W	40.6N	73.8W	0	0	0	0	1	0	0	0	0	0	0	0	0	0	1	0	0	1
																			3	2	0	2	7

TABLE II.- Continued

Route	Region / City-pair	City-pair coordinates				Distance, n.mi.	Month												Seasonal totals				
							J	F	M	A	M	J	J	A	S	O	N	D	W	Sp	Su	Au	Total
42	TRANS-AUSTRALIAN ROUTES																						
	SYD PER	33.9S	151.2E	31.9S	116.0E	1769	3	0	0	0	0	0	0	4	0	0	1	2	3	0	4	3	10
	MEL PER	37.7S	144.8E	31.9S	116.0E	1455	2	3	0	0	0	0	0	0	0	0	0	1	5	0	0	1	6
	SYD DRW	33.9S	151.2E	12.4S	130.9E	1701	0	0	0	0	0	0	0	2	0	0	0	0	0	0	2	0	2
																			8	0	6	4	18
43	SE AUSTRALIAN COAST																						
	SYD MEL	33.9S	151.2E	37.7S	144.8E	386	4	6	0	0	0	2	0	6	0	0	3	8	10	2	6	11	29
44	AUSTRALIA -- NEW ZEALAND																						
	SYD AKL	33.9S	151.2E	37.0S	174.7E	1161	1	4	0	0	8	1	2	0	2	1	3	16	5	9	4	20	38
	SYD CHC	33.9S	151.2E	43.5S	172.5E	1147	2	0	0	0	0	0	0	2	0	0	0	2	2	0	2	2	6
	AKL AKL	37.0S	174.7E	37.0S	174.7E	0	0	0	0	0	1	0	0	0	0	0	0	0	0	1	0	0	1
																			7	10	6	22	45
45	AUSTRALIA -- OCEANIA																						
	SYD NAN	33.9S	151.2E	17.8S	177.5E	1709	2	4	0	0	0	2	0	0	0	0	4	12	6	2	0	16	24
	SYD PPG	33.9S	151.2E	14.2S	170.6W	2383	0	2	0	0	0	0	0	0	0	0	0	0	2	0	0	0	2
	SYD NOU	33.9S	151.2E	22.0S	166.2E	1066	0	0	0	0	0	0	0	2	0	0	0	0	0	0	2	0	2
																			8	2	2	16	28
46	WITHIN OCEANIA																						
	PPG PPT	14.2S	170.6W	17.6S	149.6W	1228	0	0	2	0	8	0	0	0	0	1	1	8	2	8	0	10	20
47	WITHIN NW EUROPE																						
	LHR FRA	51.5N	.5W	50.1N	8.5E	351	3	4	3	0	3	1	0	0	1	4	5	3	10	4	1	12	27
	LHR BRU	51.5N	.5W	50.9N	4.5E	191	3	0	2	0	1	0	0	0	4	4	2	0	5	1	4	6	16
	LHR AMS	51.5N	.5W	52.3N	4.8E	202	0	0	0	2	4	0	0	0	0	0	0	1	0	6	0	1	7
	MUC FRA	48.1N	11.7E	50.1N	8.5E	174	1	0	0	2	0	0	0	0	3	0	0	0	1	2	3	0	6
	PIK LHR	55.4N	4.6W	51.5N	.5W	276	0	0	0	0	0	0	0	0	0	0	1	0	0	0	0	1	1
	MUC SNN	48.1N	11.7E	52.7N	8.9W	831	0	0	0	0	0	0	0	0	0	0	1	0	0	0	0	1	1
																			16	13	8	21	58

TABLE II.- Concluded

Route	Region / City-pair	City-pair coordinates				Distance, n.mi.	Month												Seasonal totals				
							J	F	M	A	M	J	J	A	S	O	N	D	W	Sp	Su	Au	Total
48	WITHIN SE EUROPE																						
	FCO IST	41.8N	12.3E	41.0N	28.8E	747	2	2	2	0	0	0	0	0	0	0	6	7	6	0	0	13	19
	ATH FCO	37.8N	23.8E	41.8N	12.2E	585	0	1	0	0	0	0	0	4	0	0	0	2	1	0	4	2	7
	ATH BEG	37.8N	23.8E	44.8N	20.3E	449	0	0	0	0	0	0	0	2	0	0	0	0	0	0	2	0	2
																			7	0	6	15	28
49	WITHIN SE ASIA																						
	SIN BKK	1.4N	103.9E	13.9N	100.7E	774	1	4	0	0	0	0	0	0	0	0	3	3	5	0	0	6	11
	BKK HKG	13.9N	100.7E	22.3N	114.1E	915	1	0	2	1	1	0	0	0	1	2	1	1	3	2	1	4	10
	MNL HKG	14.5N	121.0E	22.3N	114.1E	611	4	2	2	0	0	0	0	2	0	0	0	0	8	0	2	0	10
	GUM MNL	13.4N	144.4E	14.5N	121.0E	1364	0	2	2	0	2	0	0	0	0	0	0	2	4	2	0	2	8
	SIN HKG	1.4N	103.9E	22.3N	114.2E	1388	2	0	0	0	4	0	0	0	0	0	0	0	2	4	0	0	6
	KUL SIN	3.1N	101.5E	1.4N	103.9E	176	0	0	0	0	0	0	0	0	0	0	0	1	0	0	0	1	1
																			22	8	3	13	46
50	WITHIN CENTRAL AND SOUTH AMERICA																						
	CCS GIG	10.6N	67.0W	22.8S	43.2W	2444	0	0	0	5	0	0	0	0	1	0	0	0	0	5	1	0	6
	GUA CCS	14.7N	90.5W	10.6N	67.0W	1397	0	0	0	3	1	0	0	0	1	0	0	0	0	4	1	0	5
	GUA SJO	14.7N	90.5W	9.9N	84.2W	468	0	0	0	0	2	0	0	0	0	0	0	0	0	2	0	0	2
	SJO PTY	9.9N	84.2W	9.0N	79.4W	289	0	0	0	0	2	0	0	0	0	0	0	0	0	2	0	0	2
	GIG VCP	22.8S	43.2W	23.0S	47.1W	216	0	0	0	0	0	0	0	0	2	0	0	0	0	0	2	0	2
	GIG PTY	22.8S	43.2W	9.0N	79.4W	2857	0	0	0	0	0	0	0	0	1	0	0	0	0	0	1	0	1
	PTY GUA	9.0N	79.4W	14.7N	90.5W	736	0	0	0	0	0	0	0	0	1	0	0	0	0	0	1	0	1
																			0	13	6	0	19
51	WITHIN AFRICA																						
	MRU JNB	20.4S	57.7E	26.1S	28.2E	1658	2	2	0	0	0	0	0	0	0	0	0	0	4	0	0	0	4
52	WITHIN INDIAN SUBCONTINENT																						
	KHI DEL	24.9N	67.2E	28.6N	77.1E	575	0	0	0	1	1	1	0	0	0	0	0	0	0	3	0	0	3

Grand totals:

Winter (W):	532 flights
Spring (Sp):	484 flights
Summer (Su):	276 flights
Autumn (Au):	456 flights
Total	1748 flights

TABLE III.- SUMMARY OF CLOUD-ENCOUNTER OBSERVATIONS

(a) Pressure altitude

		18.5-28.5 kft	28.5-33.5 kft	33.5-38.5 kft	38.5-43.5 kft	Above 43.5 kft	Total
Observations in vicinity of clouds	Winter	238	1779	2244	592	0	4853
	Spring	195	797	1912	880	0	3784
	Summer	108	478	1080	389	0	2055
	Autumn	143	1014	1270	287	0	2714
	Total	684	4068	6506	2148	0	13406
Observations in clear air	Winter	1020	6288	10059	4794	65	22226
	Spring	593	2592	9915	7557	2	20659
	Summer	402	2218	7111	5945	0	15676
	Autumn	563	3872	7143	4370	7	15955
	Total	2578	14970	34228	22666	74	74516
Total		3262	19038	40734	24814	74	87922

(b) Distance from NMC tropopause

		20-15 kft below	15-10 kft below	10-5 kft below	5-0 kft below	0-5 kft above	>5 kft above	Total
Observations in vicinity of clouds	Winter	274	593	881	861	104	7	2720
	Spring	549	569	960	1118	237	12	3445
	Summer	295	437	348	354	72	4	1510
	Autumn	369	511	843	740	78	6	2547
	Total	1487	2110	3032	3073	491	29	10222
Observations in clear air	Winter	1323	1631	2022	2874	3555	2056	13461
	Spring	1848	1966	2731	4592	5350	2748	19235
	Summer	1779	2428	1928	1840	2909	2341	13225
	Autumn	1717	1869	2303	3500	3493	1279	14161
	Total	6667	7894	8984	12806	15307	8424	60082
Total		8154	10004	12016	15879	15798	8453	70304

TABLE IV. - SUMMARY OF ZONAL MEAN CLOUD-ENCOUNTER STATISTICS BY SEASON AS FUNCTIONS OF LATITUDE AND ALTITUDE

[Data from appendix D (Vol. II)]

WINTER

LATITUDE:	75N	65N	55N	45N	35N	25N	15N	5N	5S	15S	25S	35S
ALT.(KFT)												
	N											
38.5-43.5	0	125	576	981	1481	557	314	277	258	317	136	380
33.5-38.5	14	258	1211	1870	2940	2289	803	518	527	523	648	696
28.5-33.5	0	190	763	1614	1424	1307	569	286	348	379	652	531
	$\overline{TIC}$,%											
38.5-43.5		.9	0.0	4.6	3.1	.8	3.0	10.4	19.2	22.4	3.3	.8
33.5-38.5	0.0	.2	6.8	9.1	7.8	7.8	2.9	14.4	12.6	11.6	4.9	3.5
28.5-33.5		3.8	10.0	13.7	10.2	7.8	4.5	8.6	17.1	6.1	7.3	7.6
	SIGMA,%											
38.5-43.5		7.1	0.0	18.6	14.7	7.1	10.5	23.5	30.0	31.0	13.1	7.2
33.5-38.5	0.0	2.7	21.7	24.4	21.1	20.3	12.3	26.8	25.0	25.7	17.6	15.3
28.5-33.5		14.6	24.7	28.4	23.8	21.3	18.0	20.2	27.4	17.1	20.8	21.3
	TICIV,%											
38.5-43.5		54.7	0.0	65.8	50.8	31.2	20.6	40.2	47.2	41.3	26.5	36.4
33.5-38.5	0.0	43.1	54.8	50.2	39.7	37.6	32.0	41.6	37.5	45.7	40.2	41.7
28.5-33.5		42.2	46.8	48.5	42.4	43.9	58.4	35.2	36.4	29.4	42.6	39.8
	SIGMA,%											
38.5-43.5		14.3	0.0	30.9	34.3	30.4	20.2	30.4	29.9	31.4	27.7	34.2
33.5-38.5	0.0	0.0	34.2	34.5	31.6	29.5	26.9	30.8	30.6	32.3	33.6	34.0
28.5-33.5		27.8	33.7	34.1	31.7	31.3	32.5	27.1	29.9	26.8	31.9	33.1
	P(TIC>0%)											
38.5-43.5		1.6	0.0	6.9	6.0	2.7	14.3	26.0	40.7	54.3	12.5	2.1
33.5-38.5	0.0	.4	12.5	18.2	19.7	20.7	9.1	34.6	33.6	25.4	12.2	8.5
28.5-33.5		8.9	21.4	28.3	23.9	17.8	7.7	24.5	46.8	20.8	17.2	19.0
	P(TIC>10%)											
38.5-43.5		1.6	0.0	6.2	4.7	2.0	8.3	20.2	34.5	43.8	6.6	1.6
33.5-38.5	0.0	.4	10.3	14.3	15.0	16.1	6.2	26.1	24.7	20.1	8.5	6.3
28.5-33.5		8.9	17.2	22.9	18.9	14.5	7.0	18.2	34.2	14.2	12.4	13.9
	P(TIC>25%)											
38.5-43.5		1.6	0.0	5.8	4.1	1.1	5.1	15.5	29.1	32.2	5.1	.8
33.5-38.5	0.0	.4	9.2	12.4	11.2	11.3	5.0	21.6	18.2	16.4	6.6	4.6
28.5-33.5		4.2	13.9	18.2	14.2	11.4	6.0	14.0	26.7	9.5	10.6	10.2
	P(TIC>50%)											
38.5-43.5		.8	0.0	5.2	3.4	.5	1.6	10.1	18.6	19.9	2.9	.5
33.5-38.5	0.0	0.0	6.8	9.5	7.1	6.9	2.2	13.9	11.6	11.7	4.8	3.6
28.5-33.5		3.7	9.6	14.1	10.3	7.3	4.2	7.7	15.5	4.0	7.8	7.2
	$\overline{T}$(CLEAR)											
38.5-43.5		-51.8	-50.0	-52.7	-54.9	-57.3	-57.3	-56.8	-55.5	-58.1	-56.6	-56.8
33.5-38.5	-53.1	-56.3	-53.2	-53.3	-52.7	-48.2	-46.3	-45.6	-44.6	-43.5	-43.3	-48.6
28.5-33.5		-55.0	-51.4	-50.0	-48.9	-40.2	-35.2	-33.9	-32.9	-33.3	-37.1	-41.8
	$\overline{T}$(CLOUDS)											
38.5-43.5		-69.5	0.0	-68.7	-64.9	-62.9	-58.1	-57.1	-57.3	-61.6	-58.6	-62.4
33.5-38.5	0.0	-65.0	-62.0	-59.3	-56.8	-52.1	-49.4	-45.5	-43.3	-44.5	-47.2	-49.8
28.5-33.5		-60.9	-55.0	-52.1	-48.3	-43.7	-36.3	-35.8	-33.6	-33.8	-38.3	-41.5
	$\overline{\Delta Z}$(CLEAR)											
38.5-43.5		5.9	7.4	6.5	1.6	-9.9	-16.0	-17.1	-18.3	-16.5	-12.1	-3.7
33.5-38.5	4.9	3.6	3.4	1.6	-3.7	-11.9	-19.6	-21.3	-21.9	-22.1	-21.2	-12.3
28.5-33.5		1.6	-.4	-2.9	-7.2	-17.1	-25.1	-25.8	-25.9	-25.9	-22.8	-15.1
	$\overline{\Delta Z}$(CLOUDS)											
38.5-43.5		2.3	0.0	-2.3	-2.6	-8.4	-15.0	-16.8	-16.4	-15.8	-15.6	-5.0
33.5-38.5	0.0	-.1	-3.5	-4.2	-5.8	-10.7	-18.6	-21.3	-22.3	-21.9	-19.6	-9.4
28.5-33.5		-.5	-4.2	-6.0	-8.3	-13.5	-25.3	-25.4	-25.9	-24.6	-23.3	-12.9

TABLE IV.- Continued

SPRING

LATITUDE:	75N	65N	55N	45N	35N	25N	15N	5N	5S	15S	25S	35S
ALT.(KFT)												
	N											
38.5-43.5	0	285	1506	2495	1883	741	378	254	292	353	76	182
33.5-38.5	25	408	1885	2851	3215	2121	686	240	172	160	48	16
28.5-33.5	3	41	494	1058	783	635	229	31	10	51	22	30
	$\overline{TIC}$,%											
38.5-43.5		0.0	.0	3.6	4.3	1.5	8.3	12.3	14.9	13.5	.1	2.8
33.5-38.5	.1	.0	4.8	6.8	4.6	5.6	6.0	10.0	10.8	7.7	3.0	.4
28.5-33.5	0.0	16.9	5.2	11.6	5.0	4.7	6.8	1.4	11.1	4.0	.3	14.9
	SIGMA,%											
38.5-43.5		0.0	.3	15.2	17.1	8.9	22.1	25.7	26.2	26.1	.8	14.5
33.5-38.5	.3	.1	17.0	19.9	16.1	17.3	17.5	23.4	22.2	18.8	12.1	1.5
28.5-33.5	0.0	32.8	16.3	24.0	15.6	14.8	19.2	6.7	26.0	13.3	1.5	29.4
	TICIV,%											
38.5-43.5		0.0	2.5	40.8	44.0	21.9	39.1	40.0	36.7	38.2	3.1	57.3
33.5-38.5	1.6	.5	36.4	37.7	31.9	31.2	29.8	43.0	32.1	27.9	36.0	6.3
28.5-33.5	0.0	63.0	26.1	35.9	24.7	25.0	35.4	11.0	37.0	29.1	7.1	55.8
	SIGMA,%											
38.5-43.5		0.0	2.9	32.5	35.0	26.5	33.2	32.3	29.8	31.2	2.8	33.6
33.5-38.5	0.0	.4	32.5	32.1	30.5	29.5	28.7	30.6	27.8	26.7	23.7	0.0
28.5-33.5	0.0	33.2	28.0	30.1	27.0	25.7	29.9	15.7	36.0	23.6	0.0	31.1
	P(TIC>0%)											
38.5-43.5		0.0	.5	8.9	9.8	6.9	21.2	30.7	40.4	35.4	3.9	4.9
33.5-38.5	4.0	2.2	13.2	18.0	14.4	18.0	20.0	23.3	33.7	27.5	8.3	6.3
28.5-33.5	0.0	26.8	20.0	32.4	20.1	18.7	19.2	12.9	30.0	13.7	4.5	26.7
	P(TIC>10%)											
38.5-43.5		0.0	0.0	6.6	7.2	3.2	16.7	22.0	29.1	26.9	0.0	4.9
33.5-38.5	0.0	0.0	8.8	12.9	9.3	11.8	12.2	19.6	26.2	16.9	6.3	0.0
28.5-33.5	0.0	22.0	11.7	24.5	11.6	10.6	13.1	3.2	30.0	7.8	0.0	23.3
	P(TIC>25%)											
38.5-43.5		0.0	0.0	5.2	5.9	2.3	10.3	18.9	22.6	19.3	0.0	3.3
33.5-38.5	0.0	0.0	6.7	9.8	6.7	8.4	9.0	15.0	15.1	11.3	6.3	0.0
28.5-33.5	0.0	22.0	7.3	16.9	7.0	7.6	10.5	3.2	10.0	7.8	0.0	20.0
	P(TIC>50%)											
38.5-43.5		0.0	0.0	3.6	4.1	1.2	7.4	11.0	14.0	13.0	0.0	2.7
33.5-38.5	0.0	0.0	4.5	6.2	4.0	4.6	5.1	9.6	8.7	5.0	2.1	0.0
28.5-33.5	0.0	19.5	3.8	10.0	3.7	3.6	5.7	0.0	10.0	3.9	0.0	16.7
	$\overline{T}$(CLEAR)											
38.5-43.5		-50.4	-52.2	-56.5	-57.9	-59.5	-56.8	-58.0	-56.3	-60.3	-57.0	-57.4
33.5-38.5	-55.6	-50.2	-53.0	-54.1	-54.1	-51.2	-47.6	-48.3	-47.9	-49.5	-51.6	-54.9
28.5-33.5	-56.0	-56.7	-49.1	-48.8	-46.1	-41.8	-35.9	-36.7	-33.7	-36.4	-40.8	-48.3
	$\overline{T}$(CLOUDS)											
38.5-43.5		0.0	-60.5	-64.4	-63.9	-61.7	-58.4	-57.2	-57.7	-59.1	-58.7	-62.2
33.5-38.5	-59.0	-52.7	-59.7	-57.6	-56.6	-52.7	-47.7	-47.3	-49.1	-48.6	-49.5	-57.0
28.5-33.5	0.0	-57.3	-51.9	-49.8	-46.8	-42.5	-32.8	-35.8	-34.3	-33.7	-34.0	-49.3
	$\overline{\Delta Z}$(CLEAR)											
38.5-43.5		6.4	5.5	2.7	1.1	-7.5	-14.3	-16.5	-17.8	-16.0	-11.9	1.1
33.5-38.5	1.8	4.4	1.9	-.4	-3.2	-9.5	-15.7	-18.6	-18.9	-19.5	-14.7	-10.5
28.5-33.5	-3.1	-1.5	-2.2	-4.7	-7.7	-15.1	-19.3	-19.6	0.0	-21.1	-21.4	-9.6
	$\overline{\Delta Z}$(CLOUDS)											
38.5-43.5		0.0	1.7	-1.8	-3.7	-9.3	-15.4	-16.2	-16.5	-15.5	-15.0	-11.6
33.5-38.5	-.7	4.4	-2.4	-3.9	-5.1	-9.5	-15.6	-16.8	-19.6	-19.7	-20.6	-9.0
28.5-33.5	0.0	-2.7	-4.9	-6.8	-8.0	-13.6	-22.1	-18.2	0.0	-27.0	-26.1	-19.5

TABLE IV.- Continued

SUMMER

LATITUDE:	75N	65N	55N	45N	35N	25N	15N	5N	5S	15S	25S	35S
ALT.(KFT)												
	N											
38.5-43.5	135	1541	1699	1714	781	132	39	64	64	41	37	89
33.5-38.5	14	410	865	1765	2415	1577	187	151	143	148	225	292
28.5-33.5	0	0	100	378	628	609	196	133	195	182	189	109
	$\overline{TIC}$,%											
38.5-43.5	0.0	.1	.1	2.7	2.7	1.1	5.7	26.3	37.9	9.8	.1	.0
33.5-38.5	.0	.4	2.0	8.5	3.1	1.8	20.2	7.9	10.1	.4	5	.1
28.5-33.5			4.2	6.7	2.2	5.9	22.5	14.7	4.3	1.1	.5	4.1
	SIGMA,%											
38.5-43.5	0.0	1.9	1.8	11.9	11.3	5.1	19.2	35.4	33.8	20.7	.6	.3
33.5-38.5	.1	4.3	9.0	20.6	13.0	10.2	29.1	20.1	22.5	4.7	3.3	1.2
28.5-33.5			12.2	18.6	12.4	19.0	30.8	25.1	12.5	7.3	4.1	13.7
	TICIV,%											
38.5-43.5	0.0	11.8	11.2	27.9	26.8	12.1	32.0	52.5	51.7	36.4	3.5	1.6
33.5-38.5	.4	13.0	19.0	33.1	32.3	27.3	39.0	30.5	37.2	20.4	13.8	13.5
28.5-33.5			13.7	30.3	33.5	37.6	44.5	33.0	22.9	25.4	12.1	27.9
	SIGMA,%											
38.5-43.5	0.0	19.8	13.2	27.1	24.4	12.3	35.0	33.5	29.1	25.1	0.0	1.2
33.5-38.5	0.0	23.1	21.6	28.9	28.4	30.0	30.0	29.6	29.2	26.1	11.5	5.7
28.5-33.5			18.7	29.4	35.2	33.2	30.0	28.4	19.9	24.1	16.3	24.9
	P(TIC>0%)											
38.5-43.5	0.0	.6	1.1	9.9	10.2	9.1	17.9	50.0	73.4	26.8	2.7	2.2
33.5-38.5	7.1	2.7	10.3	25.8	9.6	6.5	51.9	25.8	27.3	2.0	3.6	.7
28.5-33.5			31.0	22.0	6.7	15.8	50.5	44.4	19.0	4.4	4.2	14.7
	P(TIC>10%)											
38.5-43.5	0.0	.1	.4	6.2	6.5	3.8	10.3	39.1	65.6	22.0	0.0	0.0
33.5-38.5	0.0	1.0	4.9	17.8	6.4	3.9	39.6	15.9	20.3	.7	2.2	.3
28.5-33.5			8.0	13.5	4.0	10.8	40.8	31.6	13.8	3.8	1.1	11.0
	P(TIC>25%)											
38.5-43.5	0.0	.1	.1	4.1	4.5	.8	5.1	34.4	53.1	17.1	0.0	0.0
33.5-38.5	0.0	.5	2.8	12.7	4.7	2.5	31.0	11.9	15.4	7	.9	0.0
28.5-33.5			5.0	10.8	2.7	8.2	35.2	24.1	7.2	1.1	1.1	6.4
	P(TIC>50%)											
38.5-43.5	0.0	.1	0.0	2.3	1.9	0.0	5.1	28.1	39.1	7.3	0.0	0.0
33.5-38.5	0.0	.2	.9	7.5	2.4	1.5	19.8	6.0	9.8	.7	0.0	0.0
28.5-33.5			2.0	5.8	2.1	5.4	21.4	9.8	2.1	1.1	0.0	2.8
	$\overline{T}$(CLEAR)											
38.5-43.5	-42.2	-47.4	-50.8	-55.6	-55.7	-58.0	-60.2	-56.0	-55.6	-56.1	-56.2	-52.3
33.5-38.5	-43.2	-49.3	-50.7	-50.2	-48.7	-48.3	-44.8	-44.4	-44.4	-45.3	-46.1	-49.4
28.5-33.5			-48.1	-42.1	-35.3	-34.4	-32.6	-34.4	-36.1	-35.7	-37.5	-48.0
	$\overline{T}$(CLOUDS)											
38.5-43.5	0.0	-61.5	-60.2	-61.0	-58.2	-52.4	-55.0	-56.7	-55.8	-56.2	-56.0	-54.5
33.5-38.5	-45.0	-55.7	-55.4	-52.3	-50.9	-50.6	-43.9	-44.7	-46.0	-49.7	-48.5	-51.0
28.5-33.5			-49.2	-42.0	-39.8	-32.4	-32.2	-32.7	-35.3	-37.1	-40.5	-48.1
	$\overline{\Delta Z}$(CLEAR)											
38.5-43.5	7.5	6.0	4.8	-1.5	-8.4	-10.8	-12.4	-19.4	-19.6	-15.9	-12.9	1.0
33.5-38.5	5.1	2.5	1.1	-6.8	-12.5	-13.6	-19.9	-20.7	-19.9	-19.4	-14.9	-2.4
28.5-33.5			-3.5	-11.0	-20.1	-21.2	-24.4	-24.4	-23.4	-22.7	-19.0	-6.2
	$\overline{\Delta Z}$(CLOUDS)											
38.5-43.5	0.0	-.6	1.6	-5.8	-12.2	-14.9	-16.3	-17.9	-19.9	-17.8	-17.9	-1.7
33.5-38.5	4.7	-.7	-2.3	-8.1	-11.1	-12.4	-20.0	-20.6	-18.0	-19.3	-14.7	-6.4
28.5-33.5			-3.6	-10.4	-13.9	-23.0	-25.0	-25.1	-23.6	-22.5	-18.4	-9.2

TABLE IV.- Concluded

AUTUMN												
LATITUDE:	75N	65N	55N	45N	35N	25N	15N	5N	5S	15S	25S	35S
ALT.(KFT)												
	N											
38.5-43.5	4	320	1255	1729	647	221	80	96	88	77	37	105
33.5-38.5	54	379	2490	2493	1215	738	269	161	202	187	132	94
28.5-33.5	9	343	1396	1558	587	293	255	90	55	80	101	120
	$\overline{TIC}$,%											
38.5-43.5	0.0	.0	.4	2.1	2.5	2.7	5.9	4.7	2.4	8.1	.0	.0
33.5-38.5	.0	2.2	5.1	6.3	6.4	3.1	6.7	10.3	7.3	8.6	5.7	5.7
28.5-33.5	0.0	16.1	8.1	10.8	4.9	5.8	5.8	9.9	11.2	2.8	13.3	5.8
	SIGMA,%											
38.5-43.5	0.0	.7	3.9	10.6	12.7	12.0	16.5	16.5	13.3	23.3	.1	.3
33.5-38.5	.1	11.6	17.5	19.1	19.4	13.0	20.1	23.1	20.3	21.8	20.4	19.7
28.5-33.5	0.0	30.9	21.0	25.4	17.8	18.1	18.4	21.6	20.3	12.5	26.3	20.0
	TICIV,%											
38.5-43.5	0.0	12.2	18.5	25.8	39.8	23.5	27.7	49.7	35.0	47.8	.8	2.0
33.5-38.5	.4	36.6	38.9	36.8	35.9	27.6	38.5	36.7	44.7	38.4	62.3	44.5
28.5-33.5	0.0	56.8	36.7	46.2	40.8	38.8	38.0	34.4	25.6	37.9	53.5	62.9
	SIGMA,%											
38.5-43.5	0.0	0.0	17.7	27.7	32.7	28.0	26.0	25.9	38.3	36.3	0.0	1.6
33.5-38.5	0.0	31.0	31.8	31.9	32.2	28.6	33.1	30.5	29.3	31.1	32.4	36.1
28.5-33.5	0.0	32.5	30.9	33.7	33.9	30.0	31.5	27.9	24.0	27.7	25.3	27.8
	P(TIC>0%)											
38.5-43.5	0.0	.3	2.4	8.2	6.3	11.3	21.3	9.4	6.8	16.9	2.7	1.9
33.5-38.5	1.9	6.1	13.1	17.2	17.9	11.4	17.5	28.0	16.3	22.5	9.1	12.8
28.5-33.5	0.0	28.3	22.0	23.4	12.1	15.0	15.3	28.9	43.6	7.5	24.8	9.2
	P(TIC>10%)											
38.5-43.5	0.0	.3	1.4	4.7	4.6	5.4	13.8	8.3	3.4	13.0	0.0	0.0
33.5-38.5	0.0	5.0	9.8	12.3	12.5	7.2	11.9	21.1	12.4	15.5	8.3	8.5
28.5-33.5	0.0	24.8	16.0	18.8	9.0	11.9	11.4	18.9	30.9	6.3	21.8	8.3
	P(TIC>25%)											
38.5-43.5	0.0	0.0	.6	3.2	3.6	3.6	8.8	7.3	3.4	10.4	0.0	0.0
33.5-38.5	0.0	3.4	7.2	8.7	8.7	4.2	8.9	14.9	11.9	12.8	6.8	7.4
28 5-33.5	0.0	21.9	11.9	15.0	6.8	8.5	7.8	15.6	16.4	5.0	21.8	7.5
	P(TIC>50%)											
38.5-43.5	0.0	0.0	.1	1.6	2.8	2.7	5.0	5.2	2.3	9.1	0.0	0.0
33.5-38.5	0.0	1.3	4.7	5.8	6.1	2.6	6.7	9.3	7.4	7.5	6.1	7.4
28.5-33.5	0.0	16.3	7.4	10.2	4.8	5.1	5.5	8.9	7.3	2.5	13.9	6.7
	$\overline{T}$(CLEAR)											
38.5-43.5	-51.5	-50.1	-53.0	-56.6	-57.3	-56.6	-56.5	-55.9	-55.7	-58.2	-56.1	-51.2
33.5-38.5	-57.3	-53.6	-51.4	-52.1	-50.6	-47.0	-46.1	-46.6	-45.4	-45.7	-47.0	-51.8
28.5-33.5	-59.0	-50.6	-47.6	-46.6	-44.5	-39.2	-32.8	-32.6	-33.9	-36.7	-41.1	-48.6
	$\overline{T}$(CLOUDS)											
38.5-43.5	0.0	-59.0	-63.1	-63.4	-56.2	-58.2	-58.1	-56.2	-57 0	-57.2	-56.0	-53.0
33.5-38.5	-62.0	-59.2	-57.8	-55.7	-51.3	-48.8	-48.4	-47.2	-43.0	-44.7	-48.2	-53.3
28.5-33.5	0.0	-52.4	-48.0	-48.1	-43.0	-41.5	-34.1	-32.2	-31.0	-32.0	-36.5	-47.9
	$\overline{\Delta Z}$(CLEAR)											
38.5-43.5	8.3	5.2	3.8	-.3	-7.6	-11.5	-15.7	-16.9	-17.6	-15.2	-10.8	2.9
33.5-38.5	4.2	3.1	-.5	-4.0	-10.2	-16.1	-19.2	-19.1	-18.7	-18.3	-13.0	-3.6
28.5-33.5	3.3	.9	-2.7	-6.7	-10.6	-20.0	-23.4	-23.1	-21.9	-21.3	-18.6	-7.5
	$\overline{\Delta Z}$(CLOUDS)											
38.5-43.5	0.0	-2.7	-1.9	-4.6	-12.8	-12.1	-16.3	-16.9	-17.0	-16.9	-17.6	5.6
33.5-38.5	.6	-.4	-3.3	-6.5	-11.6	-15.4	-18.7	-18.2	-15.4	-18.1	-16.5	-5.2
28.5-33.5	0.0	-4.0	-6.6	-7.6	-13.5	-16.1	-22.6	-20.9	-21.2	-22.2	-21.1	-10.1

TABLE V. - SUMMARY OF ZONAL MEAN CLOUD-ENCOUNTER STATISTICS BY SEASON AS FUNCTIONS OF LATITUDE AND DISTANCE FROM NMC TROPOPAUSE

[Data from appendix E (Vol. II)]

WINTER LATITUDE: TROP DIST(KFT)	75N	65N	55N	45N	35N	25N	15N	5N	5S	15S	25S	35S
N												
0- 5 ABV	6	365	936	1399	1049	100	0	0	0	0	2	68
0- 5 BLW	0	51	400	1097	1836	387	3	0	0	0	17	188
5-10 BLW	0	0	178	524	1218	773	35	8	0	0	17	285
10-15 BLW	0	0	44	232	547	1003	142	27	15	104	63	372
$\overline{TIC}$,%												
0- 5 ABV	0.0	.8	2.0	1.4	.3	0.0					0.0	0.0
0- 5 BLW		11.3	15.4	15.8	9.3	5.2	0.0				0.0	2.3
5-10 BLW			26.8	28.5	11.9	7.2	1.2	0.0			0.0	5.1
10-15 BLW			24.6	20.6	11.5	12.6	6.0	28.7	47.5	29.3	2.6	4.6
SIGMA,%												
0- 5 ABV	0.0	6.1	12.6	9.4	3.7	0.0					0.0	0.0
0- 5 BLW		24.9	29.8	29.9	23.7	16.9	0.0				0.0	9.9
5-10 BLW			35.1	37.7	25.2	19.0	4.9	0.0			0.0	17.9
10-15 BLW			32.0	32.7	24.6	25.8	17.3	34.4	23.2	33.1	7.2	16.5
TICIV,%												
0- 5 ABV	0.0	32.6	52.1	35.5	28.5	0.0					0.0	0.0
0- 5 BLW		52.4	50.1	47.2	43.1	36.7	0.0				0.0	22.6
5-10 BLW			50.2	59.0	42.4	33.0	10.2	0.0			0.0	41.8
10-15 BLW			51.5	49.8	41.6	42.4	26.7	59.7	47.5	42.3	16.4	33.6
SIGMA,%												
0- 5 ABV	0.0	21.4	39.3	31.6	22.5	0.0					0.0	0.0
0- 5 BLW		26.6	33.8	34.4	33.6	29.3	0.0				0.0	22.6
5-10 BLW			33.7	33.8	31.4	28.4	10.8	0.0			0.0	32.7
10-15 BLW			27.6	33.5	30.7	31.1	27.9	24.7	23.2	32.2	10.1	31.8
P(TIC>0%)												
0- 5 ABV	0.0	2.5	3.8	4.0	1.0	0.0					0.0	0.0
0- 5 BLW		21.6	30.8	33.5	21.7	14.2	0.0				0.0	10.1
5-10 BLW			53.4	48.3	28.0	21.9	11.4	0.0			0.0	12.3
10-15 BLW			47.7	41.4	27.6	29.7	22.5	48.1	100.0	69.2	15.9	13.7
P(TIC>10%)												
0- 5 ABV	0.0	2 5	2.8	2.9	.9	0.0					0.0	0.0
0- 5 BLW		21.6	25.0	25.4	16.4	11.1	0.0				0.0	7.4
5-10 BLW			41.6	42.6	22.4	15.7	2.9	0.0			0.0	9.1
10-15 BLW			40.9	33.2	21.9	23.6	13.4	48.1	93.3	56.7	9.5	8.9
P(TIC>25%)												
0- 5 ABV	0.0	.8	2.5	2.1	.5	0.0					0.0	0.0
0- 5 BLW		15.7	21.0	21.2	12.7	7.8	0.0				0.0	2.7
5-10 BLW			36.5	36.3	16.6	10.6	2.9	0.0			0.0	7.4
10-15 BLW			38.6	28.9	16.8	18.0	9.9	40.7	86.7	41.3	3.2	6.2
P(TIC>50%)												
0- 5 ABV	0.0	.5	2.0	1.2	.2	0.0					0.0	0.0
0- 5 BLW		11.8	15.5	16.0	9.3	4.7	0.0				0.0	1.6
5-10 BLW			26.4	30.3	11.3	5.7	0.0	0.0			0.0	4.9
10-15 BLW			22.7	21.1	10.8	12.3	5.6	33.3	40.0	26.0	0.0	4.3
$\overline{T}$(CLEAR)												
0- 5 ABV	-54.5	-56.1	-52.9	-53.3	-54.5	-52.0					-54.5	-55.4
0- 5 BLW		-55.1	-56.2	-55.2	-54.9	-51.8	-59.0				-63.7	-56.9
5-10 BLW			-51.9	-48.4	-50.5	-50.5	-56.6	-57.8			-60.4	-53.1
10-15 BLW			-41.9	-41.5	-45.9	-48.0	-51.1	-53.9	0.0	-64.4	-52.9	-48.2
$\overline{T}$(CLOUDS)												
0- 5 ABV	0.0	-61.9	-60.5	-62.8	-65.0	0.0					0.0	0.0
0- 5 BLW		-62.0	-60.5	-59.6	-59.2	-53.8	0.0				0.0	-53.2
5-10 BLW			-55.3	-52.7	-52.2	-53.1	-56.0	0.0			0.0	-50.2
10-15 BLW			-45.3	-47.3	-47.3	-49.0	-56.2	-63.0	-63.6	-65.8	-52.1	-44.4
$\overline{\Delta Z}$(CLEAR)												
0- 5 ABV	2.7	2.6	2.8	2.3	2.2	1.6					1.1	2.3
0- 5 BLW		-1.3	-2.2	-2.2	-2.4	-3.1	-3.2				-3.1	-3.2
5-10 BLW			-6.9	-7.1	-7.3	-7.7	-6.4	-7.2			-8.1	-7.4
10-15 BLW			-11.6	-11.9	-12.2	-12.6	-13.1	-13.0	0.0	-14.0	-13.2	-12.4
$\overline{\Delta Z}$(CLOUDS)												
0- 5 ABV	0.0	.9	.8	1.4	1.3	0.0					0.0	0.0
0- 5 BLW		-1.2	-2.6	-2.8	-3.0	-3.3	0.0				0.0	-3.3
5-10 BLW			-6.8	-7.2	-7.4	-8.0	-7.9	0.0			0.0	-7.5
10-15 BLW			-12.0	-12.0	-12.1	-12.4	-13.5	-13.6	-13.6	-13.9	-12.2	-13.0

TABLE V.- Continued

SPRING LATITUDE: TROP DIST(KFT)	75N	65N	55N	45N	35N	25N	15N	5N	5S	15S	25S	35S
	N											
0- 5 ABV	12	289	1616	2214	1398	93	0	0	0	0	5	72
0- 5 BLW	11	42	781	2193	2018	590	8	0	0	0	7	42
5-10 BLW	0	0	243	898	1388	1066	38	0	0	0	15	36
10-15 BLW	0	0	34	252	493	1028	446	79	21	106	48	23
	$\overline{TIC}$,%											
0- 5 ABV	0.0	.0	1.4	1.6	1.6	1.3					0.0	0.0
0- 5 BLW	.1	16.5	8.3	9.0	6.2	4.3	0.0				0.0	0.0
5-10 BLW			12.9	16.8	6.1	4.1	3.8				0.0	2.5
10-15 BLW			4.3	9.5	7.7	6.4	7.0	20.8	23.4	13.1	.2	3.8
	SIGMA,%											
0- 5 ABV	0.0	.1	9.5	10.0	10.5	7.4					0.0	0.0
0- 5 BLW	.5	32.5	21.7	22.5	19.3	16.2	0.0				0.0	0.0
5-10 BLW			23.7	28.1	17.7	13.7	16.6				0.0	7.2
10-15 BLW			14.2	22.3	20.8	18.3	20.3	34.4	32.4	23.4	1.0	17.9
	TICIV,%											
0- 5 ABV	0.0	.6	34.8	35.1	36.4	24.2					0.0	0.0
0- 5 BLW	1.6	69.2	34.2	39.5	35.7	35.4	0.0				0.0	0.0
5-10 BLW			29.1	38.5	29.8	25.5	36.1				0.0	15.0
10-15 BLW			20.8	35.7	34.1	30.4	38.2	54.8	40.9	35.6	4.5	87.8
	SIGMA,%											
0- 5 ABV	0.0	.4	34.0	31.1	36.2	21.8					0.0	0.0
0- 5 BLW	0.0	28.0	32.3	32.0	32.8	32.7	0.0				0.0	0.0
5-10 BLW			28.1	31.3	28.7	25.2	38.3				0.0	11.1
10-15 BLW			25.1	30.6	31.8	29.6	32.4	35.4	33.5	26.1	2.5	0.0
	P(TIC>0%)											
0- 5 ABV	0.0	2.4	3.9	4.7	4.3	5.4					0.0	0.0
0- 5 BLW	9.1	23.8	24.3	22.8	17.4	12.0	0.0				0.0	0.0
5-10 BLW			44.4	43.5	20.5	15.9	10.5				0.0	16.7
10-15 BLW			20.6	26.6	22.7	20.9	18.4	38.0	57.1	36.8	4.2	4.3
	P(TIC>10%)											
0- 5 ABV	0.0	0.0	2.4	3.3	2.5	3.2					0.0	0.0
0- 5 BLW	0.0	21.4	15.7	17.3	11.5	7.6	0.0				0.0	0.0
5-10 BLW			27.2	32.3	13.7	9.4	5.3				0.0	11.1
10-15 BLW			8.8	18.3	15.2	13.5	12.8	29.1	38.1	29.2	0.0	4.3
	P(TIC>25%)											
0- 5 ABV	0.0	0.0	1.8	2.3	2.0	1.1					0.0	0.0
0- 5 BLW	0.0	21.4	11.5	12.9	8.9	5.9	0.0				0.0	0.0
5-10 BLW			19.3	24.4	9.1	6.7	5.3				0.0	2.8
10-15 BLW			8.8	15.1	10.5	9.6	10.1	27.8	33.3	18.9	0.0	4.3
	P(TIC>50%)											
0- 5 ABV	0.0	0.0	1.2	1.6	1.6	1.1					0.0	0.0
0- 5 BLW	0.0	19.0	7.9	8.5	5.7	3.7	0.0				0.0	0.0
5-10 BLW			9.5	14.9	4.6	3.0	2.6				0.0	0.0
10-15 BLW			2.9	8.7	7.3	5.2	6.5	21.5	23.8	14.2	0.0	4.3
	$\overline{T}$(CLEAR)											
0- 5 ABV	-59.1	-52.4	-53.6	-55.1	-56.0	-57.6					-54.2	-58.6
0- 5 BLW	-57.8	-57.1	-57.4	-56.6	-57.0	-56.5	-58.6				-54.6	-57.2
5-10 BLW			-52.5	-51.4	-52.3	-53.5	-55.3				-54.2	-54.5
10-15 BLW			-37.3	-42.1	-45.2	-49.5	-49.9	-56.6	-48.4	-62.0	-56.6	-49.3
	$\overline{T}$(CLOUDS)											
0- 5 ABV	0.0	-55.9	-62.4	-60.8	-61.2	-61.8					0.0	0.0
0- 5 BLW	-59.0	-57.0	-58.1	-59.4	-60.2	-57.3	0.0				0.0	0.0
5-10 BLW			-52.6	-51.7	-53.2	-55.0	-61.0				0.0	-60.8
10-15 BLW			-32.9	-43.0	-45.1	-49.2	-50.4	-50.4	-63.6	-59.8	-58.0	-61.0
	$\overline{\Delta Z}$(CLEAR)											
0- 5 ABV	1.6	3.0	2.7	2.3	2.1	1.3					1.5	2.1
0- 5 BLW	-1.3	-2.1	-1.9	-2.2	-2.5	-2.8	-3.9				-3.2	-2.6
5-10 BLW			-6.6	-7.2	-7.3	-7.9	-8.6				-7.1	-7.4
10-15 BLW			-12.7	-12.2	-12.1	-12.4	-12.8	-13.5	-14.6	-13.9	-12.4	-12.9
	$\overline{\Delta Z}$(CLOUDS)											
0- 5 ABV	0.0	2.8	1.3	1.7	1.1	.4					0.0	0.0
0- 5 BLW	-.7	-3.0	-2.6	-3.0	-2.7	-2.9	0.0				0.0	0.0
5-10 BLW			-6.7	-7.1	-7.1	-7.6	-8.3				0.0	-7.5
10-15 BLW			-12.8	-12.2	-12.1	-12.8	-13.3	-12.4	-14.6	-12.9	-14.3	-14.8

TABLE V.- Continued

SUMMER LATITUDE: TROP DIST(KFT)	75N	65N	55N	45N	35N	25N	15N	5N	5S	15S	25S	35S
N												
0- 5 ABV	11	750	1341	699	117	0	0	0	0	0	2	123
0- 5 BLW	0	110	391	1103	399	18	0	0	0	0	6	160
5-10 BLW	0	0	102	854	708	431	19	1	0	2	65	117
10-15 BLW	0	0	12	653	1206	753	26	2	17	17	93	70
$\overline{TIC}$,%												
0- 5 ABV	.0	.0	.3	1.2	.5						0.0	.0
0- 5 BLW		2.3	3.8	5.7	4.7	1.0					0.0	.9
5-10 BLW			8.0	8.0	2.3	.7	1.1	0.0		0.0	.8	.8
10-15 BLW			5.9	10.1	4.0	2.9	1.4	0.0	18.7	0.0	.1	1.1
SIGMA,%												
0- 5 ABV	.1	.1	3.3	7.7	4.6						0.0	.0
0- 5 BLW		10.6	12.5	16.8	15.2	3.5					0.0	7.5
5-10 BLW			19.2	19.7	9.8	6.3	4.6	0.0		0.0	4.7	4.0
10-15 BLW			19.7	23.0	14.9	13.1	4.2	0.0	27.3	0.0	.5	6.9
TICIV,%												
0- 5 ABV	.4	2.0	13.6	22.9	27.6						0.0	.4
0- 5 BLW		15.0	18.4	32.0	35.9	6.3					0.0	18.0
5-10 BLW			26.5	31.0	23.9	17.7	20.4	0.0		0.0	17.8	15.4
10-15 BLW			71.4	34.4	31.9	29.0	12.2	0.0	31.8	0.0	3.5	25.6
SIGMA,%												
0- 5 ABV	0.0	1.3	16.7	25.6	22.2						0.0	0.0
0- 5 BLW		23.3	21.9	27.3	25.6	6.4					0.0	28.5
5-10 BLW			26.8	28.1	22.1	25.3	0.0	0.0		0.0	13.5	9.3
10-15 BLW			0.0	31.2	29.8	30.7	4.7	0.0	29.1	0.0	.8	22.3
P(TIC>0%)												
0- 5 ABV	9.1	.4	2.4	5.2	1.7						0.0	.8
0- 5 BLW		15.5	20.7	17.7	13.0	16.7					0.0	5.0
5-10 BLW			30.4	25.8	9.6	4.2	5.3	0.0		0.0	4.6	5.1
10-15 BLW			8.3	29.2	12.4	10.1	11.5	0.0	58.8	0.0	2.2	4.3
P(TIC>10%)												
0- 5 ABV	0.0	0.0	1.0	3.0	.9						0.0	0.0
0- 5 BLW		5.5	8.4	12.7	9.5	5.6					0.0	2.5
5-10 BLW			16.7	16.9	5.9	1.6	5.3	0.0		0.0	3.1	3.4
10-15 BLW			8.3	19.1	7.9	6.2	7.7	0.0	35.3	0.0	0.0	2.9
P(TIC>25%)												
0- 5 ABV	0.0	0.0	.3	1.7	.9						0.0	0.0
0- 5 BLW		3.6	5.6	8.3	8.0	0.0					0.0	.6
5-10 BLW			11.8	12.5	4.0	1.2	0.0	0.0		0.0	1.5	.9
10-15 BLW			8.3	14.5	5.8	3.9	0.0	0.0	29.4	0.0	0.0	1.4
P(TIC>50%)												
0- 5 ABV	0.0	0.0	.1	.7	0.0						0.0	0.0
0- 5 BLW		1.8	1.8	4.4	3.8	0.0					0.0	.6
5-10 BLW			5.9	7.1	1.4	.5	0.0	0.0		0.0	0.0	0.0
10-15 BLW			8.3	9.8	3.3	2.5	0.0	0.0	23.5	0.0	0.0	1.4
$\overline{T}$(CLEAR)												
0- 5 ABV	-44.7	-50.8	-51.9	-53.9	-52.6						-50.0	-49.2
0- 5 BLW		-57.6	-54.4	-54.4	-53.9	-52.6					-47.0	-51.4
5-10 BLW			-49.1	-52.6	-52.9	-52.7	-58.5	-60.0		-48.0	-47.0	-49.2
10-15 BLW			-33.9	-48.8	-50.1	-49.3	-55.9	-60.5	-47.3	-53.1	-47.5	-43.6
$\overline{T}$(CLOUDS)												
0- 5 ABV	-45.0	-57.0	-59.3	-59.2	-55.5						0.0	-54.0
0- 5 BLW		-59.1	-54.9	-56.6	-55.6	-51.7					0.0	-53.5
5-10 BLW			-45.5	-54.2	-52.4	-52.7	-66.0	0.0		0.0	-48.0	-48.3
10-15 BLW			-31.0	-49.7	-51.8	-50.6	-38.7	0.0	-48.3	0.0	-47.0	-37.7
$\overline{\Delta Z}$(CLEAR)												
0- 5 ABV	4.7	3.2	2.8	2.0	2.3						.7	2.2
0- 5 BLW		-1.9	-1.9	-2.5	-3.1	-3.8					-3.0	-2.8
5-10 BLW			-6.8	-7.6	-7.8	-7.9	-9.0	-9.7		-8.8	-8.2	-7.1
10-15 BLW			-12.2	-12.5	-12.7	-12.7	-12.7	-12.9	-13.7	-13.0	-12.7	-12.3
$\overline{\Delta Z}$(CLOUDS)												
0- 5 ABV	4.7	1.9	1.2	1.3	.7						0.0	4.7
0- 5 BLW		-1.4	-2.3	-2.7	-2.9	-3.3					0.0	-3.0
5-10 BLW			-7.1	-7.4	-8.0	-8.3	-8.9	0.0		0.0	-9.4	-8.0
10-15 BLW			-10.9	-12.3	-12.9	-12.9	-14.7	0.0	-13.3	0.0	-12.7	-12.1

TABLE V.- Concluded

AUTUMN LATITUDE: TROP DIST(KFT)	75N	65N	55N	45N	35N	25N	15N	5N	5S	15S	25S	35S
N												
0- 5 ABV	39	538	1619	1230	146	4	0	0	0	0	4	57
0- 5 BLW	0	203	1656	1798	422	24	0	0	0	0	14	105
5-10 BLW	0	45	712	1486	694	106	0	0	0	0	32	83
10-15 BLW	0	0	214	757	732	402	47	9	39	55	78	34
$\overline{TIC}$,%												
0- 5 ABV	.0	.9	.6	.6	0.0	0.0					0.0	.0
0- 5 BLW		16.5	8.0	6.7	1.2	.9					0.0	1.2
5-10 BLW		55.6	14.3	12.5	5.0	3.9					0.0	8.0
10-15 BLW			7.5	9.3	7.5	5.3	6.7	0.0	22.5	2.3	2.3	11.4
SIGMA,%												
0- 5 ABV	.1	6.9	5.5	5.3	0.0	0.0					0.0	.1
0- 5 BLW		29.9	21.3	20.3	8.0	4.4					0.0	8.9
5-10 BLW		38.6	27.0	26.3	18.0	14.7					0.0	22.5
10-15 BLW			19.0	22.8	20.4	17.2	19.6	0.0	30.1	9.5	13.2	26.7
TICIV,%												
0- 5 ABV	.4	31.7	29.8	23.9	0.0	0.0					0.0	5
0- 5 BLW		49.3	39.5	37.3	32.3	22.0					0.0	31.6
5-10 BLW		67.6	38.5	42.3	41.2	34.1					0.0	60.2
10-15 BLW			28.1	41.1	35.6	29.8	35.0	0.0	46.2	25.3	45.3	64.4
SIGMA,%												
0- 5 ABV	0.0	24.6	26.3	23.8	0.0	0.0					0.0	.2
0- 5 BLW		32.3	31.5	33.8	26.0	0.0					0.0	33.3
5-10 BLW		31.6	32.0	33.0	34.3	29.8					0.0	26.0
10-15 BLW			27.8	31.6	31.1	30.4	32.0	0.0	27.7	20.1	38.0	25.0
P(TIC>0%)												
0- 5 ABV	2.6	3.0	1.9	2.5	0.0	0.0					0.0	5.3
0- 5 BLW		33.5	20.2	18.0	3.8	4.2					0.0	3.8
5-10 BLW		82.2	37.2	29.5	12.1	11.3					0.0	13.3
10-15 BLW			26.6	22.6	21.2	17.9	19.1	0.0	48.7	9.1	5.1	17.6
P(TIC>10%)												
0- 5 ABV	0.0	2.2	1.3	1.5	0.0	0.0					0.0	0.0
0- 5 BLW		29.1	15.5	12.4	2.8	4.2					0.0	1.9
5-10 BLW		75.6	27.2	22.7	8.8	8.5					0.0	12.0
10-15 BLW			16.4	17.3	15.2	10.0	10.6	0.0	41.0	7.3	3.8	17.6
P(TIC>25%)												
0- 5 ABV	0.0	1.7	1.0	1.0	0.0	0.0					0.0	0.0
0- 5 BLW		23.2	11.4	9.1	2.1	0.0					0.0	1.9
5-10 BLW		71.1	19.9	17.6	6.6	5.7					0.0	10.8
10-15 BLW			11.2	13.3	10.4	8.2	8.5	0.0	38.5	3.6	2.6	14.7
P(TIC>50%)												
0- 5 ABV	0.0	.6	.4	.5	0.0	0.0					0.0	0.0
0- 5 BLW		16.3	7.4	6.1	.9	0.0					0.0	1.0
5-10 BLW		55.6	13.5	11.5	5.2	3.8					0.0	10.8
10-15 BLW			6.1	9.1	7.1	4.7	8.5	0.0	20.5	1.8	2.6	14.7
$\overline{T}$(CLEAR)												
0- 5 ABV	-57.7	-53.0	-52.0	-54.4	-54.6	-61.3					-48.3	-51.2
0- 5 BLW		-53.9	-52.4	-54.4	-55.1	-58.7					-50.4	-51.9
5-10 BLW		-52.9	-48.6	-50.5	-51.5	-54.7					-53.6	-49.9
10-15 BLW			-40.2	-45.6	-49.5	-50.3	-57.4	-52.1	-42.3	-53.8	-47.3	-43.8
$\overline{T}$(CLOUDS)												
0- 5 ABV	-62.0	-57.7	-59.2	-62.3	0.0	0.0					0.0	-52.0
0- 5 BLW		-54.8	-57.5	-58.5	-57.7	-58.0					0.0	-57.3
5-10 BLW		-50.1	-49.0	-51.2	-53.1	-55.1					0.0	-50.0
10-15 BLW			-40.9	-48.5	-49.2	-50.2	-56.8	0.0	-42.5	-40.0	-49.5	-43.2
$\overline{\Delta Z}$(CLEAR)												
0- 5 ABV	3.2	2.8	2.4	2.1	1.5	.4					1.6	3.0
0- 5 BLW		-1.5	-2.3	-2.5	-3.0	-2.3					-2.5	-2.3
5-10 BLW		-6.2	-7.2	-7.4	-7.8	-8.2					-8.3	-7.5
10-15 BLW			-11.9	-12.3	-12.5	-12.7	-13.7	-13.5	-14.6	-13.5	-13.2	-12.1
$\overline{\Delta Z}$(CLOUDS)												
0- 5 ABV	.6	1.0	.7	1.0	0.0	0.0					0.0	3.1
0- 5 BLW		-2.5	-2.7	-3.2	-3.4	-2.7					0.0	-3.2
5-10 BLW		-6.6	-7.2	-7.6	-8.4	-8.5					0.0	-7.7
10-15 BLW			-12.6	-11.6	-12.4	-13.3	-14.6	0.0	-14.8	-13.6	-13.6	-12.2

TABLE VI.- CUMULATIVE FREQUENCY DISTRIBUTION OF MEAN PARTICLE CONCENTRATIONS[a] AS A FUNCTION OF THE AVERAGE TIME IN CLOUDS (TIC) DURING AN OBSERVATION PERIOD (ALL GASP OBSERVATIONS INCLUDED)

PD5 (m^{-3})	Percentage of observation periods with - [b]							
	TIC = 0%	TIC > 0%	TIC ⩾ 10%	TIC ⩾ 25%	TIC ⩾ 50%	TIC ⩾ 75%	TIC ⩾ 90%	TIC ⩾ 100%
>0	31.5	90.0	94.0	96.9	99.0	100.0	100.0	100.0
$>10^2$	18.1	87.1	92.0	95.8	98.5	99.9	100.0	100.0
$>3 \times 10^2$	9.8	84.1	90.4	94.7	98.1	99.9	100.0	100.0
$>10^3$	4.8	80.2	88.1	93.0	97.1	99.9	100.0	100.0
$>3 \times 10^3$	2.4	76.0	85.2	91.1	96.3	99.8	100.0	100.0
$>10^4$	.7	68.9	80.1	87.3	94.0	99.5	100.0	100.0
$>3 \times 10^4$	.1	57.6	71.6	80.7	90.8	98.8	100.0	100.0
$>5 \times 10^4$	0.0	49.9	64.4	74.4	86.9	97.5	100.0	100.0
$>7 \times 10^4$	0.0	43.5	57.1	67.4	81.0	93.8	98.9	100.0
$>10^5$	0.0	36.6	48.9	58.3	71.6	86.1	92.7	100.0
$>3 \times 10^5$	0.0	15.2	20.6	25.6	33.0	41.5	32.6	7.1
$>7 \times 10^5$	0.0	4.3	5.8	7.2	9.1	10.1	3.2	
$>10^6$		2.4	3.3	4.2	5.3	5.5	1.1	
$>3 \times 10^6$		.3	.4	.6	.7	.6		
$\overline{PD5}$	449	164 722	218 194	265 206	325 829	379 870	281 870	211 736
σ(PD5)	16 403	359 583	407 224	451 673	478 388	483 474	197 044	64 922
N	47 374	8 302	5 989	4 429	2 884	1 592	565	42

[a]All particles with diameters >3 μm.

[b]Example: In clear air (TIC = 0%), there are $>3 \times 10^3$ particles/m^3 in 2.4% of cases.
For TIC > 0%, this concentration is exceeded in 76% of cases.
For TIC ⩾ 50%, this concentration is exceeded in 96.3% of cases.

TABLE VII.- CUMULATIVE PROBABILITY DISTRIBUTION OF TIC AS A FUNCTION OF ALTITUDE WITH ALL SEASONS AND LATITUDES INCLUDED

Altitude, kft	Percentage of observation periods with -										
	TIC = 0%	TIC > 0%	TIC > 10%	TIC > 20%	TIC > 30%	TIC > 40%	TIC > 50%	TIC > 60%	TIC > 70%	TIC > 80%	TIC > 90%
18.5 to 23.5 kft	68.4	31.6	29.0	27.2	27.2	25.4	22.8	21.9	20.2	18.4	18.3
23.5 to 28.5 kft	80.0	20.0	14.5	13.2	11.6	11.0	9.8	8.6	7.4	6.0	2.1
28.5 to 33.5 kft	78.8	21.2	16.0	13.2	11.2	9.4	8.0	6.7	5.3	3.9	1.6
33.5 to 38.5 kft	84.2	15.8	11.3	9.1	7.7	6.4	5.3	4.3	3.4	2.4	1.0
38.5 to 43.5 kft	91.5	8.5	6.1	5.0	4.2	3.5	3.0	2.5	1.9	1.4	.6
43.5 to 48.5 kft	100.0	0.0	0.0	0.0	0.0	0.0	0.0	0.0	0.0	0.0	0.0
Total	85.2	14.8	10.8	8.8	7.4	6.3	5.3	4.3	3.4	2.5	1.0

TABLE VIII.- ZONAL MEAN VALUES OF $\overline{TIC}$ AND PCE, FOR THREE ALTITUDE BANDS

Code: $\overline{TIC}$, % / PCE, % — No. of independent observations

Latitude	Winter						Spring						Summer						Autumn					
	Altitude, kft						Altitude, kft						Altitude, kft						Altitude, kft					
	28.5-33.5		33.5-38.5		38.5-43.5		28.5-33.5		33.5-38.5		38.5-43.5		28.5-33.5		33.5-38.5		38.5-43.5		28.5-33.5		33.5-38.5		38.5-43.5	
80°N-70°N			0.0 0.0	2			0.0 0.0	1	.1 .3	4					0.0 7.1	2	0.0 0.0	15	0.0 0.0	1	0.0 1.9	6	0.0 0.0	1
70°N-60°N	3.8 8.9	20	.2 .4	25	.9 1.6	13	16.9 26.8	5	0.0 2.2	35	0.0 0.0	29			0.4 2.7	39	0.1 0.6	139	16.1 28.3	32	2.2 6.1	36	0.0 0.3	31
60°N-50°N	10.0 21.4	83	6.8 12.5	108	0.0 0.0	50	5.2 20.0	64	4.8 13.2	171	0.0 0.5	129	4.2 31.0	38	2.0 10.3	99	0.1 1.1	148	8.1 22.0	152	5.1 13.1	213	0.4 2.4	106
50°N-40°N	13.7 28.3	206	9.1 18.2	211	4.6 6.9	92	11.6 32.4	203	6.8 18.0	320	3.6 8.9	234	6.7 22.0	99	8.5 25.8	185	2.7 9.9	160	10.8 23.4	199	6.3 17.2	238	2.1 8.2	143
40°N-30°N	10.2 23.9	248	7.8 19.7	291	3.1 6.0	133	5.0 20.1	207	4.6 14.4	381	4.3 9.8	195	2.2 6.7	158	3.1 9.6	244	2.7 10.2	91	4.9 12.1	132	6.4 17.9	145	2.5 6.3	74
30°N-20°N	7.8 17.8	182	7.8 20.7	199	0.8 2.7	48	4.7 18.7	130	5.6 18.0	198	1.5 6.9	69	5.9 15.8	98	1.8 6.5	126	1.1 9.1	12	5.8 15.0	43	3.1 11.4	68	2.7 11.3	20
20°N-10°N	4.5 7.7	73	2.9 9.1	84	3.0 14.3	26	6.8 19.2	41	6.0 20.0	78	8.3 21.2	33	22.5 50.5	22	20 2 51.9	19	5.7 17.9	3	5.8 15.3	30	6.7 17.5	27	5.9 21.3	8
10°N-0°	8.6 24.5	41	14.4 34.6	63	10.4 26.0	33	1.4 12.9	9	10.0 23.3	28	12.3 30.7	34	14.7 44.4	10	7.9 25.8	14	26.3 50.0	8	9.0 28.9	15	10.3 28.0	22	4.7 9.4	12
0°-10°S	17.1 46.8	33	12.6 33.6	51	19.2 40.7	24	11.1 30.0	1	10.8 33.7	16	14.9 40.4	28	4.3 19.0	20	10.1 27.3	16	37.9 73.4	6	11.2 43.6	5	7.3 16.3	16	2.4 6.8	10
10°S-20°S	6.1 20.8	62	11.6 25.4	67	22.4 54.3	33	4.0 13.7	18	7.7 27.5	20	13.5 35.4	41	1.1 4.4	19	0.4 2.0	14	9.8 26.8	4	2.8 7.5	16	8.6 22.5	20	8.1 16.9	8
20°S-30°S	7.3 17.2	63	4.9 12.2	62	3.3 12.5	12	0.3 4.5	7	3.0 8.3	9	0.1 3.9	9	0.5 4.2	18	0.5 3.6	22	0.1 2.7	3	13.3 24.8	12	5.7 9.1	12	0.0 2.7	4
30°S-40°S	7.6 19.0	89	3.5 8.5	78	0.8 2.1	33	14.9 26.7	11	0.4 6.3	5	2.8 4.9	18	4.1 14.7	27	0.1 0.7	33	0.0 2.2	8	5.8 9.2	25	5.7 12.8	14	0.0 1.9	10

TABLE IX.- ZONAL MEAN VALUES OF $\overline{TIC}$ AND PCE FOR FOUR TROPOPAUSE SEPARATION BANDS

Code: $\overline{TIC}$, % / PCE, % — No. of independent observations

Latitude	Winter				Spring				Summer				Autumn			
	Separation from tropopause, kft				Separation from tropopause, kft				Separation from tropopause, kft				Separation from tropopause, kft			
	10-15 BLO	5-10 BLO	0-5 BLO	0-5 ABV	10-15 BLO	5-10 BLO	0-5 BLO	0-5 ABV	10-15 BLO	5-10 BLO	0-5 BLO	0-5 ABV	10-15 BLO	5-10 BLO	0-5 BLO	0-5 ABV
80°N-70°N				0.0 1 0.0			0.1 2 9.1	0.0 3 0.0				0.0 3 9.1				0.0 5 2.6
70°N-60°N			11.3 12 21.6	0.8 38 2.5			16.5 6 23.8	0.0 37 2.4			2.3 11 15.5	0.0 84 0.4		55.6 11 82.2	16.5 30 33.5	0.9 62 3.0
60°N-50°N	24.6 16 47.7	25.8 40 53.4	15.4 58 30.8	2.0 98 3.8	4.3 18 20.6	12.9 51 44.4	8.3 109 24.3	1.4 170 3.9	5.9 10 8.3	8.0 38 30.4	3.8 90 20.7	0.3 145 2.4	7.5 58 26.6	14.3 113 37.2	8.0 188 20.2	0.6 173 1.9
50°N-40°N	20.6 77 41.4	28.5 118 48.3	15.8 177 33.5	1.4 177 4.0	9.5 122 26.6	16.8 200 43.5	9.0 313 22.8	1.6 280 4.7	10.1 117 29.2	8.0 149 25.8	5.7 164 17.7	1.2 110 5.2	9.3 165 22.6	12.5 232 29.5	6.7 216 18.0	0.6 147 2.5
40°N-30°N	11.5 144 27.6	11.9 208 28.0	9.3 238 21.7	0.3 128 1.0	7.7 161 22.7	6.1 270 20.5	6.2 313 17.4	1.6 205 4.3	4.0 168 12.4	2.3 126 9.6	4.7 63 13.0	0.5 20 1.7	7.5 143 21.2	5.0 130 12.1	1.2 76 3.8	0.0 27 0.0
30°N-20°N	12.6 152 29.7	7.2 111 21.9	5.2 66 14.2	0.0 15 0.0	6.4 164 20.9	4.1 190 15.9	4.3 75 16.2	1.3 18 5.4	2.9 80 10.1	0.7 43 4.2	1.0 5 16.7		5.3 42 17.9	3.9 21 11.3	0.9 6 4.2	0.0 2 0.0
20°N-10°N	6.0 23 22.5	1.2 6 11.4	0.0 1 0.0		7.0 63 18.4	3.8 12 16.6	0.0 2 0.0		1.4 4 11.5	1.1 2 5.3			6.7 6 19.1			
10°N-0°	28.7 7 48.1	0.0 2 0.0			20.8 12 38.0				0.0 1 0.0	0.0 1 0.0			0.0 2 0.0			
0°-10°S	47.5 1 100.0				23.4 2 57.1				18.7 1 58.8				22.5 4 48.7			
10°S-20°S	29.3 12 69.2				13.1 13 36.8				0.0 3 0.0	0.0 1 0.0			2.3 9 9.1			
20°S-30°S	2.6 17 15.9	0.0 6 0.0	0.0 4 0.0	0.0 1 0.0	0.2 8 4.2	0.0 3 0.0	0.0 2 0.0	0.0 1 0.0	0.1 17 2.2	0.8 13 4.6	0.0 2 0.0	0.0 14 0.0	2.3 14 13.2	0.0 8 0.0	0.0 3 0.0	0.0 2 0.0
30°S-40°S	4.6 59 13.7	5.1 40 12.3	2.3 25 10.1	0.0 11 0.0	3.8 12 4.3	2.5 11 16.7	0.0 8 0.0	0.0 10 0.0	1.1 24 4.3	0.8 27 5.1	0.9 28 5.0	0.0 15 0.8	11.4 16 17.6	8.0 18 13.3	1.2 16 3.8	0.0 8 5.3

TABLE X.- PROBABILITY OF ENCOUNTERING VARIOUS LEVELS OF AVERAGE CLOUDINESS ON SEVEN LONG-RANGE AIRLINE ROUTES, AS ESTIMATED FROM A GAMMA PROBABILITY DISTRIBUTION

Code:	No. of flights	$P(TIC_F \geq 5\ \%)$, %
	TIC_R, %	$P(TIC_F \geq 10\ \%)$, %
	$P(TIC_F < 1\ \%)$, %	$P(TIC_F \geq 25\ \%)$, %
	$P(TIC_F < 5\ \%)$, %	$P(TIC_F \geq 50\ \%)$, %

Route	Altitude, kft					
	28.5-33.5		33.5-38.5		38.5-43.5	
California - Hawaii	22	52.4	177	37.2	2	
	9.4	32.5	5.5	17.4		
	17.3	8.9	24.7	2.1		
	47.6	1.2	62.8	≈0		
East Coast - West Coast (USA)	3		58	46.2	13	14.0
			7.5	25.9	2.4	2.8
			20.1	5.3	41.3	≈0
			53.8	0.4	86.0	≈0
West Coast - Northwest Europe	6	53.8	26	16.9	26	17.8
	9.9	34.0	2.7	4.0	2.8	4.4
	16.7	9.9	38.6	0.1	37.7	0.1
	46.2	1.4	83.1	≈0	82.2	≈0
East Coast - Northwest Europe	38	52.1	99	47.7	24	23.1
	9.3	32.2	7.9	27.4	3.4	7.1
	17.5	8.7	19.5	6.0	33.5	0.3
	47.8	1.1	52.3	0.6	76.9	≈0
Australia - SE Asia	16	49.4	20	51.0	No data	
	8.4	29.2	8.9	30.9		
	18.7	7.0	18.0	7.9		
	50.6	0.7	49.0	0.9		
West Coast - Japan (westbound)	4		30	26.2	14	12.1
			3.8	9.1	2.2	2.1
			31.3	0.5	43.5	≈0
			73.8	≈0	87.9	≈0
West Coast - Japan (eastbound)	No data		12	51.0	29	24.7
			8.9	30.9	3.6	8.1
			18.0	7.9	32.3	0.3
			49.0	0.9	75.3	≈0

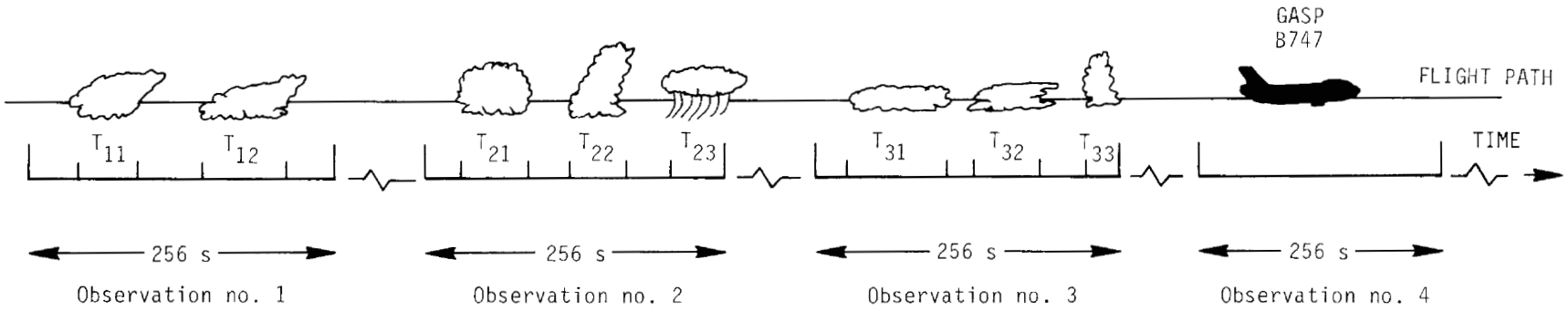

TIC_1 = Percent of time in clouds during observation 1 = $\frac{T_{11} + T_{12}}{256} \times 100$

TIC_2 = Percent of time in clouds during observation 2 = $\frac{T_{21} + T_{22} + T_{23}}{256} \times 100$

TIC_3 = Percent of time in clouds during observation 3 = $\frac{T_{31} + T_{32} + T_{33}}{256} \times 100$

TIC_4 = Percent of time in clouds during observation 4 = 0/256 = 0

$\overline{TIC}$ ≡ Average percent of time in clouds during all observations = $\frac{TIC_1 + TIC_2 + TIC_3 + TIC4}{4}$

PCE ≡ Probability of cloud encounter in an observation = $\frac{\text{3 Observations with clouds in vicinity}}{\text{4 Observations total}} = 0.75$

TICIV ≡ Average percent of nonzero time in clouds during an observation = $\frac{TIC_1 + TIC_2 + TIC_3}{3}$

INTERRELATION: $\overline{TIC} = PCE \times TICIV$

PROOF: $\frac{TIC_1 + TIC_2 + TIC_3 + TIC_4}{4} = 0.75 \times \frac{TIC_1 + TIC_2 + TIC_3 + \overbrace{TIC_4}^{0}}{3}$

Figure 1.- Example of interrelation of $\overline{TIC}$, PCE and TICIV for a set of four observation periods.

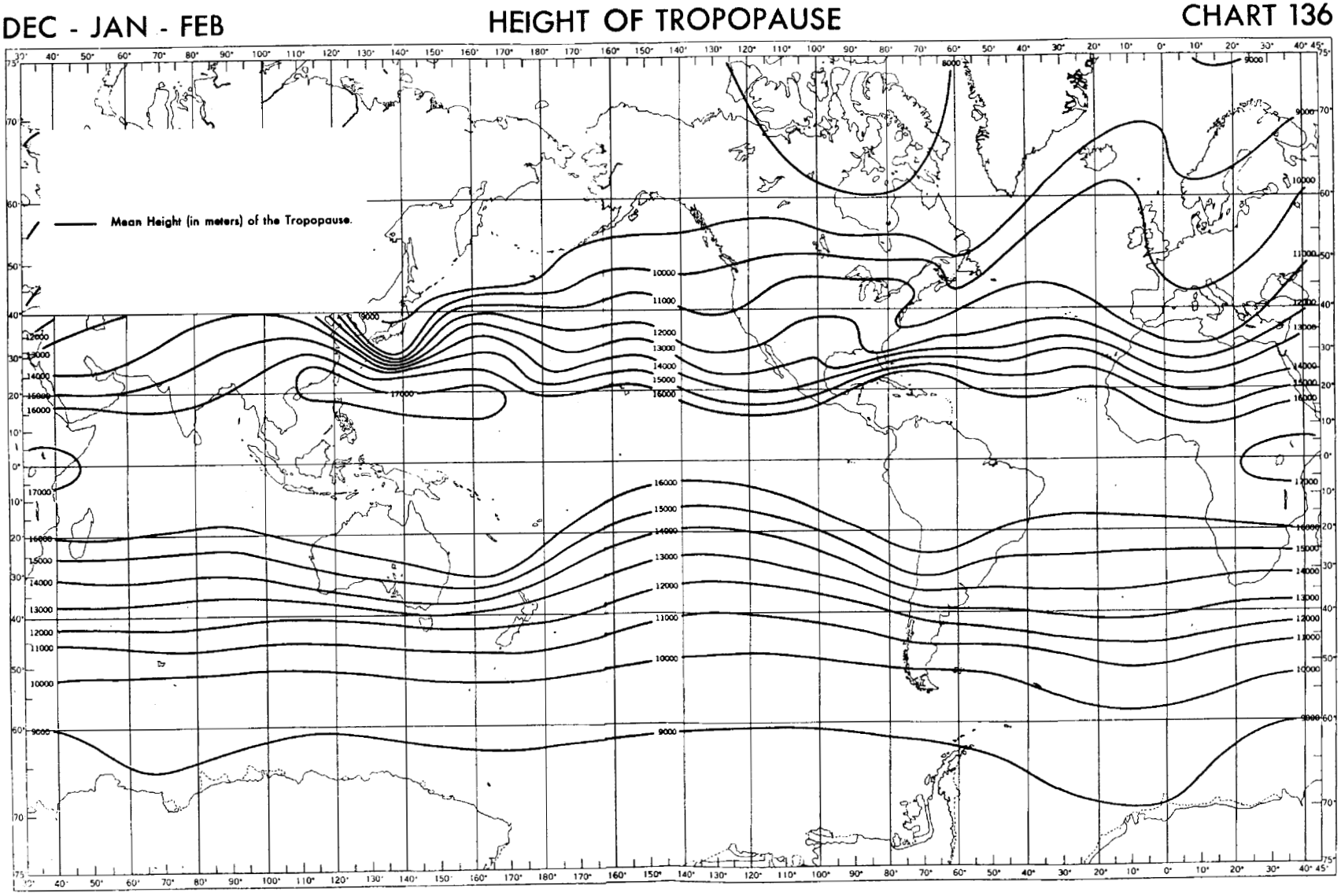

(a) Winter.

Figure 2.- The average height of the tropopause. (From ref. 37.)

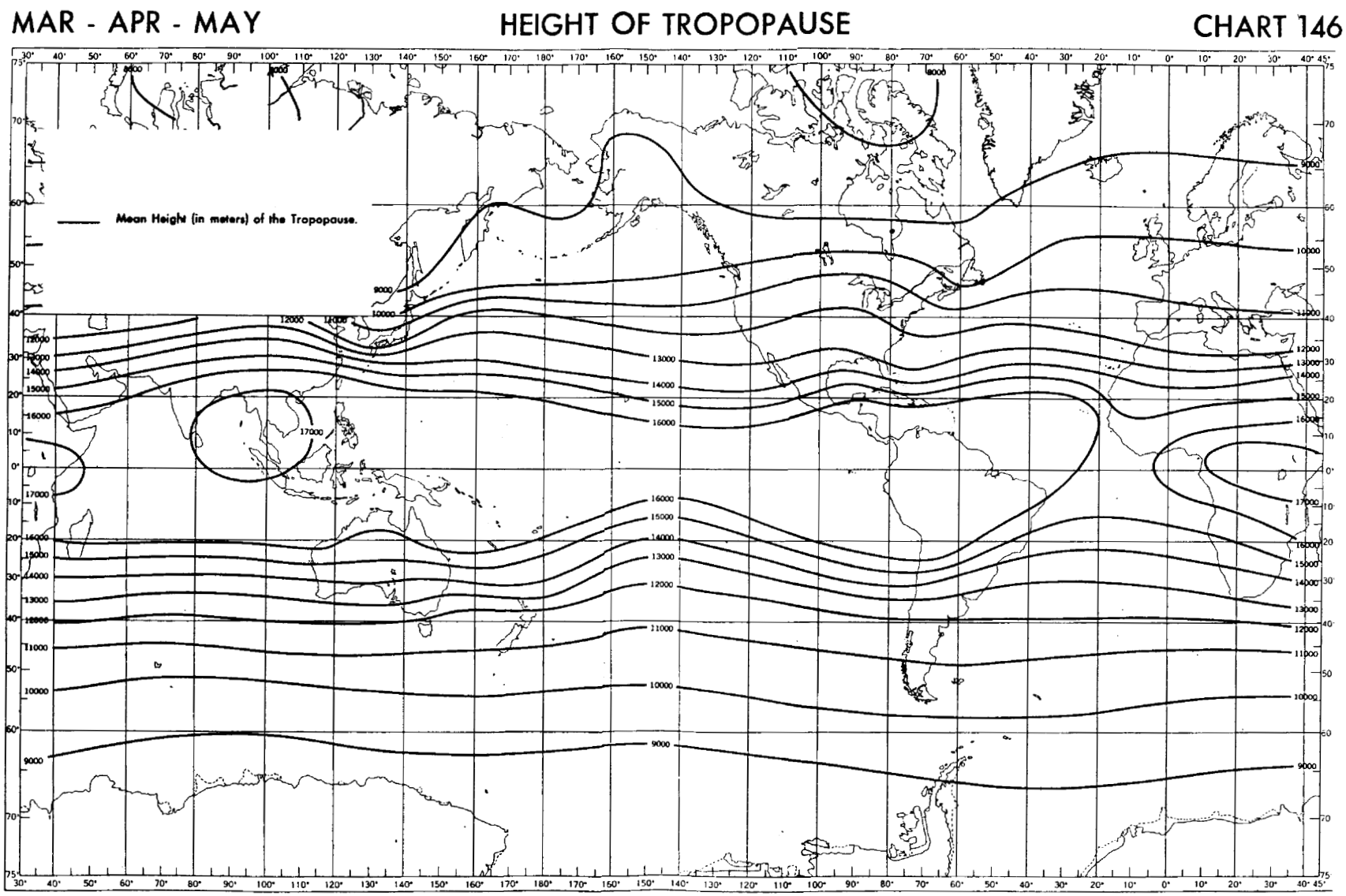

(b) Spring.

Figure 2.- Continued.

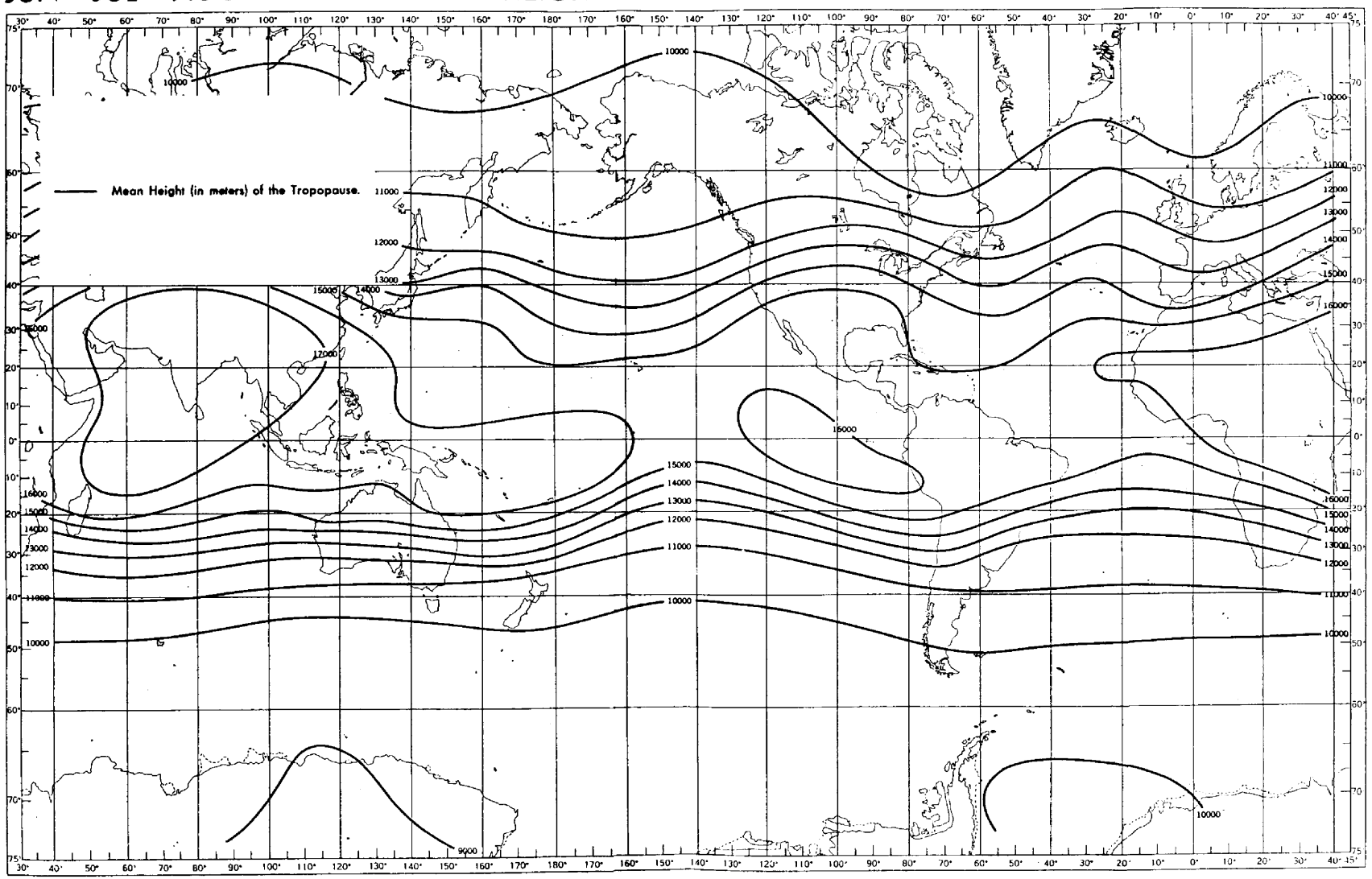

(c) Summer.

Figure 2.- Continued.

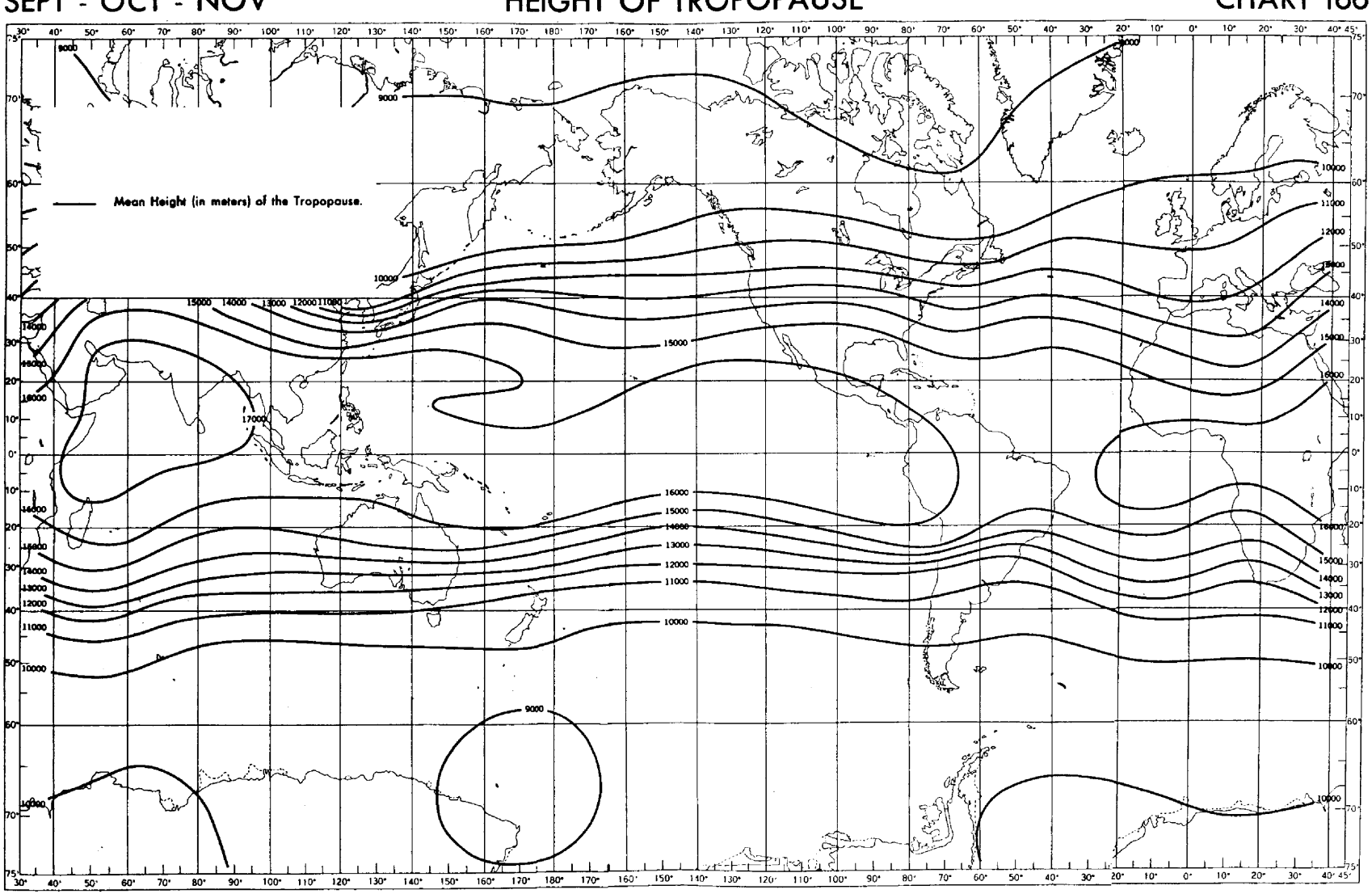

(d) Autumn.

Figure 2.- Concluded.

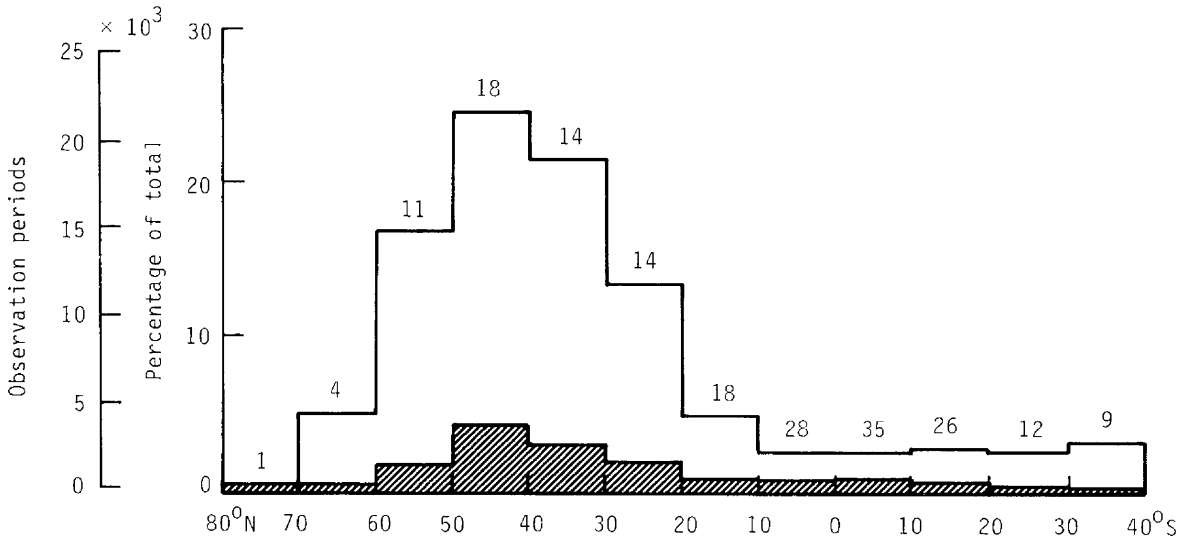

(a) By latitude.

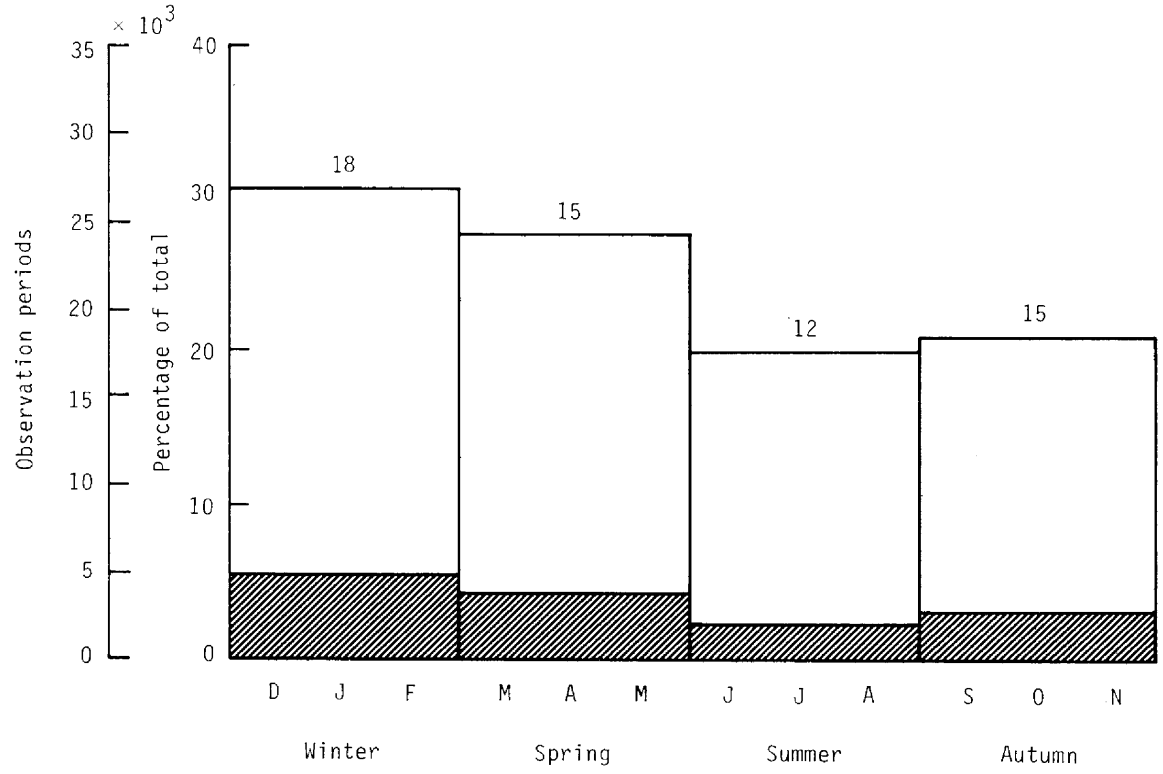

(b) By season.

Figure 3.- Distribution of cloud observation periods by latitude and season. Shading denotes observation periods with TIC > 0. Numbers above bars are percentage PCE for each interval.

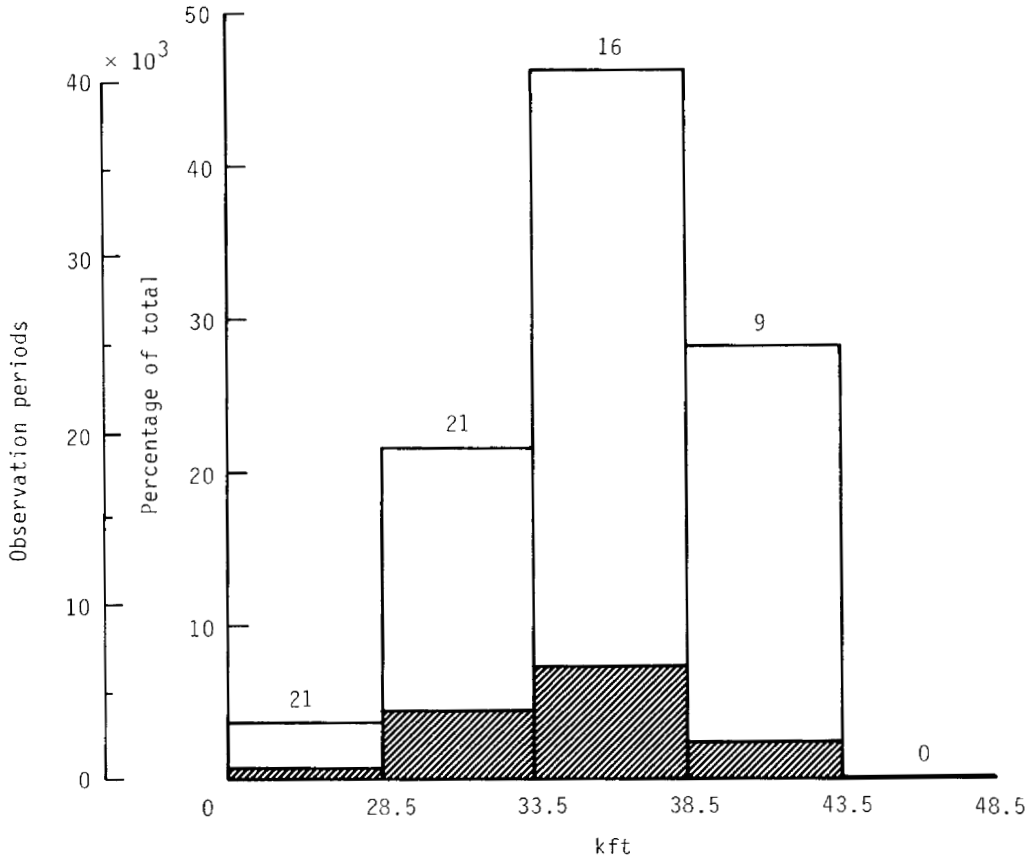

(a) By altitude.

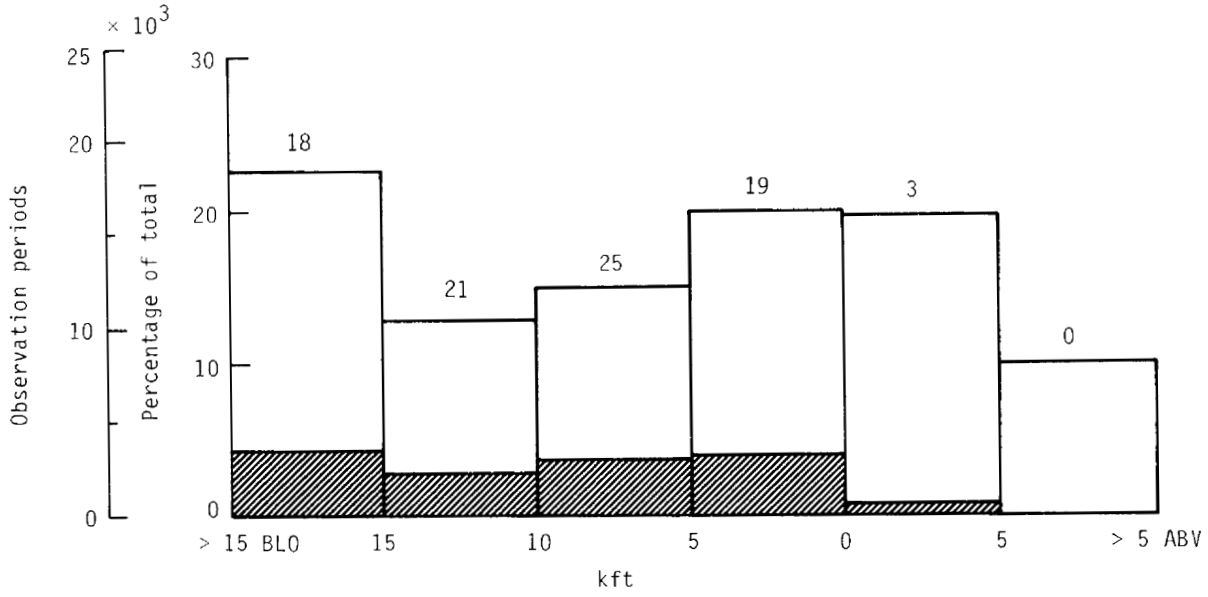

(b) By distance from tropopause.

Figure 4.- Distributions of cloud observation periods by altitude and distance from tropopause. Shading denotes observation periods with TIC > 0. Numbers above bars are percentage PCE for each interval.

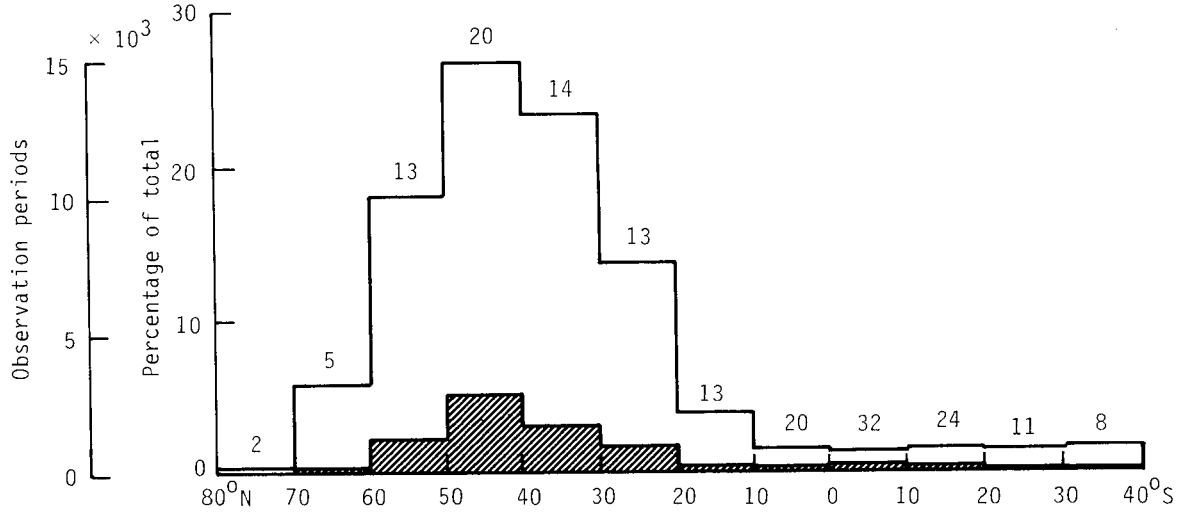

(a) By latitude.

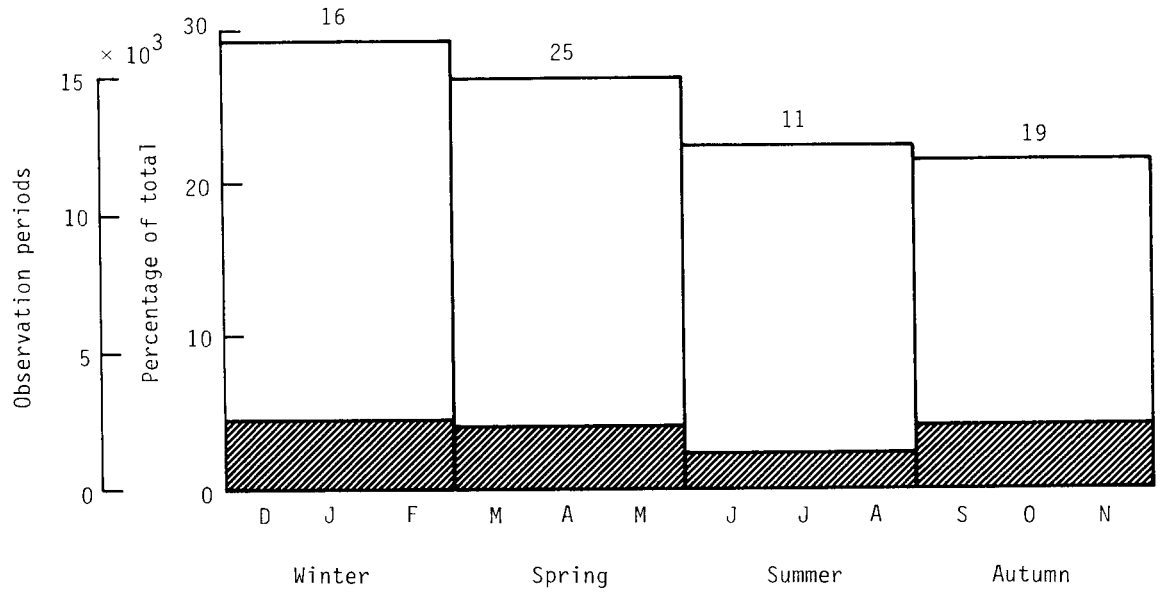

(b) By season.

Figure 5.- Distribution of cloud observation periods with accompanying particle-concentration data by latitude and season. Shading denotes observation periods with TIC > 0. Numbers above bars are percentage PCE for each interval.

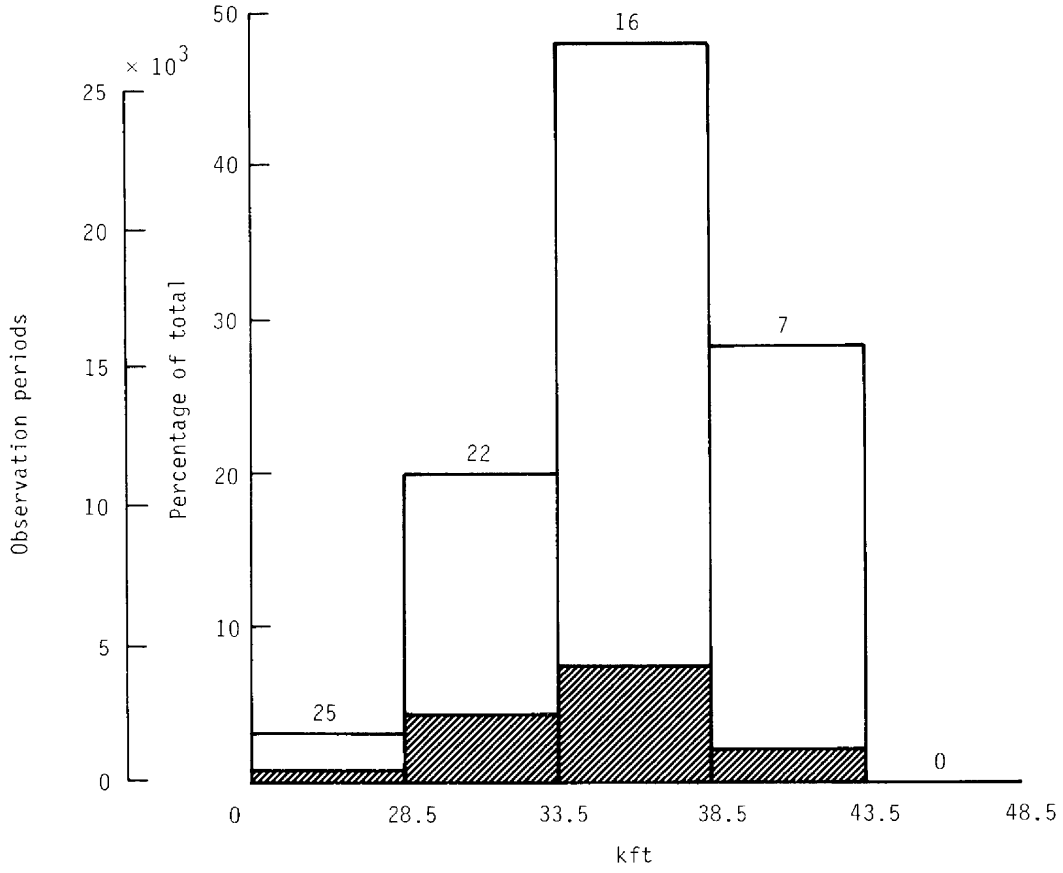

(a) By altitude.

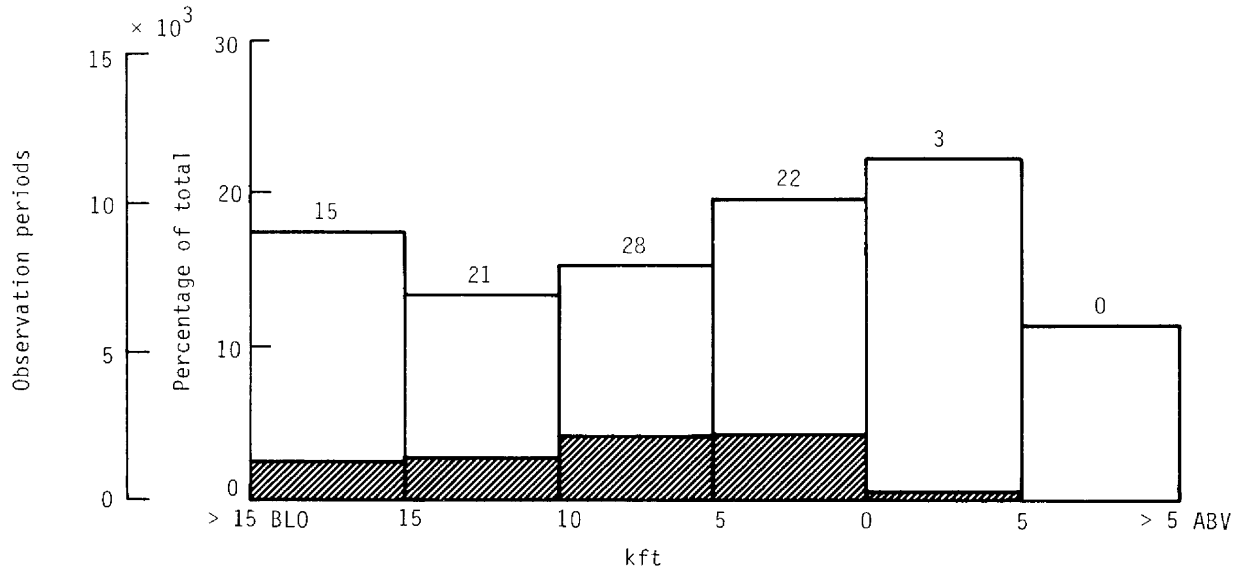

(b) By distance from tropopause.

Figure 6.- Distribution of cloud observation periods with accompanying particle-concentration data by altitude and distance from the tropopause. Shading denotes observation periods with TIC > 0. Numbers above bars are percentage PCE for each interval.

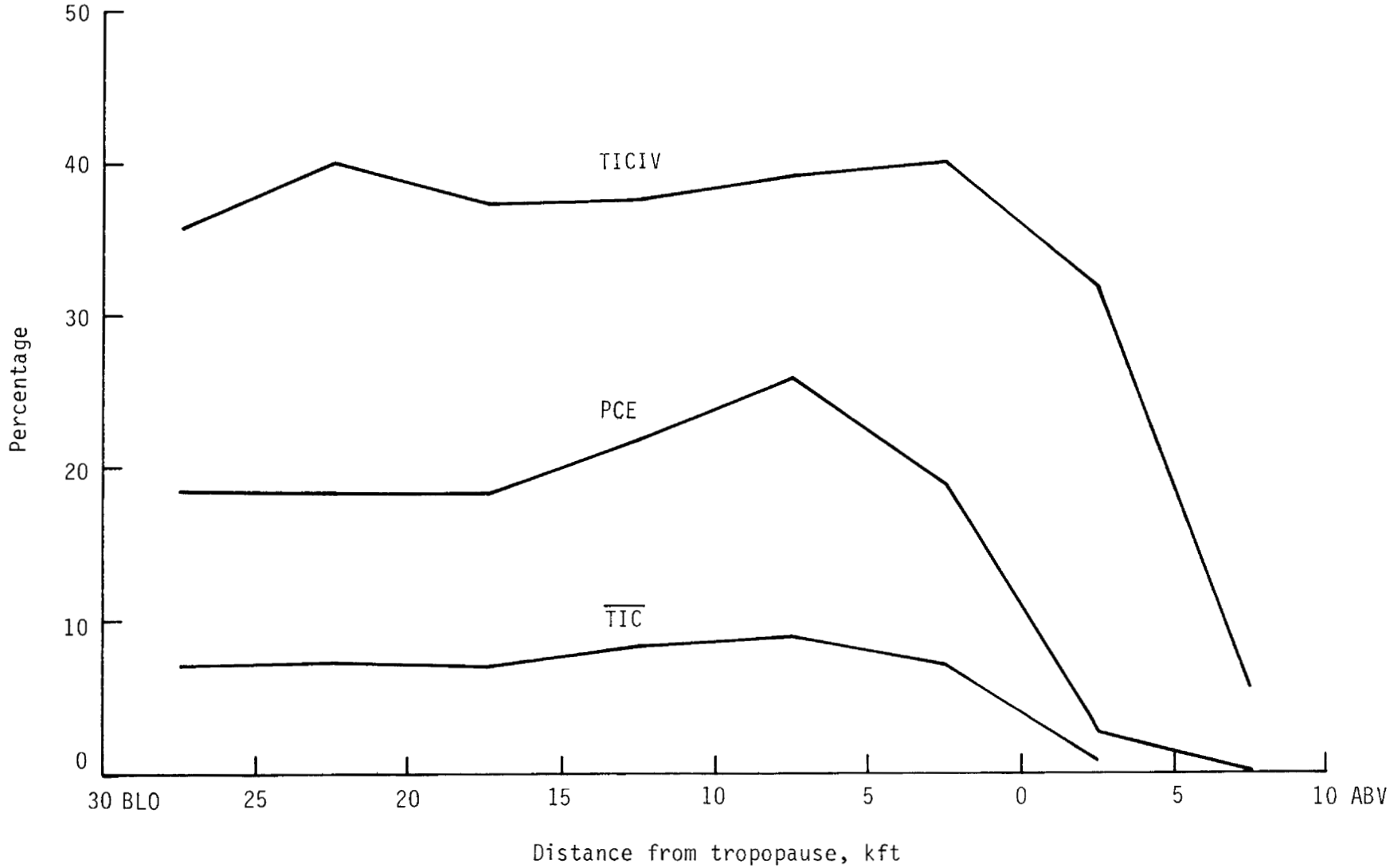

Figure 7.- Variation of global annual mean values of cloudiness parameters with distance from the tropopause.

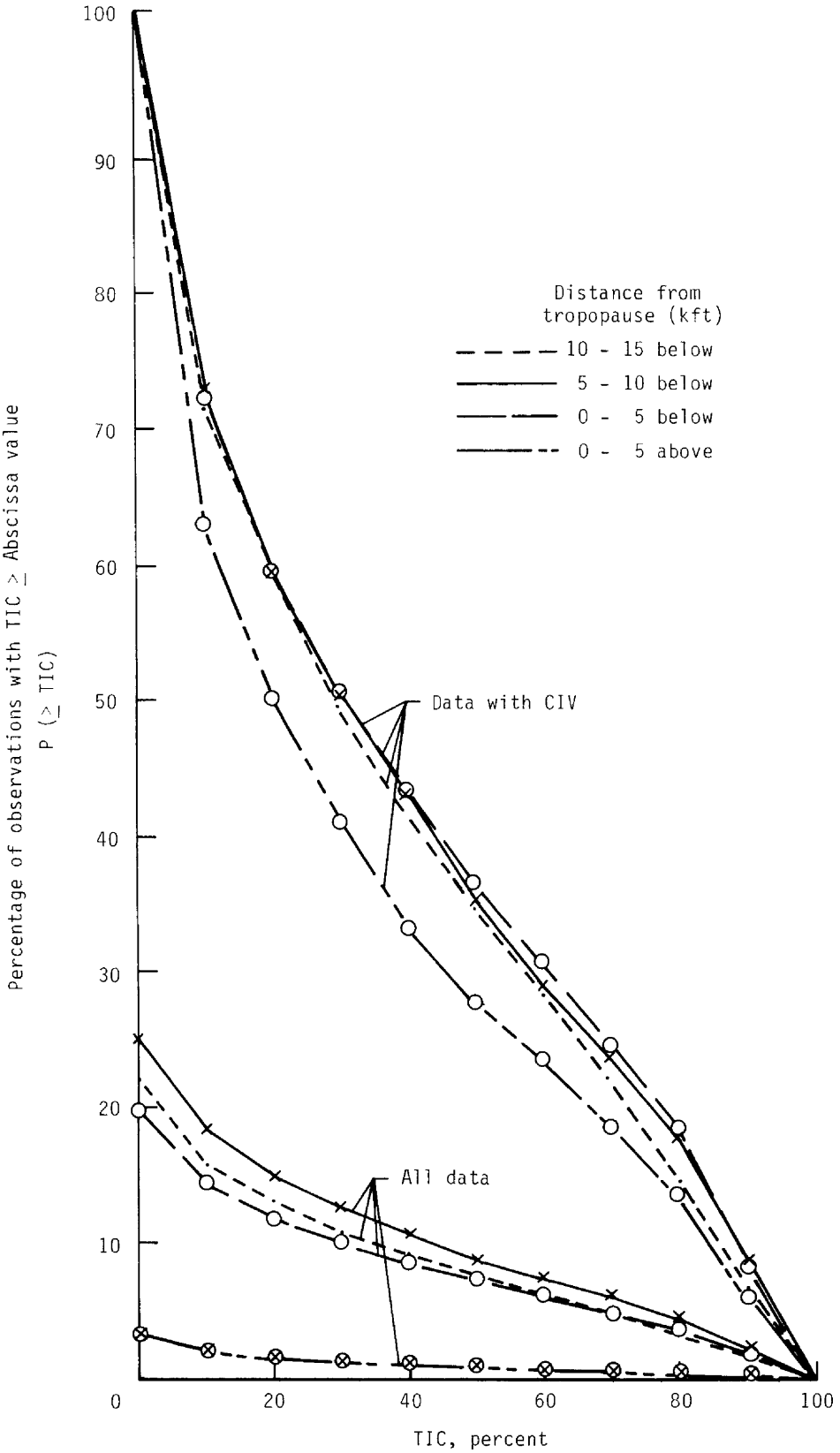

Figure 8.- Cumulative probability distributions of the values of TIC for the global annual data set. Plots are grouped separately for all data and for data with clouds in the vicinity (CIV).

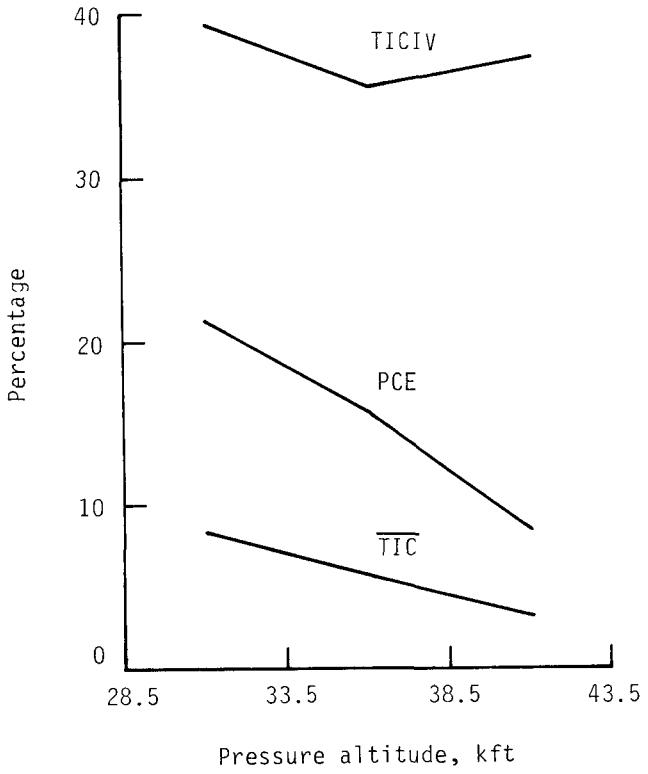

(a) Cloudiness parameters.

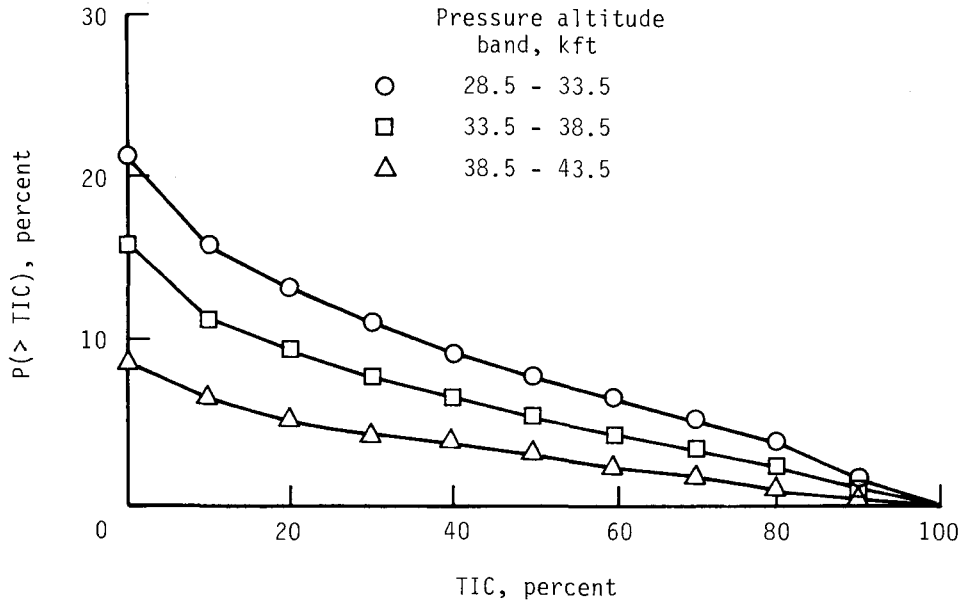

(b) Cumulative probability distribution.

Figure 9.- Variation of global annual mean cloudiness with pressure altitude.

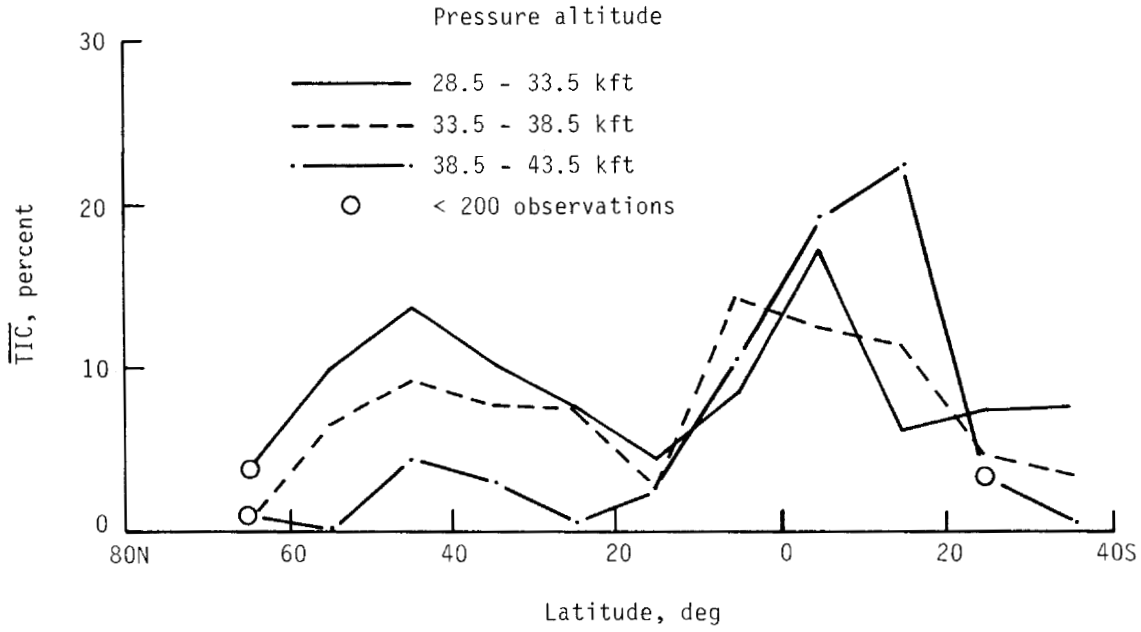

(a) Winter.

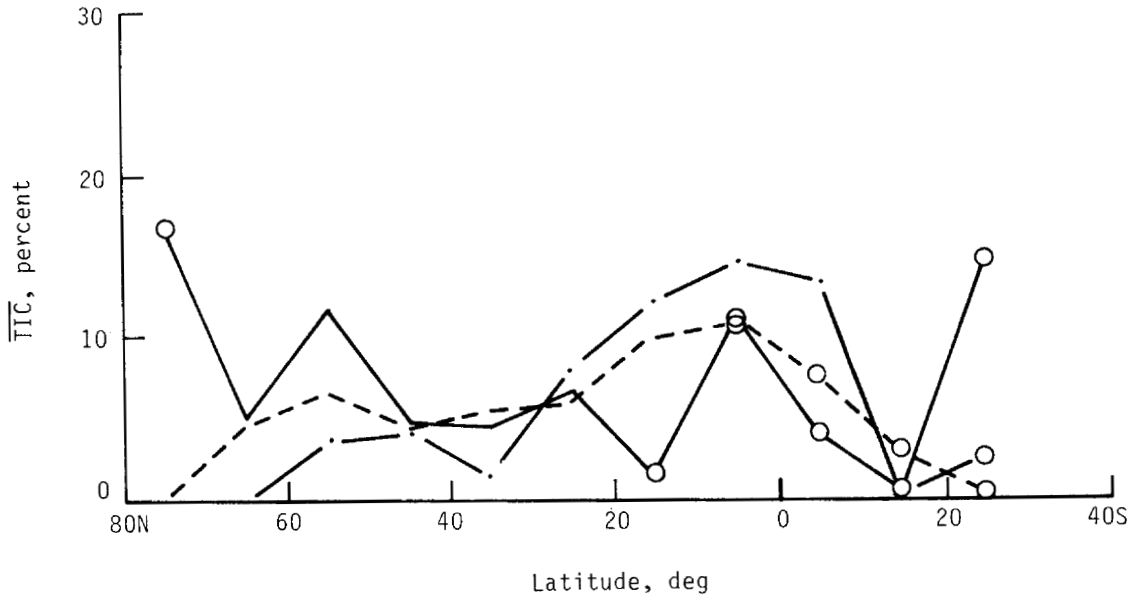

(b) Spring.

Figure 10.- Variation of average time in clouds with latitude and height for Northern Hemisphere seasons. Symbols are plotted where there are fewer than 200 observations.

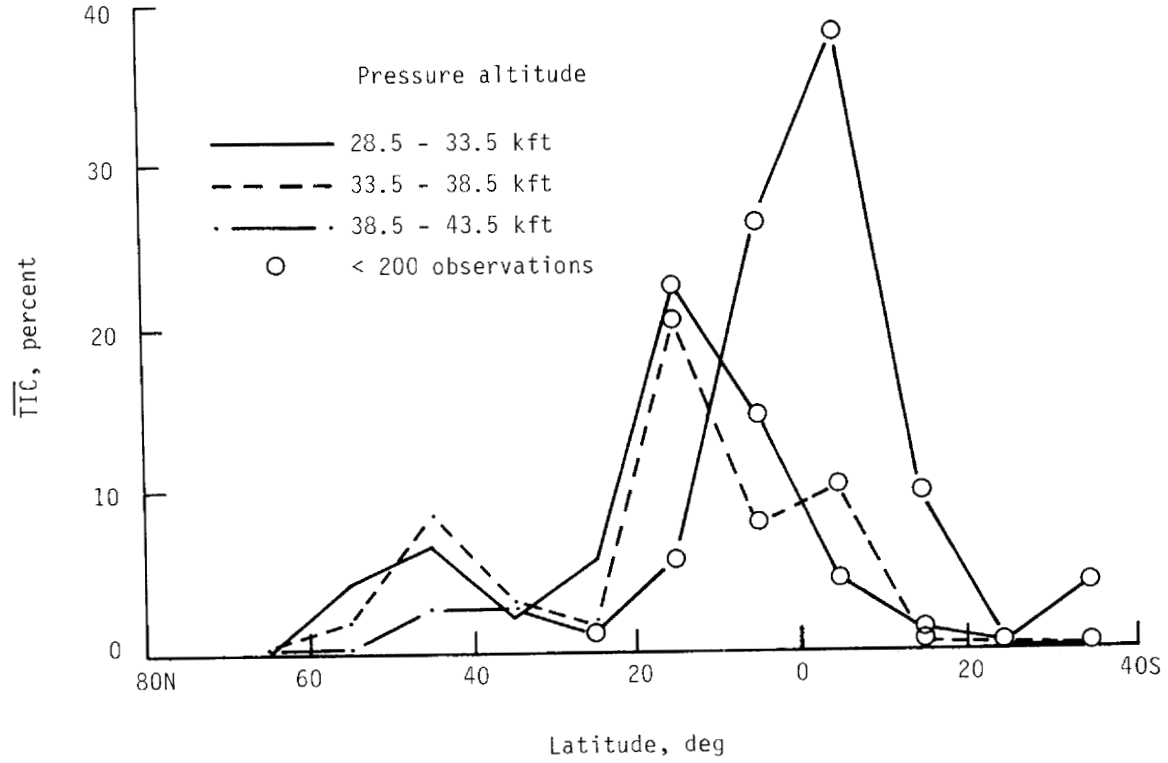

(c) Summer.

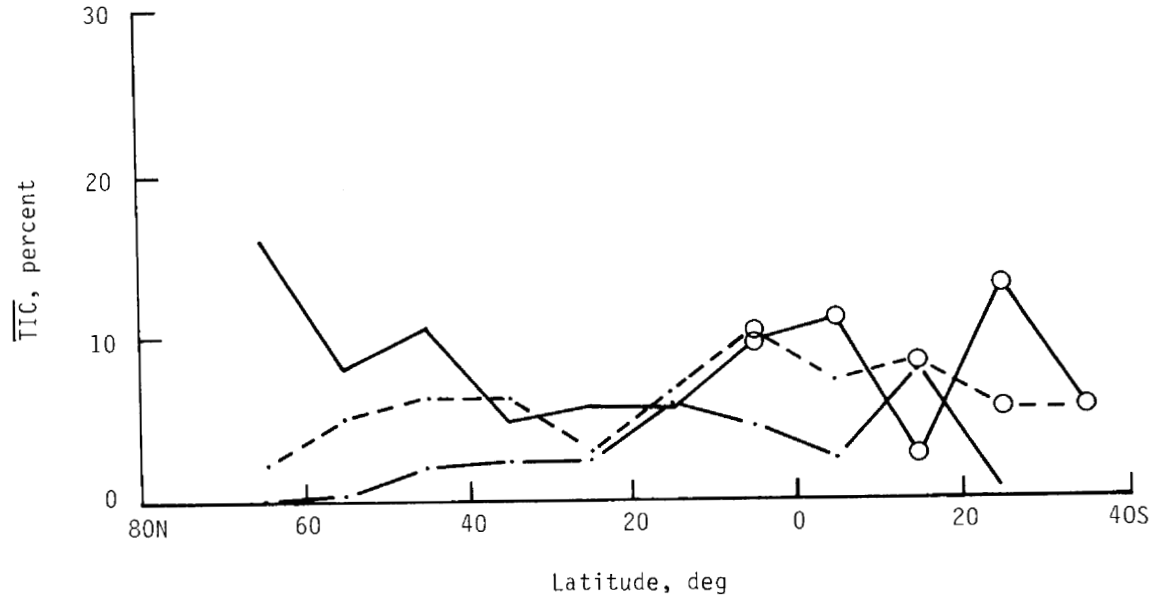

(d) Autumn.

Figure 10.- Concluded.

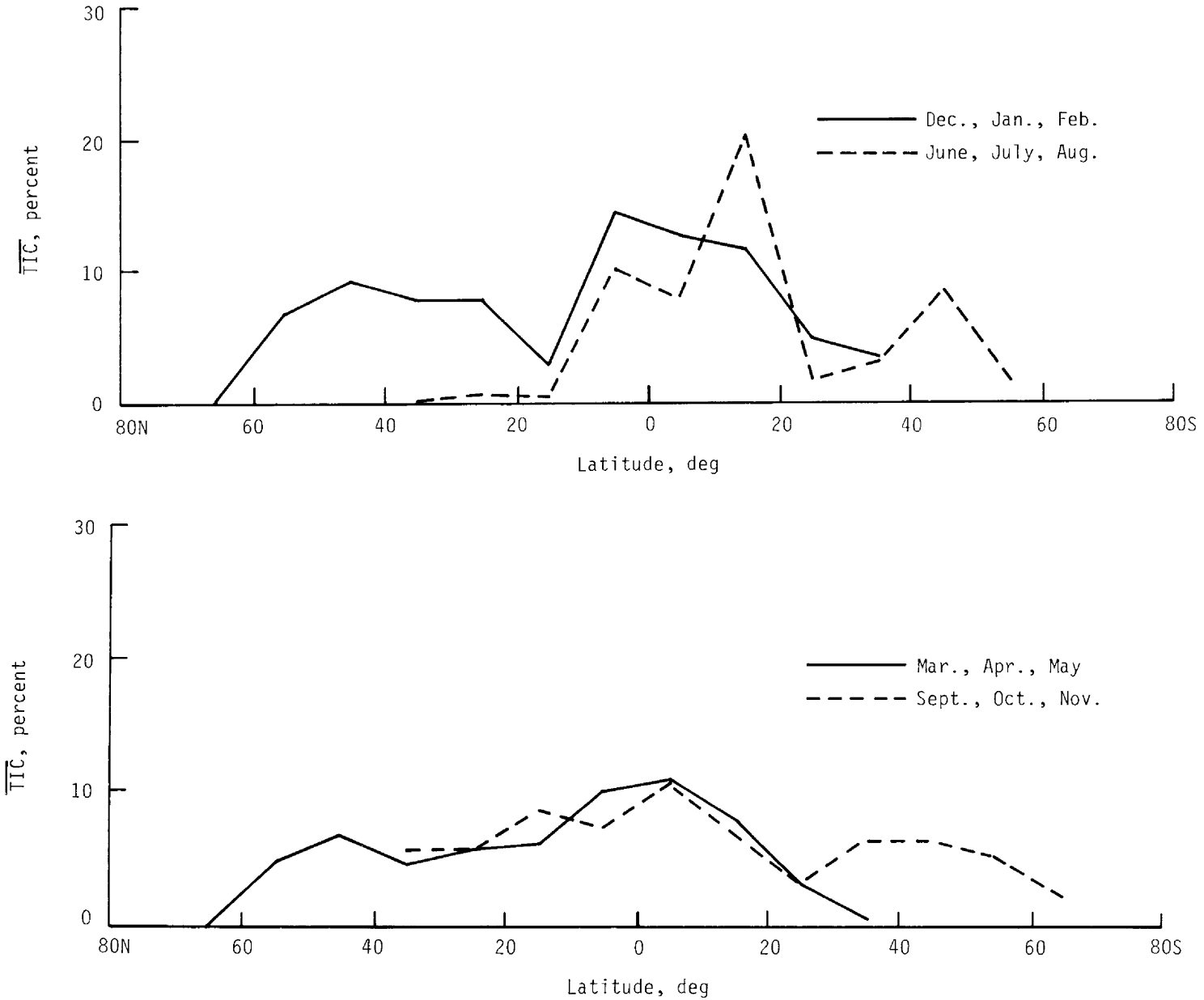

Figure 11.- Seasonal symmetry of average time in clouds with latitude. Altitude = 33.5 to 38.5 kft.

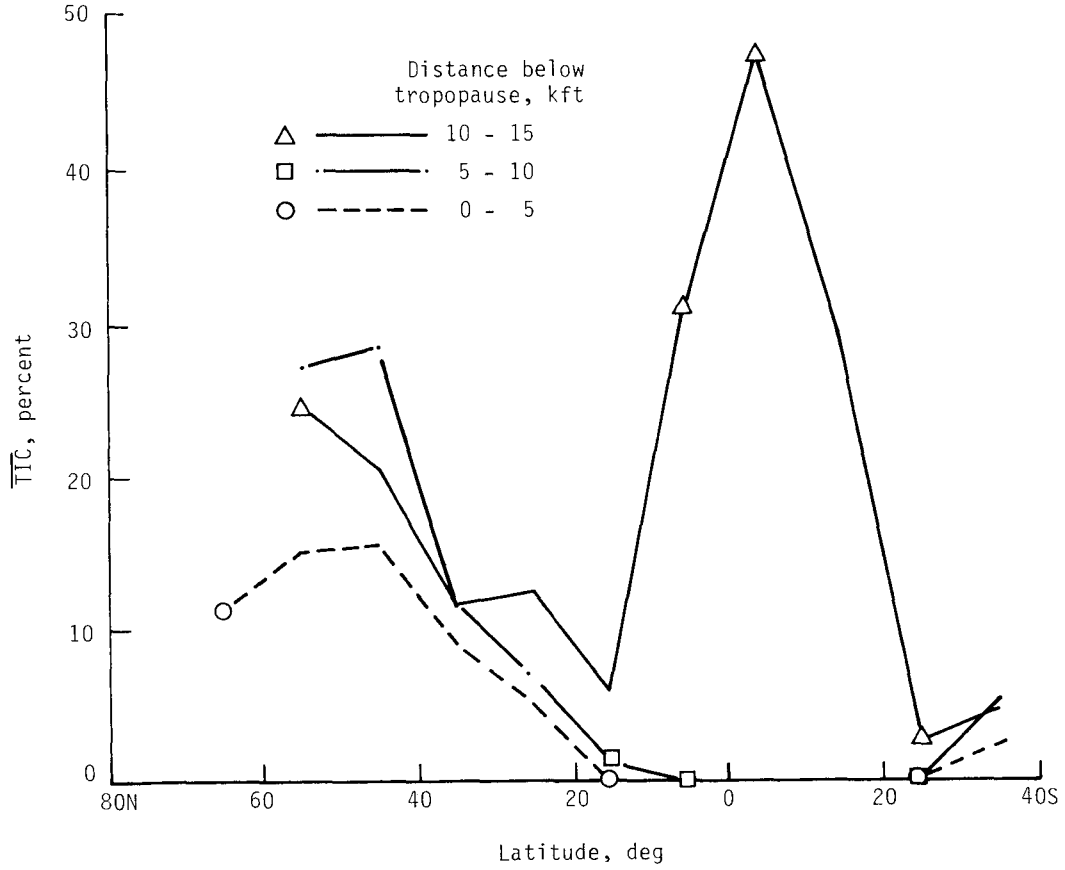

(a) Winter.

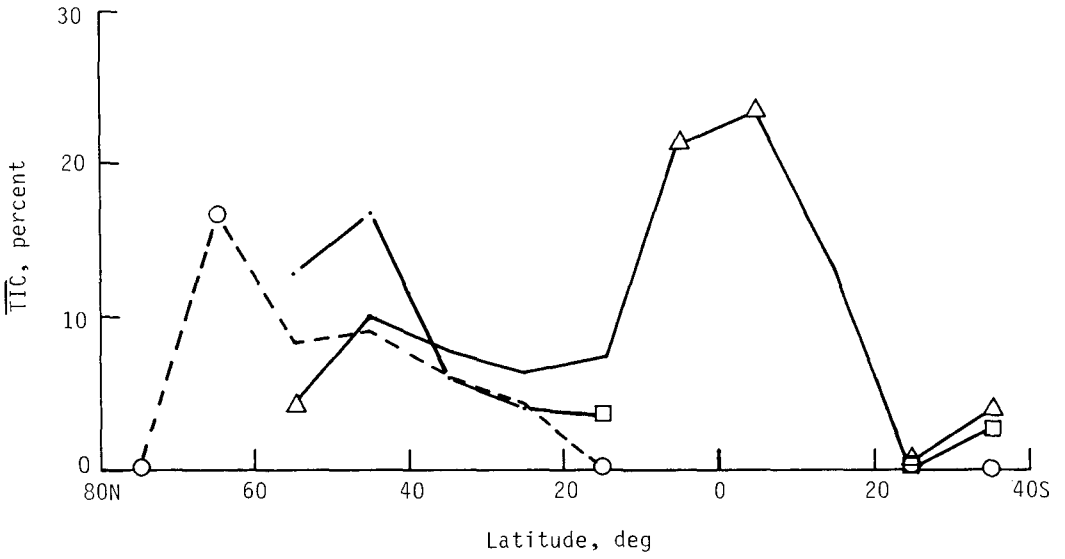

(b) Spring.

Figure 12.- Variation of average time in clouds with latitude and distance from the NMC tropopause for Northern Hemisphere seasons. Symbols are plotted where there are fewer than 100 observations.

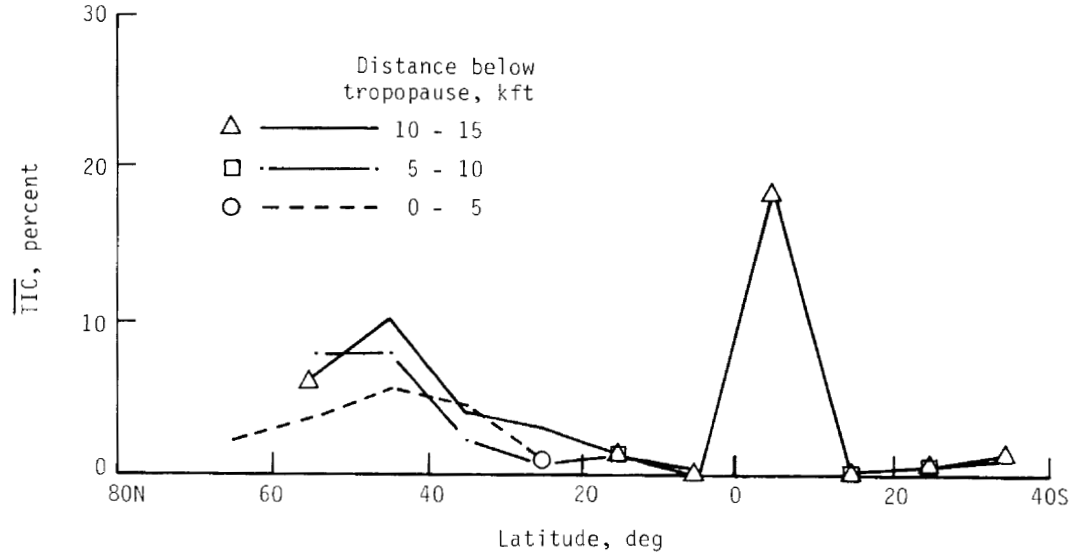

(c) Summer.

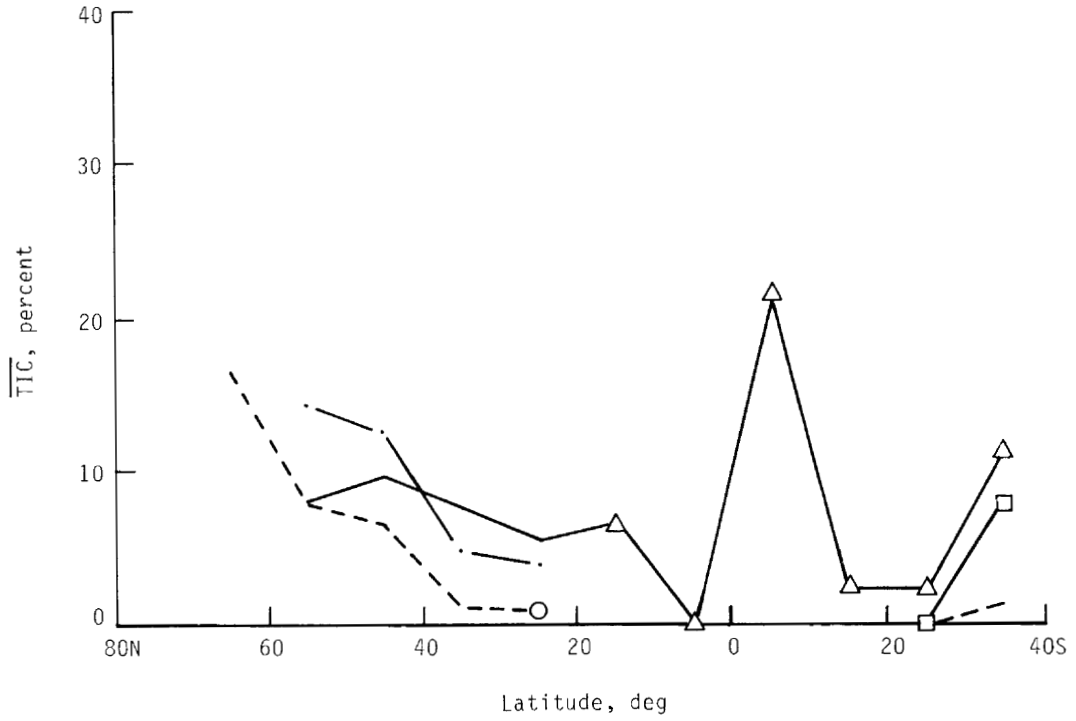

(d) Autumn.

Figure 12.- Concluded.

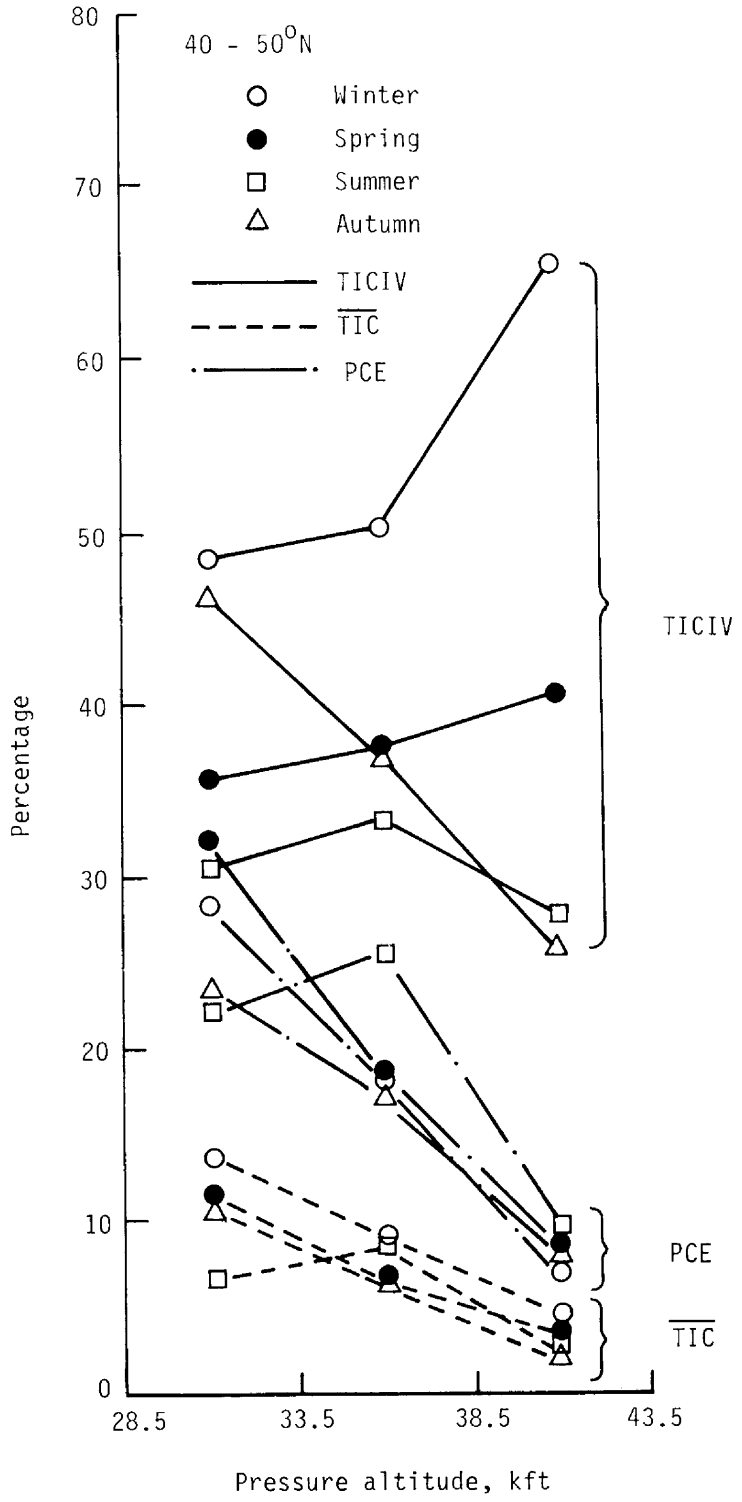

Figure 13.- Variation of cloudiness parameters with pressure altitude and Northern Hemisphere seasons at 40°N to 50°N latitude.

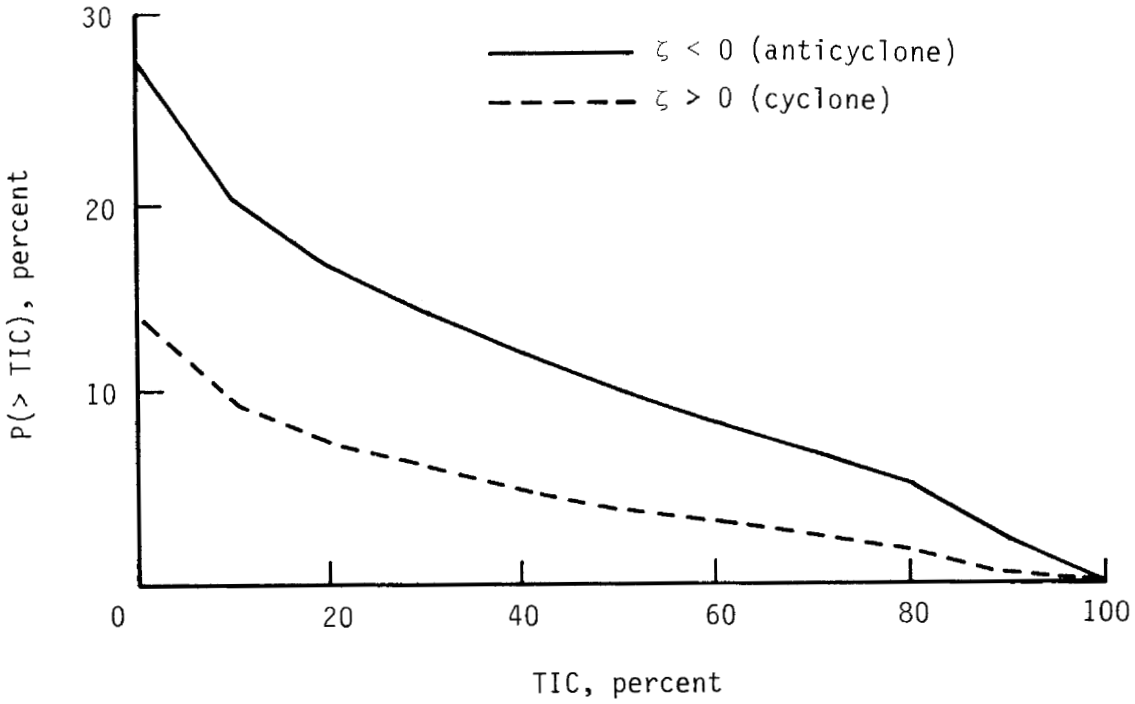

Figure 14.- Cumulative probability distribution of TIC at 0 to 10 kft below the tropopause in cyclones and anticyclones.

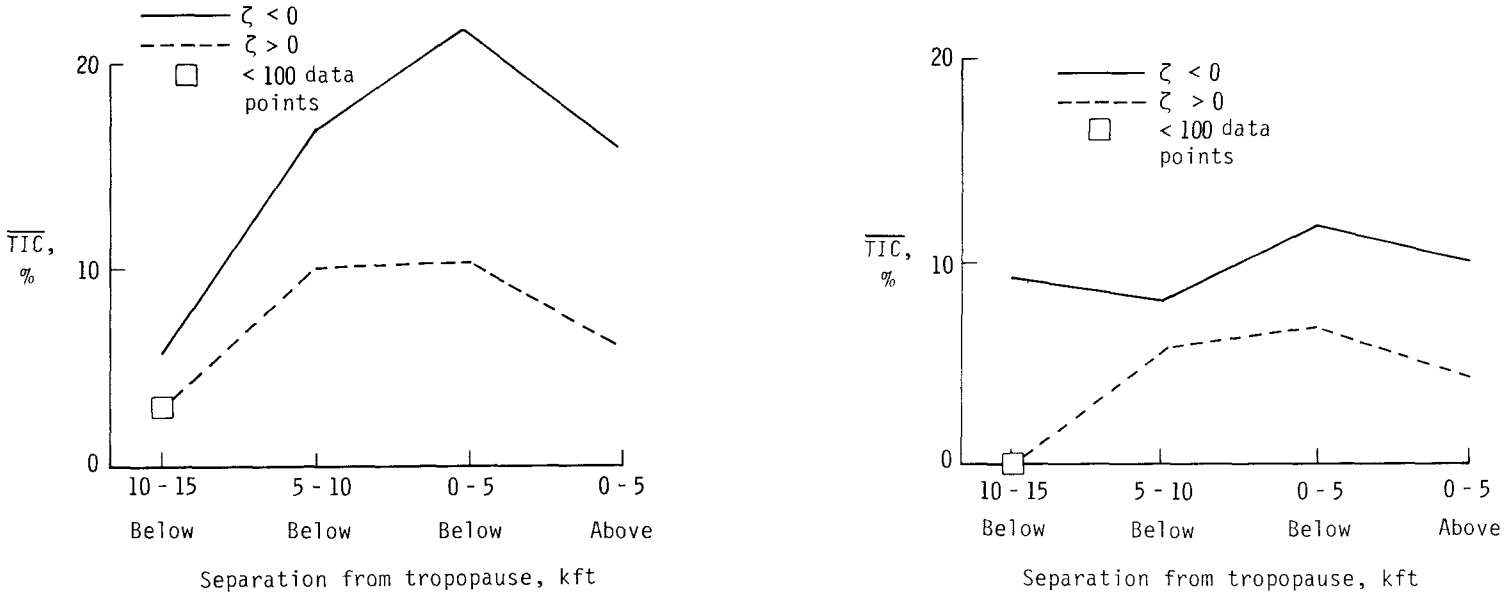

Figure 15.- Cloudiness parameter $\overline{TIC}$ in cyclones (relative vorticity $\zeta > 0$) and anticyclones ($\zeta < 0$) as a function of distance from the NMC tropopause for Northern Hemisphere seasons at 30°N to 70°N latitude. Symbol is plotted where there are fewer than 100 data samples.

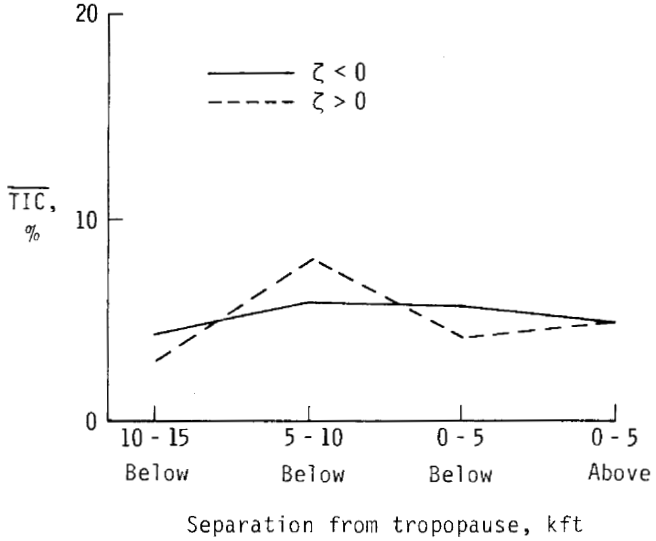

(c) Summer.

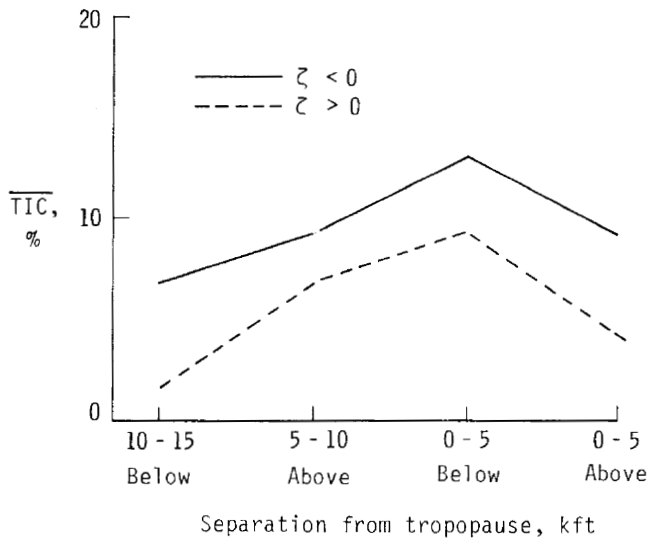

(d) Autumn.

Figure 15.- Concluded.

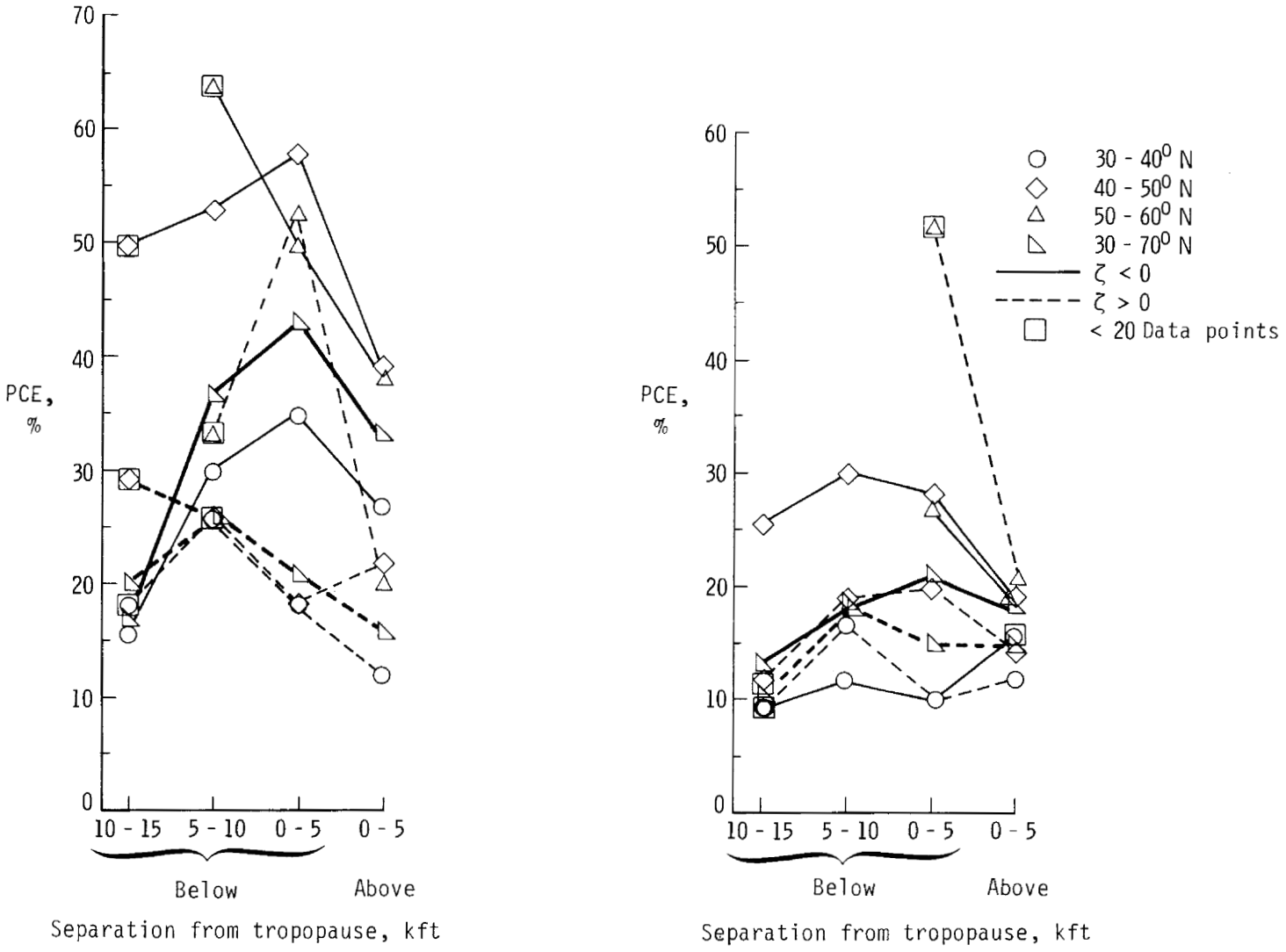

Figure 16.- Cloudiness parameter PCE as a function of distance from NMC tropopause, latitude, and sign of relative vorticity ζ, in Northern Hemisphere winter and summer.

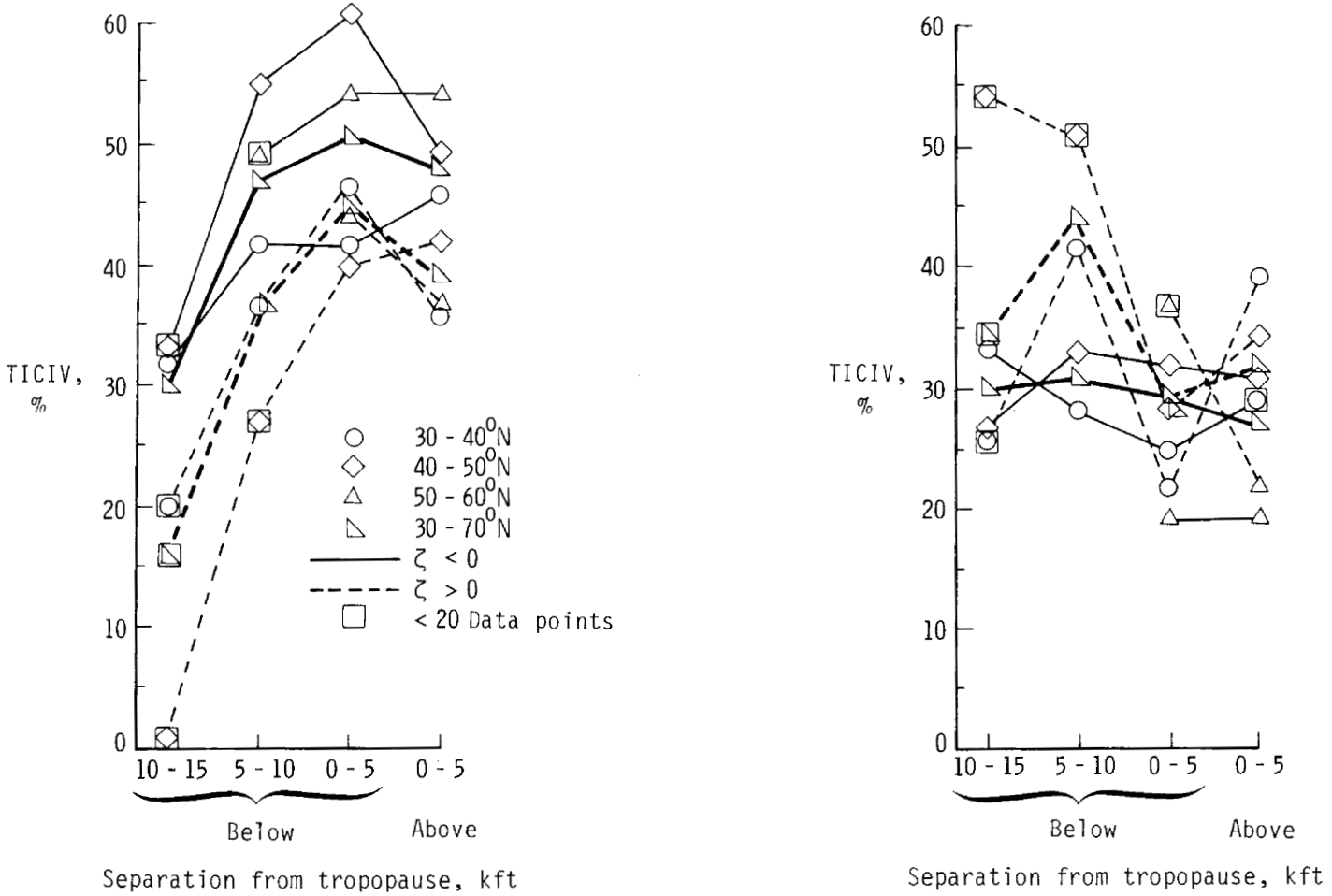

(a) Winter.

(b) Summer.

Figure 17.- Cloudiness parameter TICIV as a function of distance from NMC tropopause, latitude, and sign of relative vorticity ζ, in Northern Hemisphere winter and summer.

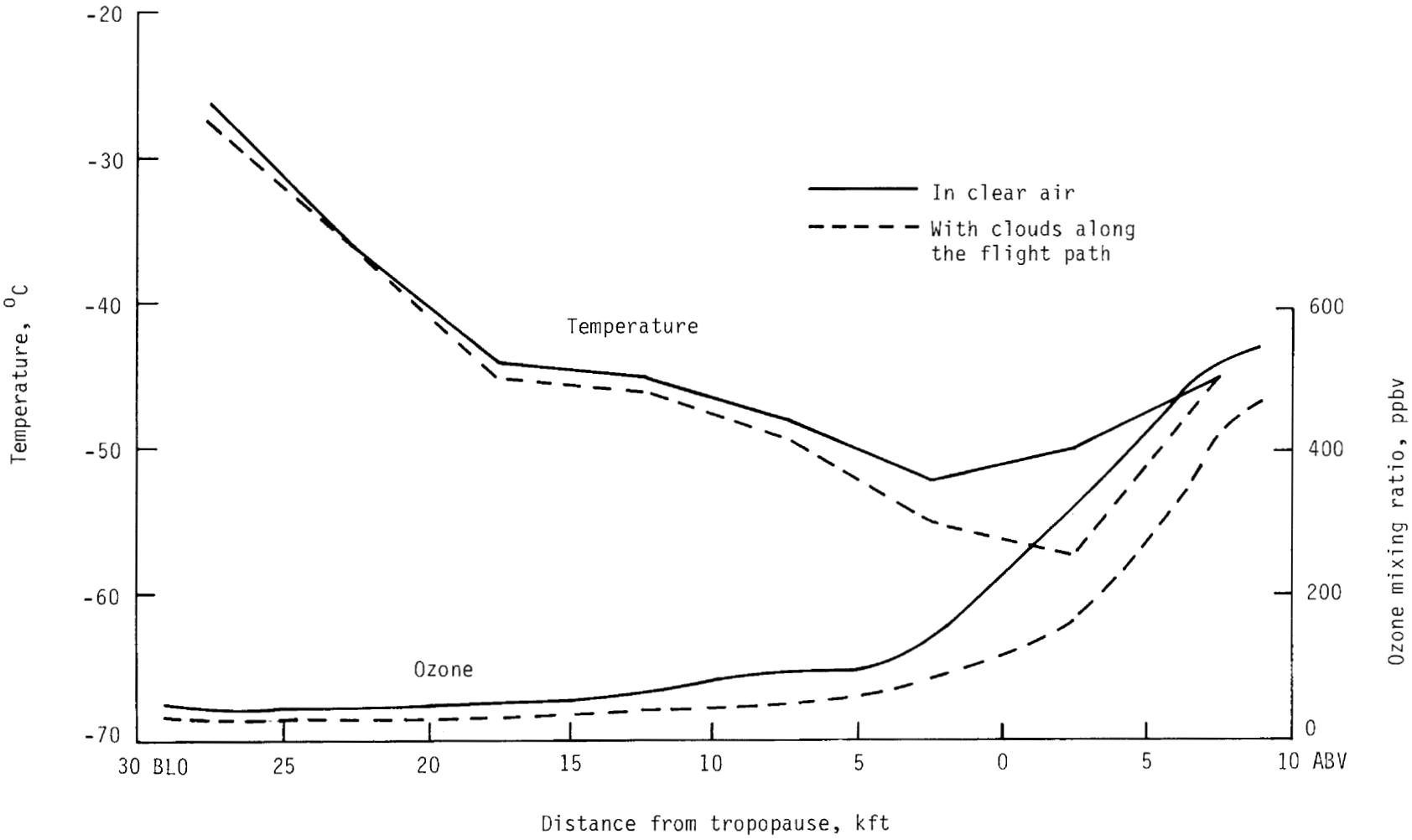

Figure 18.- Temperature and ozone in clear air and in cloudy air as a function of distance from the NMC tropopause.

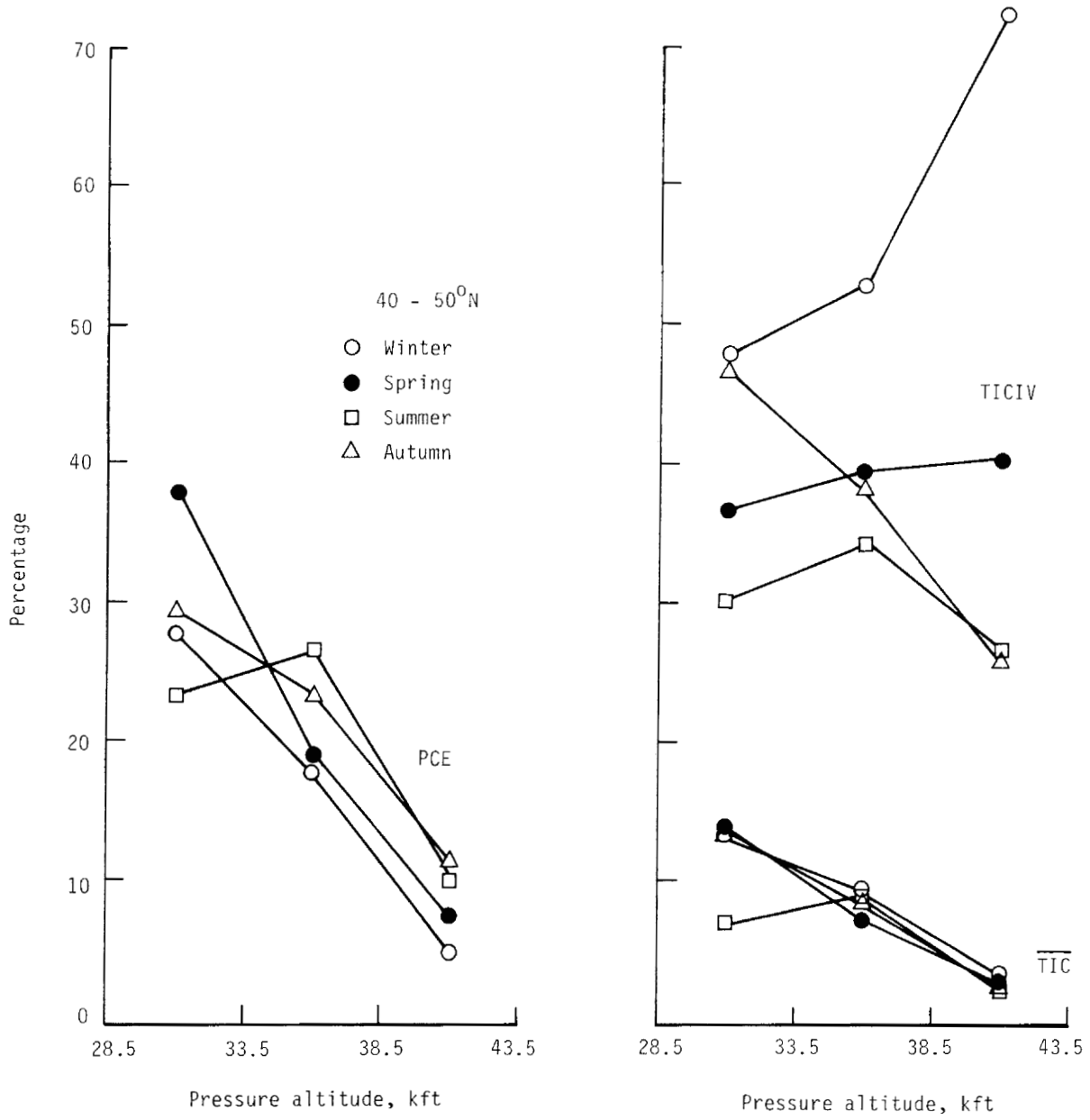

Figure 19.- Variation of cloudiness parameters with pressure altitude and Northern Hemisphere seasons at 40°N to 50°N for only those observations also having particle-concentration data.

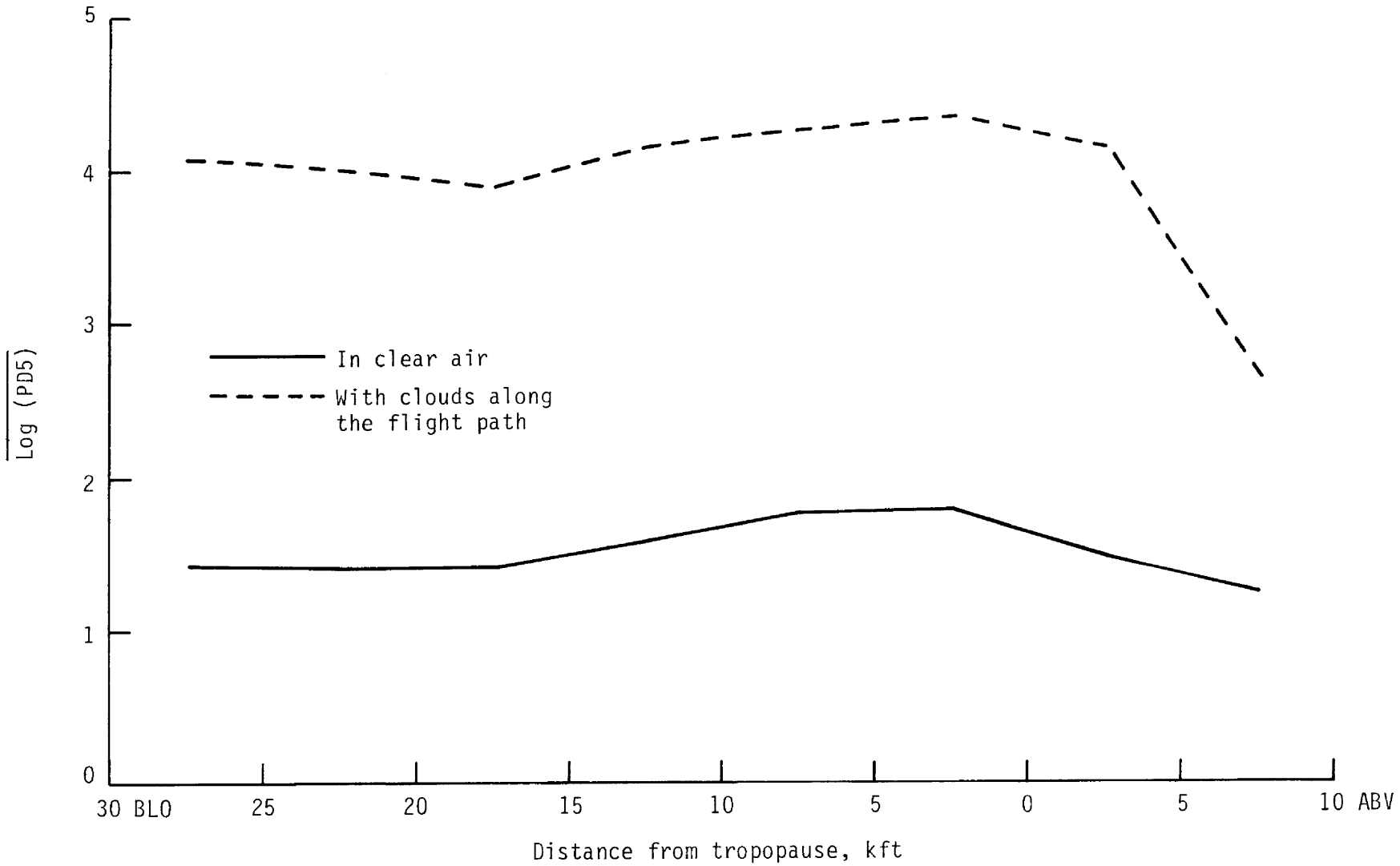

Figure 20.- Average value of log PD5, the concentration of particles with D > 3 μm, in clear and cloudy air as a function of distance from the NMC tropopause.

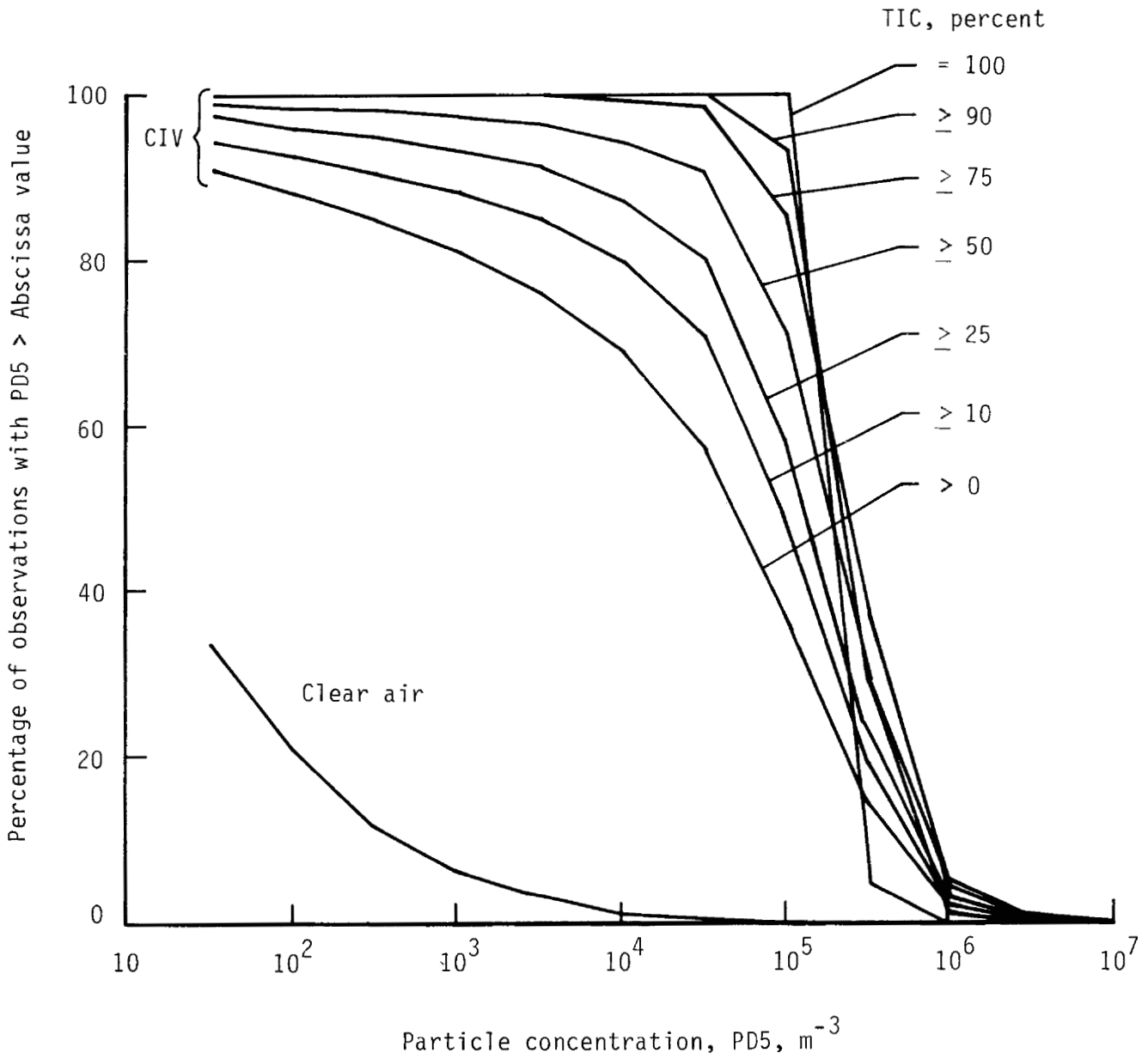

Figure 21.- Cumulative frequency distributions of PD5 in and out of clouds.

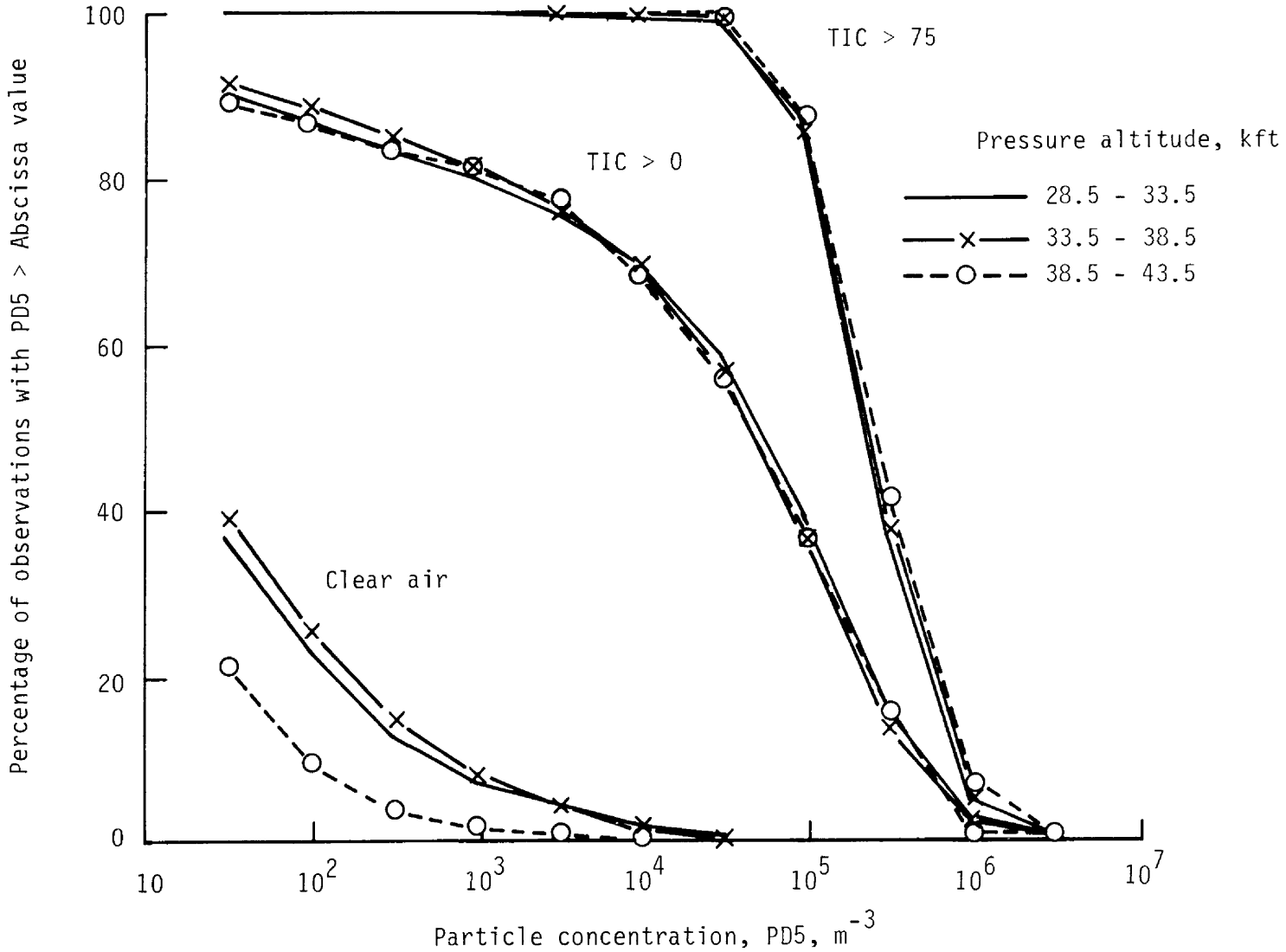

(a) By pressure altitude.

Figure 22.- Cumulative frequency distributions for PD5, as a function of pressure altitude and distance from the NMC tropopause.

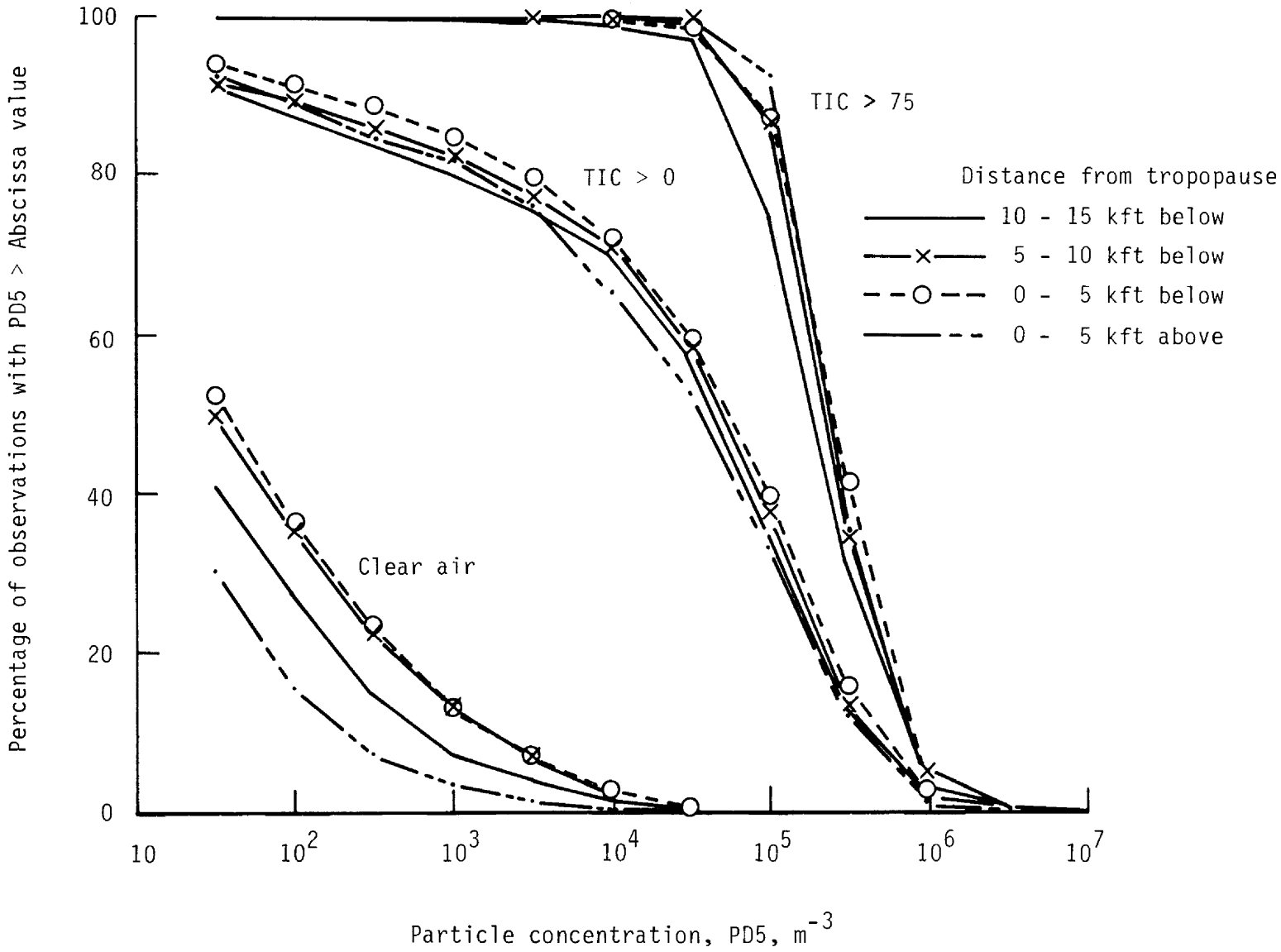

(b) By distance from tropopause.

Figure 22.- Concluded.

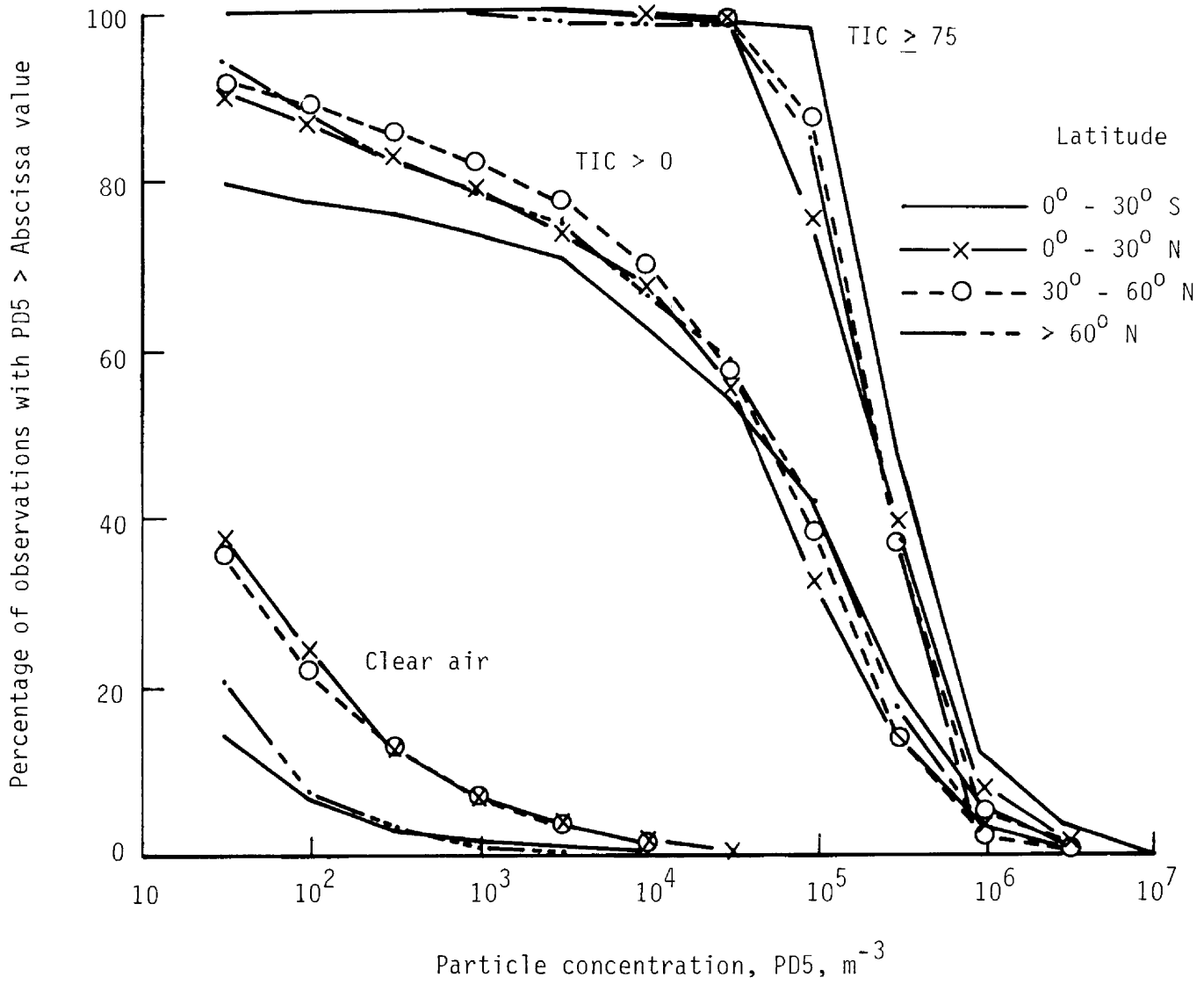

(a) By latitude.

Figure 23.- Cumulative frequency distributions of PD5, as a function of latitude and Northern Hemisphere seasons.

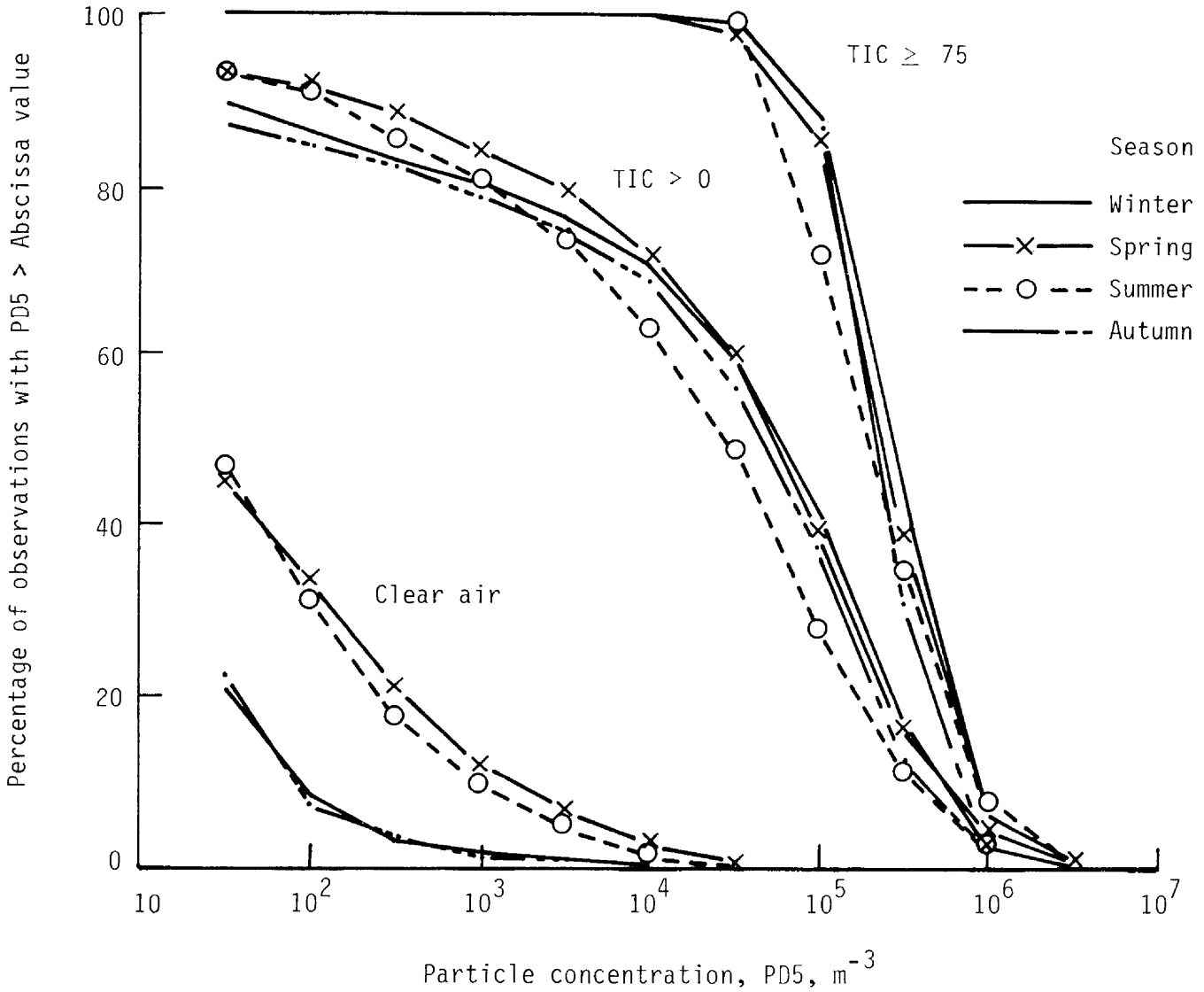

(b) By season.

Figure 23.- Concluded.

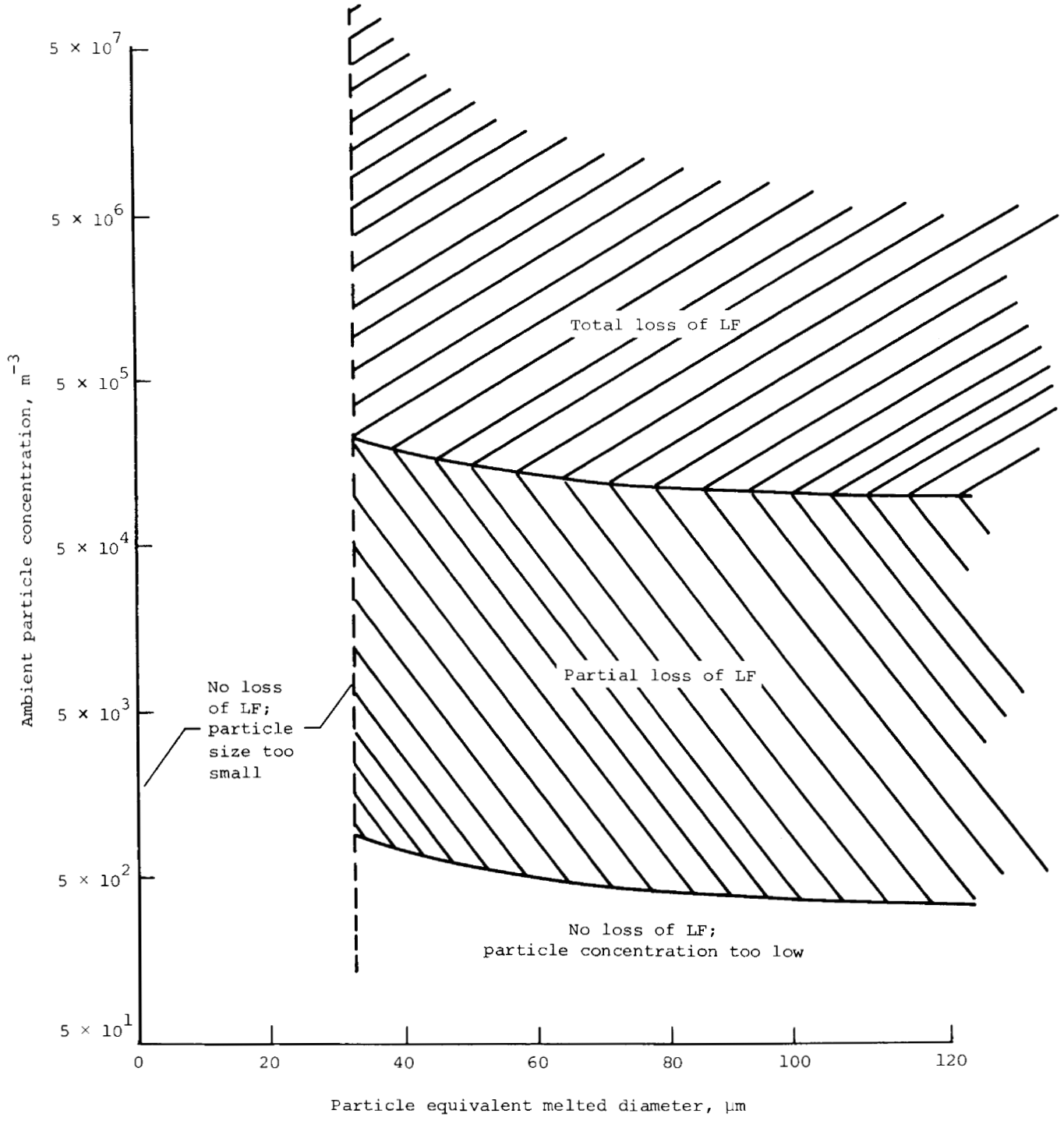

Figure 24.- Estimated LF degradation within clouds at 40 kft and Mach 0.75 (based on ref. 10).

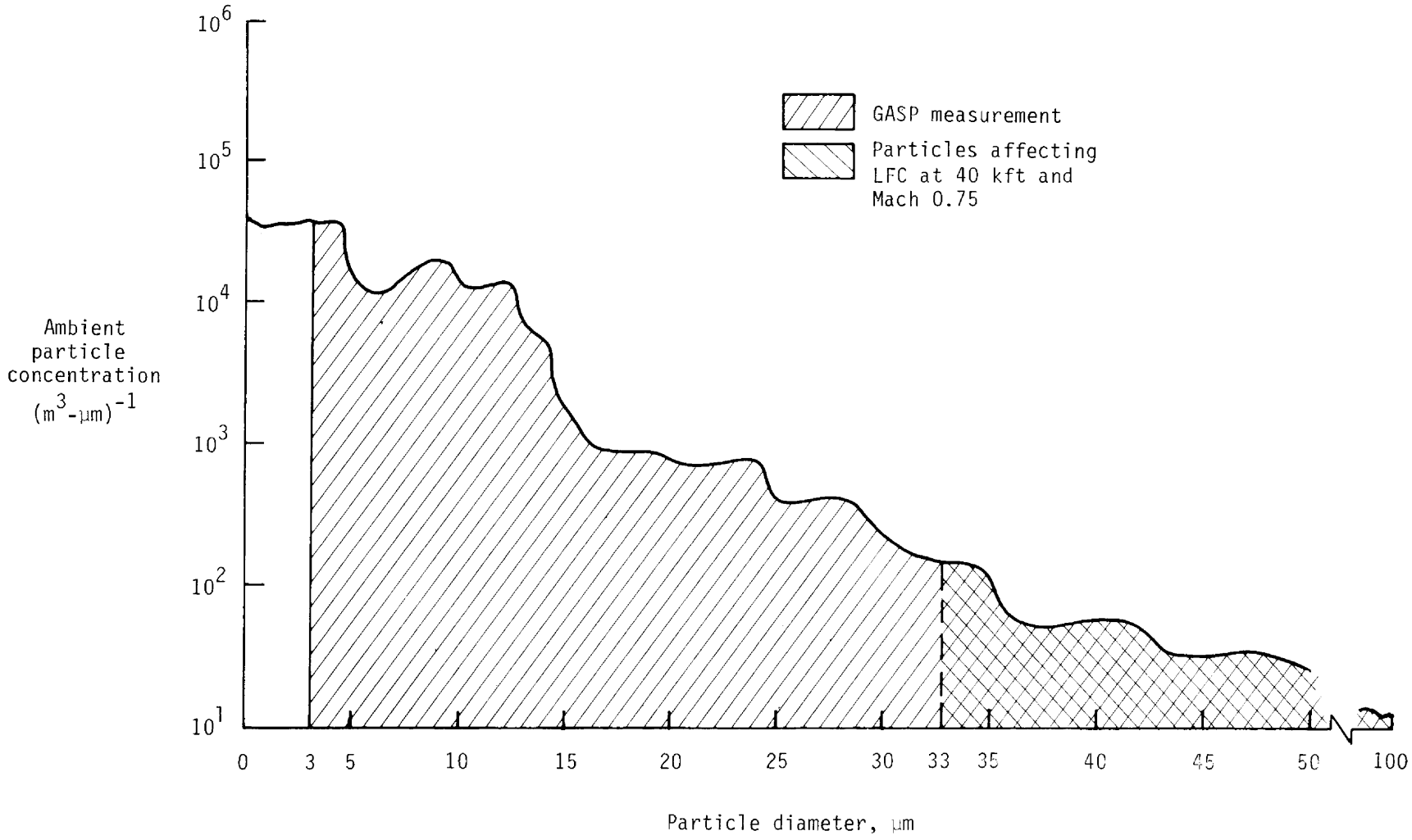

Figure 25.- The range of particle sizes measured by the GASP cloud detector and the range of particle sizes affecting LFC. The flux of particles (integral with size of concentration) in each range is denoted by appropriate hatched areas. The concentration of particles depicted here is typical of that obtained in a thin cloud.

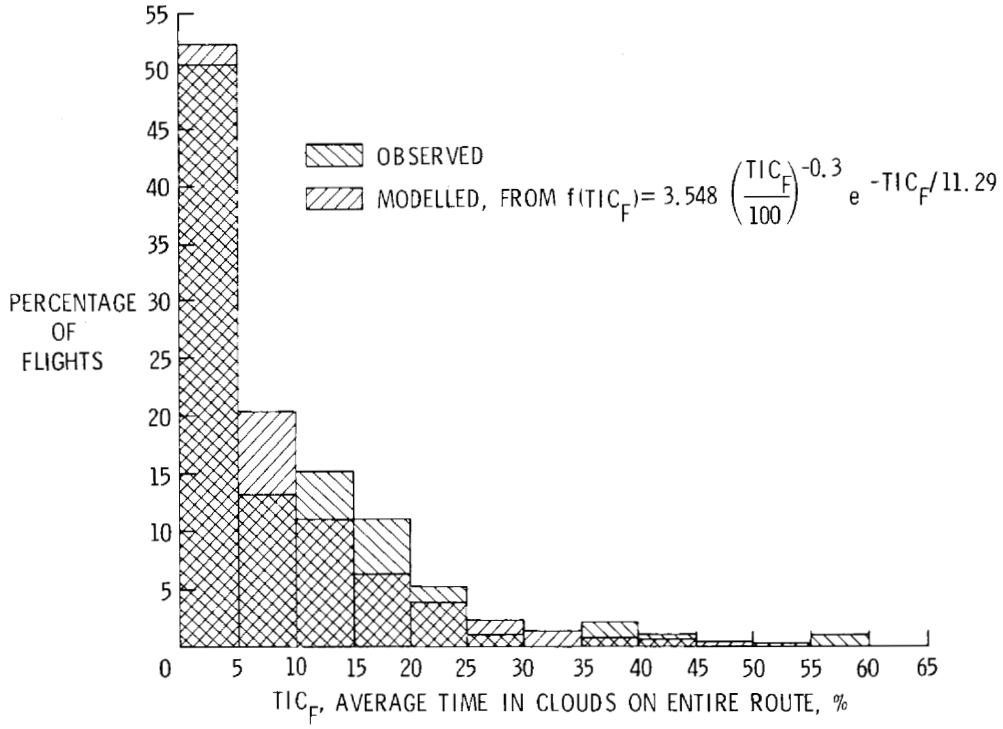

(a) Average altitude of 33.5 to 38.5 kft.

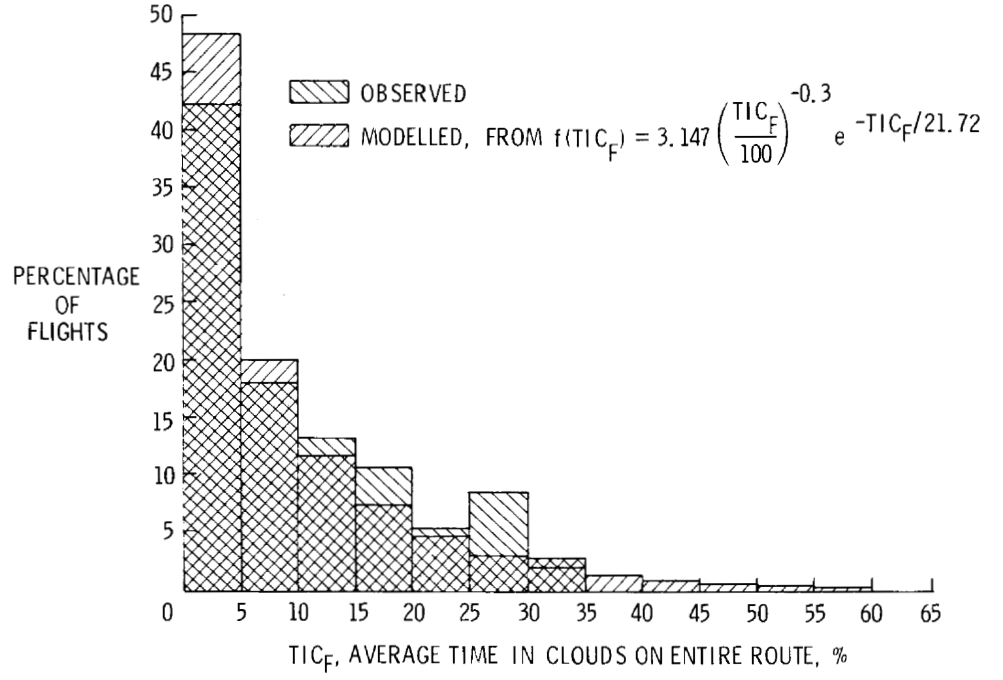

(b) Average altitude of 28.5 to 33.5 kft.

Figure 26.- Observed and theoretical frequency distributions of average time in clouds on GASP flights between the U.S. East Coast and Northwest Europe.

1. Report No.	2. Government Accession No.	3. Recipient's Catalog No.
NASA TM-85835		

4. Title and Subtitle	5. Report Date
GASP CLOUD- AND PARTICLE-ENCOUNTER STATISTICS, AND THEIR APPLICATION TO LFC AIRCRAFT STUDIES VOLUME I: ANALYSIS AND CONCLUSIONS	October 1984
	6. Performing Organization Code 505-45-63-35
7. Author(s) William H. Jasperson, Gregory D. Nastrom, Richard E. Davis, and James D. Holdeman	8. Performing Organization Report No. L-15789
	10. Work Unit No.
9. Performing Organization Name and Address NASA Langley Research Center Hampton, VA 23665	11. Contract or Grant No.
	13. Type of Report and Period Covered Technical Memorandum
12. Sponsoring Agency Name and Address National Aeronautics and Space Administration Washington, DC 20546	14. Sponsoring Agency Code

15. Supplementary Notes

William H. Jasperson and Gregory D. Nastrom: Control Data Corp., Minneapolis, MN.
Richard E. Davis: Langley Research Center, Hampton, VA.
James D. Holdeman: Lewis Research Center, Cleveland, OH.

16. Abstract

Summary studies are presented for the entire cloud observation archive from the NASA Global Atmospheric Sampling Program (GASP). Studies are also presented for GASP particle-concentration data gathered concurrently with the cloud observations. Cloud encounters are shown on about 15 percent of the data samples overall, but the probability of cloud encounter is shown to vary significantly with altitude, latitude, and distance from the tropopause. Several meteorological circulation features are apparent in the latitudinal distribution of cloud cover, and the cloud-encounter statistics are shown to be consistent with the classical mid-latitude cyclone model. Observations of clouds spaced more closely than 90 minutes are shown to be statistically dependent. The statistics for cloud and particle encounter are utilized to estimate the frequency of cloud encounter on long-range airline routes, and to assess the probability and extent of laminar flow loss due to cloud or particle encounter by aircraft utilizing laminar flow control (LFC). It is shown that the probability of extended cloud encounter is too low, of itself, to make LFC impractical. This report is presented in two volumes. Volume I contains the narrative, analysis, and conclusions. Volume II contains five supporting appendixes.

17. Key Words (Suggested by Author(s))	18. Distribution Statement
Probability of cloud encounter Cloud-encounter statistics Aircraft measurements Global Atmospheric Sampling Program (GASP) Statistical analysis Laminar-flow-control loss probability Meteorological parameters	Unclassified - Unlimited Subject Category 47

19. Security Classif. (of this report)	20. Security Classif. (of this page)	21. No. of Pages	22. Price
Unclassified	Unclassified	90	A05

For sale by the National Technical Information Service, Springfield, Virginia 22161 NASA-Langley, 1984